A STUDY OF THE CHEMISTRY OF SOME

TRANSITION METAL IONS IN CERAMIC GLAZES

A thesis submitted for the degree of

Doctor of Philosophy

by

Peter A. Gillespie

University of Aston in Birmingham
Gosta Green
Birmingham B4 7ET   September 1979

A STUDY OF THE CHEMISTRY OF SOME

TRANSITION METAL IONS IN CERAMIC GLAZES

by

Peter A. Gillespie

A thesis submitted for the degree of
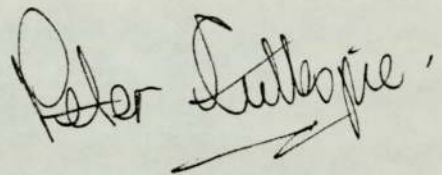Doctor of Philosophy, September 1979

ABSTRACT

The general introduction gives a brief history of the development
of ceramic articles from early Egyptian times to the present day,
outlining the importance of the independent development of Chinese
ceramics as well as the recent development of the British pottery
industry. The value of a number of spectroscopic techniques in investi-
gating the chemistry of transition metal ions in ceramic glazes is
evaluated.

Chapter three outlines the room temperature and liquid nitrogen
temperature Mössbauer and magnetochemistry results for a number of
Iron (III) dipyridyl complexes in order to evaluate the use of Mössbauer
spectroscopy in the investigation of iron in weak ligand fields similar
to those encountered in a glaze environment.

Chapter four describes the Mössbauer X-ray Diffraction and Electron
Spin Resonance results for a number of iron containing glazes. Iron is
introduced in various forms and firings are performed under oxidizing
and inert conditions. The Mössbauer results indicate that the final
environment of iron in the fully matured glaze depends upon the method
of introduction. Comparison of the Mössbauer parameters for a number of
Chinese ceramic glaze samples also serves to illustrate this point.

ESR of Copper containing glazes are also reported. Copper (II) is
found to exist in a highly distorted octahedral environment. Visible
spectra of Chromium containing glazes are also reported and compared
with some highly acidic chromium (III) solution spectra in order to
gain a quantitative estimate of the sort of ligand field strengths
normally encountered in a glaze environment. Replacement of Strontium
for Calcium in Iron, Copper and Chromium containing glazes in no way
alters the environment of the transition metal ions.

MOSSBAUER   GLAZES   IRON   ESR

The work described in this thesis was carried out between 1975 and 1978 at the University of Aston in Birmingham. It has been carried out independently and has not been submitted for any other degree.

Peter A. Gillespie

ACKNOWLEDGEMENTS

LIST OF CONTENTS

CHAPTER FOUR

AN INVESTIGATION OF THE ROLE PLAYED BY TRANSITION METAL IONS
IN CERAMIC GLAZES

CHAPTER ONE

A GENERAL INTRODUCTION TO THE CHEMISTRY OF

TRANSITION METAL IONS IN CERAMIC GLAZES

1.1   THE HISTORY OF CERAMICS[1]

The exact date of the earliest man-made ceramic articles is not known with any certainty. Crude clay-ware has, in recent years, been unearthed in Northern Europe, North and South America and Mesopotamia which can be dated back to about 5000 BC. This indicates that ceramic technology probably developed independently in various parts of the world from about this time. The development of ceramics from crudely shaped to beautifully engineered articles can be sketchily traced in many different cultures.

Egyptian pottery can be found in old tombs and temples which have been ascribed to the Memphite period (5000 - 3000 BC). These articles are generally crude in shape but well polished so that they in fact appear to be glazed. The earliest example of glazing was found on Egyptian decorative tiles from about 3500 BC which consist of a sandy body covered in a blue copper glaze. Tableaux found on the walls of Egyptian tombs have given detailed information on the methods used in the production of ceramic articles in the Theban period (3000 - 1700 BC). By the end of this period, glazed earthenware had been developed as many examples of this type of ware have been found in pyramids and temples.

Ceramic technology followed similar lines in Babylon and Assyria with enamelling being used to add different colours. Persian pottery

succeeded this by the addition of metal oxides to an alkaline base to give coloured glazes. Greek pottery workers, on the other hand, did not continue along these conventional lines, but concentrated more on delicacy of shape, preferring to cover their articles in a thin transparent gloss. The ancient Romans also did some work of this nature, but they are largely remembered for their bricks and tiles, some Roman buildings being preserved to this day, many with their original vitrified stoneware pipes and baths. Although the Romans introduced their ceramic ware throughout Europe, the style always remained independent of individual location but was characteristically Roman. Two distinctive types of Roman pottery have been classified, Samian ware which is red and the less common black Etruscan ware. The progress of ceramic art in Europe was severely retarded for several centuries on the decline of the Roman Empire.

On the other side of the world, the development of pottery ran along completely independent lines. The first records of bricks and tiles being made in China relate to the period of the Emperor Wu (140 - 88 BC), although historians claim that the first articles were produced in about 2500 BC. These articles were extremely crude and the better known fine Chinese pottery probably does not date back further than 200 BC.

Chinese pottery is generally described by association with the various dynasties of Emperors. The Han Dynasty (206 BC - 220 AD) is associated with a stoneware type article having either a blue or a brown glaze. The Sui Dynasty (581 - 617 AD) saw the development of the first translucent porcelains and also the use of kaolin to produce

opaque chinaware. This period is also the one associated with the development of Celadon green glazes. The Tang Dynasty (618 - 906 AD) saw the use of higher firing temperatures to improve the quality of the porcelain, which led to great advances in the production of procelain and stoneware sculptures. This was followed by the Sung Dynasty (960 - 1280 AD) which produced a greater variety of glazes and colourings and was the period when export of ware to Europe first began. The Ming Dynasty° (1368 - 1643 AD) is often thought to be the one which produced some of the most technically perfect colours and decorations and it was followed by the more recent Manchu Dynasty (1643 - 1912 AD) which saw an increase in the standard of pottery ware to the extent that some of these glazes have a quality which is difficult to reproduce in Europe today.

After the withdrawal of the Romans from most of Europe, only the crudest earthenware was produced until the Moorish invasion of Spain. They introduced ware with a porous body covered in a white opaque glaze of high lustre, which was at first reproduced in Majorca and was therefore called Majolica. This was copied throughout Europe, especially in Italy, where a characteristic style emerged known as faience. The French were also able to exploit this kind of ware in the seventeenth and eighteenth centuries as many local clays were found that produced high quality porous pottery. The French tended to apply a tin glaze, which gave a white matt finish. The popularity of faience declined when the Germans developed European porcelain after discovering their own sources of kaolin. They followed Chinese production methods closely and thereby established their own porcelain industry.

British pottery, on the other hand, was relatively slow to develop and was rather crude by comparison with European pottery even as late as the seventeenth century. Slip ware was first manufactured about this time in Staffordshire by the Toft brothers. Around 1690, the Elers brothers used washed Staffordshire clays for the production of dense ware but it was not until well into the eighteenth century that china clay was used to give whiter earthenware bodies. This was something of a turning point as the development of English chinaware progressed at an extremely fast rate until the beginning of the nineteenth century when the production of bone china made it world famous. In the present century, the trend has been in Britain towards greater mechanisation in order to produce a more reproducible ware rather than towards the development of new materials or bodies.

1.2   PRESENT DAY TECHNOLOGY[2]

The manufacture of ceramics can be conveniently described by two distinct stages. The preparation and firing of the body followed by the application and firing of the glaze. The composition of a ceramic article usually depends upon the raw materials available to the artist and hence is very much dependent on location, pottery centres having grown up around abundant clay sites. The commonest types of bodies consist of mixtures of kaolinite, quartz and various feldspathic or micaceous materials, which are ground together and mixed with water to form a slip. The body is then shaped either by hand or by machine, depending on whether it is being produced by craft pottery or tech-

nologist, and then fired over a period of hours. The firing cycle is designed to take the body through certain critical temperatures at an extremely slow rate so as to not damage the article.

The first stage of the firing, up to about 110 ^{o}C, serves to dry the article. Heating too fast through this temperature range will deform or pit the ceramic. Similar care has to be taken when chemically bound water is released at about 550 ^{o}C and also when passing through the various phase transition temperatures of quartz which are accompanied by changes in volume. The maximum temperature of this firing, called the biscuit firing, depends upon the composition of the body and on the degree of sintering that is required. Sintering of a single component is the process whereby particles which are in contact combine on the application of heat in order to decrease their surface area and thereby increase their density. This is complicated in ceramic bodies by the presence of alkali fluxes which become molten at relatively low temperatures and tend to dissolve the more refractory components to a degree which is highly dependent on temperature. If a body of maximum density is produced by heating to relatively high temperatures, then the body is said to be totally vitrified. This is by no means always the case as many ceramic articles, particularly earthenware, are porous and have not therefore been fired to a high enough temperature to allow total vitrification to occur.

Until this century, clay bodies were fired in large kilns or bottle ovens heated by solid fuels such as wood or coal. The ware was first of all placed in refractory containers known as saggers to avoid contact between the articles whilst allowing them to be

stacked together to a considerable height. The saggers also served
to protect the ware from flying ash and from direct scorching by
flames. Solid fuels are now generally not used by the technologist
and only used by some craft potters in order to reproduce certain
effects, such as reduction, which can be difficult to achieve by
other means.

Gaseous fuels are now used extensively throughout Europe. In
France and Holland, natural gas is very cheap so is used to a large
extent while town gas is used a great deal in Britain. This has the
disadvantage that it may contain traces of sulphur which is particularly
harmful to pottery, leaving black scorch marks. Kerosene, butane and
propane fuel sources are most consistent in composition as is North
Sea gas which is now tending to replace town gas in Britain. Electric
kilns have the advantage of giving a more controlled heat but the
silicon carbide elements are very expensive. Also some of the unusual effects
created by firing are due to the atmospheres generated by the various
fuels so that reproduction of certain finishes is sometimes difficult
using an electric kiln.

After the biscuit firing, the article is glazed. This is the
process of applying a thin layer of glass to the article to give it
greater mechanical strength and to improve its aesthetic appeal. The
glaze is applied as a slip and can be sprayed, painted or dipped onto
the fired body. The body is then fired again, carefully as before
in order to avoid damage, to the temperature at which glass formation
occurs. The temperature of the glost firing, as this second firing
is called, depends upon the sort of finishing that is required.

Generally, low temperature glazes, high in alkali metal oxide concentration, are more brilliant than high temperature glazes which contain a greater proportion of more refractory materials such as silica or alumina.

Also it is important that the glaze is under compression in the finished article to give greater overall strength. If the expansion of the glaze were greater than that of the body on heating, then the glaze would contract to a greater extent on cooling, putting it under tension and hence creating small cracks known as 'crazing'. The coefficient of thermal expansion of glazes for a given temperature range is largely independent of composition whereas the coefficient of the body is more easily varied by change in composition. Therefore in order to correctly match a body and glaze, the body composition is often modified so that it is fair to say that the body composition is governed to a large extent by the glaze.

1.3   STRUCTURE OF SILICATES

Silicate materials have extremely complex, often polymeric, structures which are sometimes difficult to characterise and describe. Silicates are based on the silicon oxygen tetrahedron consisting of one silicon atom surrounded by four oxygen atoms at a distance of 1.62 Å. The bonds are quite polar although there is an element of $d\pi$ - $p\pi$ bonding which diminishes the availability of the d electronic

orbitals to nucleophilic attack giving greater stability, particularly to the more polymeric species. This is illustrated in figure 1.

The simplest silicate species of this type is known as zircon, $ZrSiO_4$, where Zirconium has a co-ordination number of eight. Substitution of Zirconium ions by either Mg^{2+} or Fe^{2+} gives another simple silicate, olivine, where the metal ions are now six co-ordinated.

Silicon-Oxygen Tetrahedron   dπ - pπ bonding
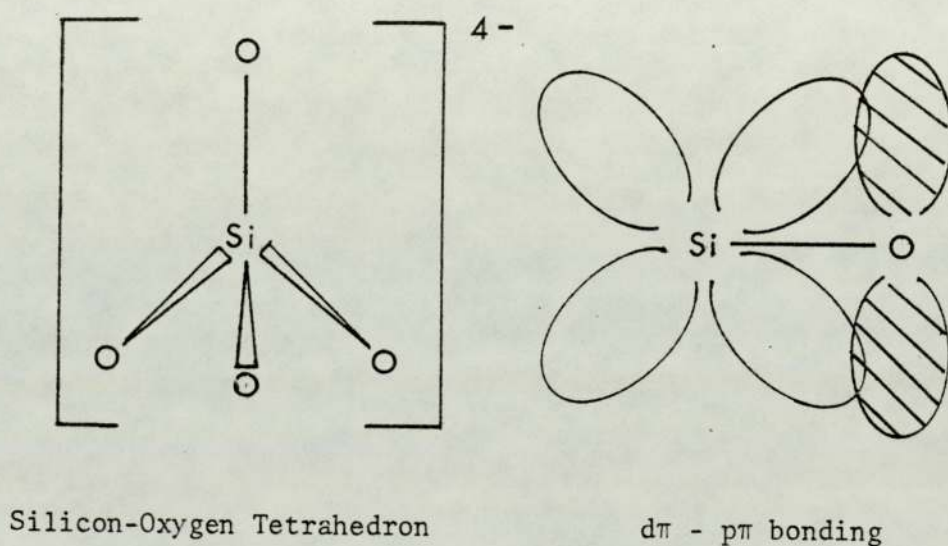
FIGURE 1

If two orthosilicate tetrahedra are linked together by the sharing of one oxygen atom by two silicon atoms, then the rare pyrosilicate anion is formed, figure 2.

The pyrosilicate ion
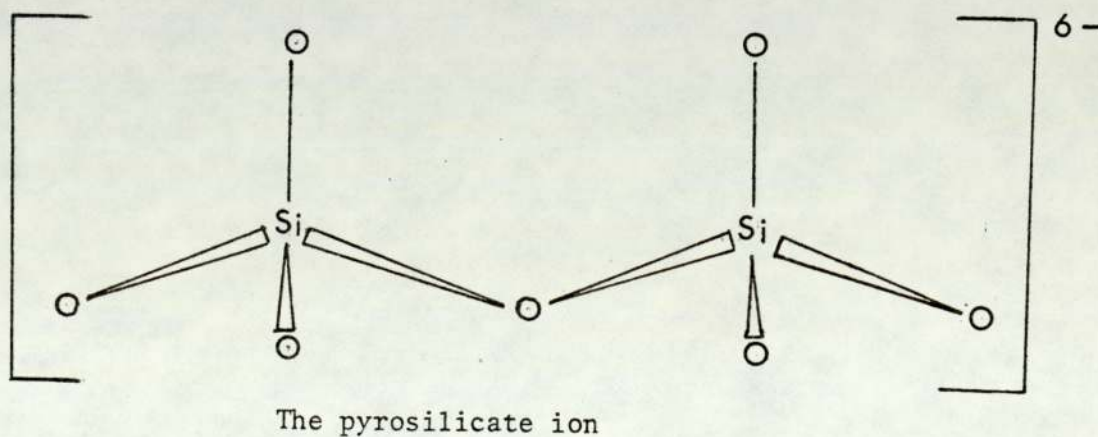
FIGURE 2

This ion is only produced at high temperatures and is often found in the slag in furnaces. If a number of silicon-oxygen tetrahedra are linked together in a linear chain, a group of silicates known as pyroxenes are formed with the general formula $(SiO_3^{2-})_n$. These chains are held together by charge balancing cations which sit between them and interact ionically to give strongly bound structures.

The silicate tetrahedra can also link together to form rings which are held together by cations as in previous examples. Beryl consists of rings made up from six tetrahedra which are bound together by Be^{2+} and Al^{3+} cations. The natural red colour of this mineral is due to Cr^{3+} impurities. This fact serves to illustrate that these silicate structures are in fact ideal structures and that they rarely occur in nature without a certain amount of impurity.

Silicon-oxygen rings containing six silicon atoms can fuse together to form a series of polymeric structures known as amphiboles, with the general formula $(Si_4O_{11}^{6-})_n$. These are ladder chains and they are important in another sense for Al^{3+} cations often substitute for silicon in four co-ordinate positions. So aluminium can have two roles, one as a charge balancing cation, usually six co-ordinated and situated between chains or rings, and another in a substitution role in place of silicon. Other more complex ring structures can occur, some with a mixture of rings containing four silicon atoms with rings containing six silicon atoms. Potash Feldspar, $KAlSi_3O_8$, has a ring structure in which the substitution of silicon by aluminium is quite advanced and it forms an extremely rigid three-dimensional ring structure which does not begin to melt until above 1100 ^{o}C.

The structure of potash feldspar is illustrated in figure 3. Potassium cations and oxygen anions have a charge balancing role and they usually fit into interstices in the ring network. Water can play an important role in silicate structures as is shown in the idealised structure of Kaolinite, figure 4.

Potash Feldspar
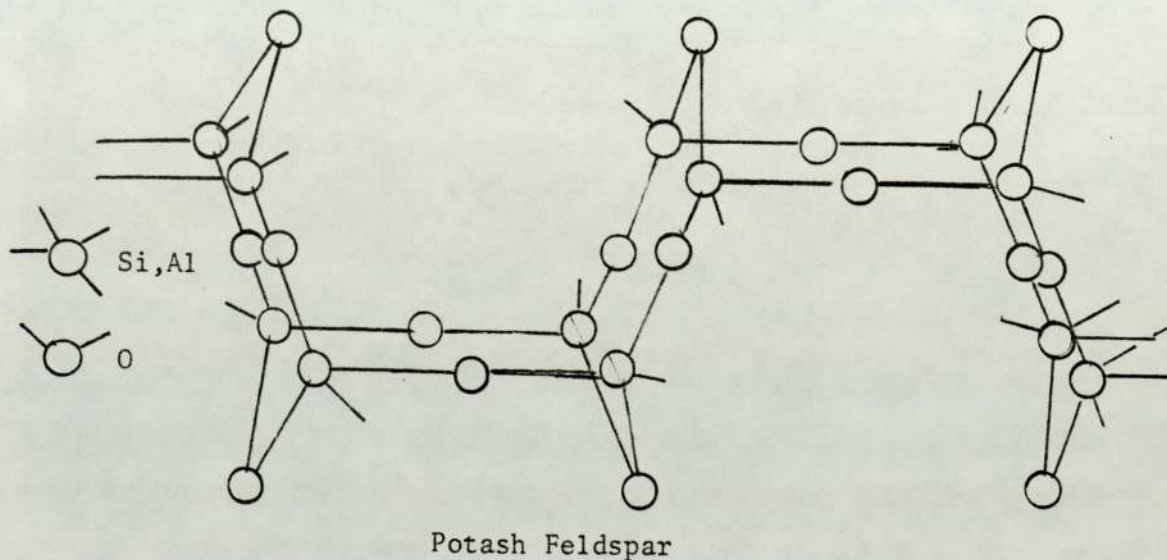
FIGURE 3

In fact substitution of Silicon by Aluminium occurs to various degrees depending upon the location of the Kaolinite find.

(a) hydroxyl layer

(b) aluminium layer

(c) condensed oxygen hydroxyl layer

(d) silicon layer

(e) oxygen layer
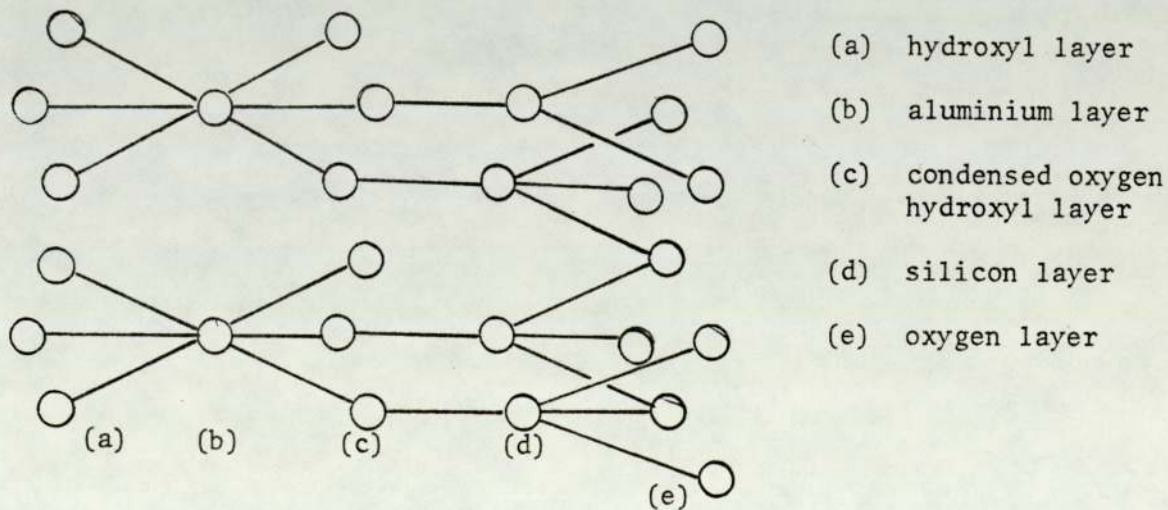
Kaolinite

FIGURE 4

This structure can be considered to be a condensation between Gibbsite, $Al(OH)_3$ and SiO_2. Silica itself has a number of crystallographic forms as shown in figure 5.

$$\alpha \text{ Quartz} \xrightarrow{\ 870\ ^{o}C\ } \alpha \text{ Tridymite} \xrightarrow{\ 1470\ ^{o}C\ } \alpha \text{ Cristobalite}$$

$$\updownarrow \quad 573\ ^{o}C \qquad \updownarrow \quad 120\text{-}160\ ^{o}C \qquad \updownarrow \quad 200\text{-}280\ ^{o}C$$

$$\beta \text{ Quartz} \qquad\qquad \beta \text{ Tridymite} \qquad\qquad \beta \text{ Cristobalite}$$
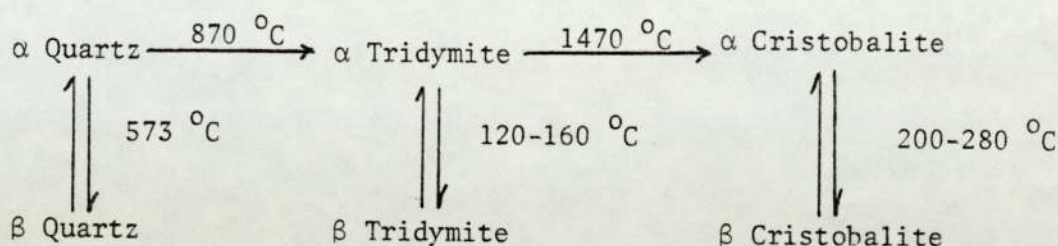
FIGURE 5

Quartz is a helical arrangement of silicon oxygen tetrahedra and is the only stable form at room temperature. Tridymite consists of a ring network of silicon oxygen tetrahedra which is stable between 870 ^{o}C and 1470 ^{o}C, whilst Cristobalite is stable above 1470 ^{o}C and is isomorphous with Diamond. These physical changes require the breaking of bonds to occur so that the transformation between the three forms is quite slow. On the other hand, each of these has an α and a β form. The transition between α and β requires only a change in unit cell dimensions and involves no breaking of bonds and is therefore rapid and readily reversible.

1.4   THE STRUCTURE OF GLAZES

During the last fifty years, a number of theories of glass formation and structure have been postulated, the most relevant to the study of ceramic glazes being the crystallite theory and the random network

theory. The crystallite theory suggests that when glass fusions are cooling, crystallites or small crystals are formed which then make up the main body of the glass. These crystals need only be very small in size and they only need to merge slowly into their amorphous surroundings so that only a limited short range order exists.

The random network theory of Zachariason and Warren[3] has been the subject of much serious criticism but it does provide the practical ceramicist with a good working model. The theory is based upon the fact that the main building unit in silicates is the silicon-oxygen tetrahedron, many of which can be arranged in a three dimensional repeating pattern forming a network by sharing of some of the oxygen corner atoms.

Glazes and glasses also contain other metallic cations which according to this theory take up various positions in the interstices of the silicate network. The silicon-oxygen tetrahedron is known as a network former while the species from which the cations are derived are known as network modifiers. Zachariason set out a number of conditions which must be fulfilled for any oxide to exist in the vitreous or 'glassy' state.

(1) The free energy of the vitreous oxide should not be much higher than that of the crystalline oxide.

(2) The oxygen atoms in the network cannot be shared by more than two atoms of silicon or metal.

(3) The co-ordination number of the cations should be low.

(4) The polyhedra may have common angles but not common faces or edges.

The following oxides all exist independently in the vitreous state as well as in mixtures with other oxides.

$$B_2O_3 \qquad P_2O_3 \qquad Al_2O_3 \qquad Sb_2O_3$$

$$SiO_2 \qquad GeO_2 \qquad P_2O_5 \qquad As_2O_3$$

$$SbO_5$$
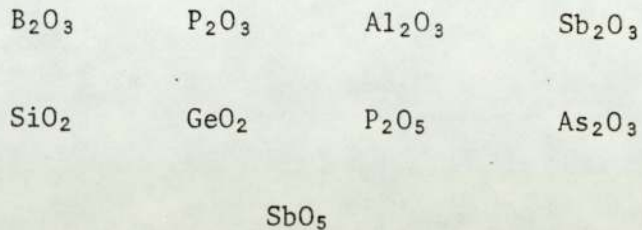
The random network theory outlined above provides a good working model for glaze technologists but the most recent ideas indicate that this approach has to be modified for results indicate that glass cannot be assumed to be a simple supercooled liquid since external conditions when altered during the firing process have been found to induce changes in structure.

Shteinberg[4], whilst concentrating most of her work on strontium, challenges the basic concept that bivalent cations are modifiers but suggests that they are in fact the chief building unit as previously suggested by Belov[5], working with X ray diffraction. The strong silicate structure is considered to adapt itself to the cation size rather than the cation merely filling suitable sites in a rigid lattice. The small cations though are still considered to be modifiers, as in the Zachariason model, although Shteinberg has shown that when a mixture of large and small cations are involved, the small cations can significantly alter the physical properties of the glaze, an effect which is more noticeable at certain cation radius ratios. She suggests that perhaps the structure is affected not so much by the ratio of the radii of the cations as by the ratio of the strength of their bonds with oxygen. Although Shteinberg's work involved the use

of Strontium primarily for aesthetic reasons after the movement away from lead containing glazes, she claims to have proved the theory of Belov that divalent cations have a major effect on the structure of silicate glasses.

1.5 THE ROLE OF RAW MATERIALS

Many raw materials are used in the preparation of ceramic glazes and with the recent trend towards the use of industrial waste products much research is being carried out to find applications for abundant materials especially those that have no other industrial value. There is no universal method of classification of glaze formulae, the particular method used in a particular case depending upon the point of view of the worker, whether he be glass technologist, craft potter or chemist.

One customary method is to classify glaze materials into acidic, basic and amphoteric oxides, the molar sum of each group being expressed as an integer, as follows for potash feldspar.

$$K_2O \qquad Al_2O_3 \qquad 6\ SiO_2$$

| basic | amphoteric | acidic |

Or for a low temperature lead glaze:

$$0.7\ PbO \qquad 0.4\ Al_2O_3 \qquad 2.0\ SiO_2$$
$$0.1\ MgO \qquad 0.6\ B_2O_3$$
$$0.2\ CaO$$

The acidic oxides such as silica are described as glaze network formers whilst the basic oxides such as calcium oxide, magnesium oxide, etc., are described at glaze network modifiers so that the system, although empirical, falls into line with the random network theory.

Another method of representing glaze recipes is by the so called Seger formula. This is of great practical importance although again it contains no structural information. Its value lies in the fact that it does not show the composition of the fired glaze but shows the composition of the materials in the unfired recipe. This is of considerable use to the craft potter and is also a sound platform for the chemist who may then wish to proceed to describe the chemical changes that occur during the firing process.

It is perhaps important at this stage to emphasise the fact that the method of introduction of various species affects the properties of the glaze[6]. It is quite possible for two glazes to have the same molecular formula but different physical properties purely because the constituent elements were introduced through the addition of different chemical species.

The most common method of introduction of a large number of elements into glazes is by using abundant silicate materials such as potash feldspar, kaolinite, montmorillonite, etc.. Other components are added as required to give the glaze its desired properties. The silica content can be increased by the addition or either quartz or flint while the aluminium content can be

increased by the addition of alumina, Al_2O_3. Group I and II metal oxides are used to act as network modifiers to produce low temperature fusing mixtures by combination with various silica and alumina based formers. The modifiers are not necessarily added as the oxides, but often in the carbonate or nitrate form, thermal decomposition of the anion occurring to yield an oxygen anion and liberating gaseous products.

Borates are important glaze constituents for they fuse with silica at comparatively low temperatures, therefore alkali borates are often used for earthenware glazes as a convenient way of intro-ducing group one metals into a low firing temperature glaze. Alkaline earth metals are introduced to improve hardness, chemical resistance and strength. Glazes with high calcium or magnesium contents are highly refractory and care must be taken to avoid crystallization on cooling. Strontium can be used to form brilliant glazes with excellent ceramic properties. According to Shteinberg[4], these are as good as lead glazes having a similar finish as well as excellent chemical resistance. The colour and aesthetic properties of glazes are governed largely by the addition of transition metal ions and by firing under different conditions and with different metal concen-trations, as illustrated in figure 6.

Lead has been used as a raw material in the oxide form to produce a full range of high quality glazes, but its use has been restricted in many countries by government legislation in order to minimise the associated toxic effects. It is felt by many craft potters that iron could be a possible substitute for lead, although by comparison many

Cr^{III} ⟶ green

Fe^{II} ⟶ blue

Fe^{III} ⟶ green - brown - amber

            —increase in conc.⟶

Co^{II} ⟶ blue

Cu^{I} ⟶ red

Cu^{II} ⟶ blue ——— green

        —increase in conc.⟶
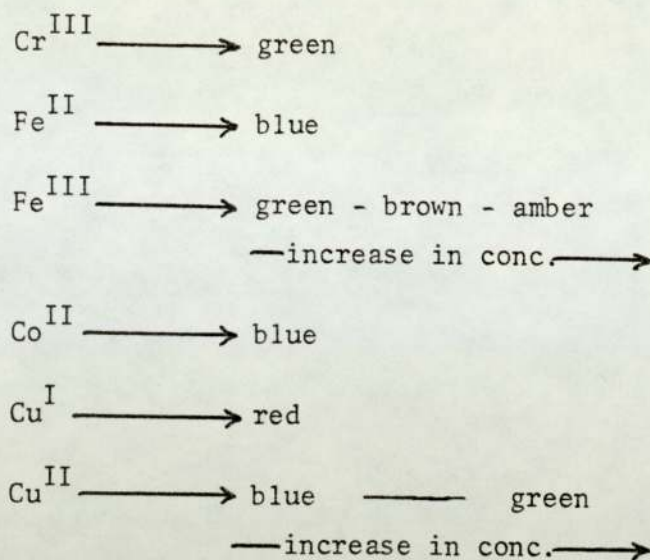
Colour of some transition metal ions in glazes

FIGURE 6

iron glazes lack aesthetic appeal, particularly those produced under oxidizing conditions.

1.6   THE PRESENT PROBLEM

Considerable difficulty has been experienced in the past whilst investigating the structure of silicate species. X ray diffraction can give some information on the general structure of silicate lattices although this technique is quite insensitive to small impurities and is of no value when amorphous phases are encountered. Infra-red spectroscopy has been employed also but difficulties in interpretation occur due to the insensitivity of this technique to

either impurities or slight structural modifications. Any technique used in this form of research has to be non-destructive in order to obtain any valuable information. Considering the problem related to the movement away from lead glazes, as described in the previous section, towards the possible use of iron substitutes, it is felt ^{57}Fe Mössbauer spectroscopy lends itself very much towards this sort of research.

Mössbauer spectroscopy[7] is the resonant non-recoil emission and subsequent re-absorption of a gamma ray by the nucleus. This technique has to be performed in the solid state, is extremely sensitive to oxidation state and can give detailed information about the environment and symmetry of the nucleus. Naturally abundant iron contains 2.2% ^{57}Fe so that one possible disadvantage of this technique is that it requires large amounts of iron in order to obtain a spectrum. This problem can be surmounted either by isotopic enrichment or by low temperature measurement which increases the recoil free fraction and facilitates easier measurement over a shorter period of time. The purpose of the present work is to use this technique to elucidate certain problems in the pottery industry in conjunction with a number of other spectroscopic techniques such as X ray diffraction and visible and electron spin resonance spectroscopy.

The research project is part technological in objective. The craft potter in the past has often obtained high quality iron glazes by firing iron (III) under reducing conditions and then trapping the iron (II) formed on reduction in a glass. Reduction is usually effected by the use of reducing fuels or by the addition at high kiln temperatures of organic compounds such as naphthalene. Reduction to the iron (II) state

gives more desirable aesthetic effects as in Chinese stoneware and procelain which are noted for their soft colours and greater variety of finishes.

One of the major objectives of this work is to establish if reduction is absolutely necessary to produce the desired effects. Reduction is often expensive, can be hazardous to health as well as possibly being unreliable as reproduction can be difficult unless the same firing conditions are repeated exactly. The possibility of using an inert atmosphere and introducing iron in the divalent form is investigated in this work to establish whether oxidation can be prevented, thereby trapping Fe (II) in a glaze environment.

Also it has been found by experimental study of the visible spectra of the large number of complexes containing various metal ions and various ligands, that generally speaking ligands can be arranged in a series according to their capacity to cause d orbital splittings in octahedral complexes[8]. This series is known as the spectrochemical series and for the more common ligands the order of increasing d level splittings is $I^- < Br^- < Cl^- < OH^- < NCS^- <$ pyridine $\simeq NH_3 <$ bipyridyl $<$ 1-10 phenanthroline $< NO_2^- < CN^-$. Visible spectra of transition metal containing glasses have been extensively studied[9] and the spectra obtained have indicated that the transition metal ion is invariably under the influence of relatively weak crystal fields. In view of this, the use of Mössbauer spectroscopy in the study of Fe (II) and Fe (III) in weak field environments is initially studied.

Another major objective of this work is to determine the chemical changes affecting the transition metal environments in

ceramic glazes using Mössbauer spectroscopy in conjunction with other
spectroscopic techniques. The work concentrates mainly on iron and
copper and attempts to reproduce ceramic glaze finishes under more
scientifically controlled conditions than those used by the craft
potter. The Mössbauer results are compared with results for similar
systems including spectral results for a selection of Chinese glazes
as reported by Hedges[10]. Other spectroscopic results particularly
for the strontium containing glazes are reviewed in terms of
Shteinberg's theory of glass structure. Electron spin resonance
studies are employed mainly to elucidate the structure and symmetry
of copper (II) in copper containing glazes whilst visible spectroscopy
is used in the study of some chromium containing glazes. Throughout
the course of this work, X ray diffraction is used in order to
identify various species that are formed at different stages of the
firing process.

1.7 THE USEFULNESS OF VARIOUS TECHNIQUES IN SOLVING THE PRESENT PROBLEM

1.7.1 Mössbauer Spectroscopy

Mössbauer spectroscopy is the non-recoil resonant absorption of
a gamma ray by the nucleus. The position of the absorption peak is
described by δ, the isomer shift parameter, which is measured with
reference to a standard absorber such as iron metal. The actual
value of the energy of the quantized nuclear states depends upon a
contact term which describes the interaction between the nucleus and

the electronic environment of the atom or ion. Only the s electrons have a probability of being present inside the nucleus so that the isomer shift is a direct comparison of different s electron densities. This parameter is sensitive to shielding of the s electrons by d or p electrons so that for iron it is possible to differentiate between different oxidation states. Figure 7 shows the energy level diagram for the ground and excited nuclear states before and after interaction with the electronic environment.

$I = 3/2$

14·4 keV

$\simeq 10^{-4}$ eV

$I = 1/2$

Bare Nucleus

Electrostatic Energy Shift

$\simeq 10^{-4}$ eV
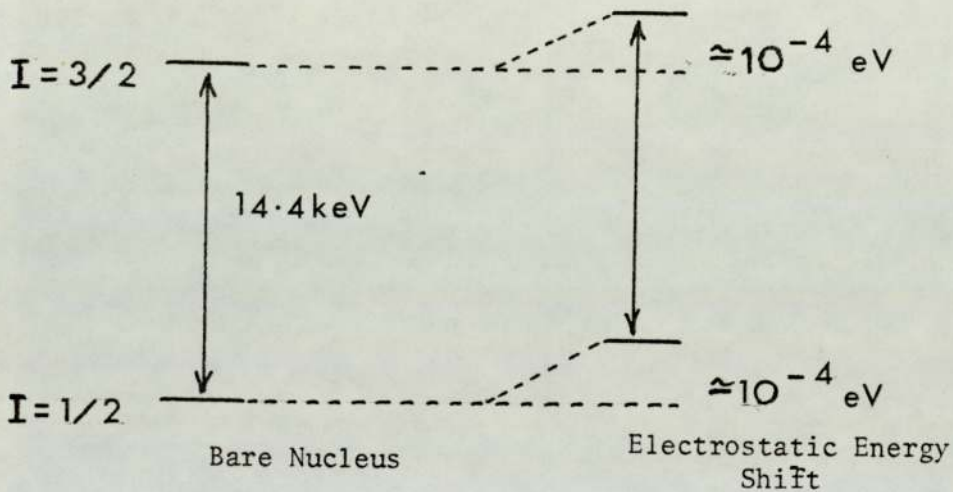
FIGURE 7

The quadrupole splitting, Δ, arises from the interaction of a quadrupole nucleus with an electric field gradient. The ground state nucleus ($I = \frac{1}{2}$) has no quadrupole moment so is unaffected by the presence of an electric field gradient. However, the excited state ($I = {}^3/_2$) is split into two components so that two peaks are observed as indicated in figure 8.
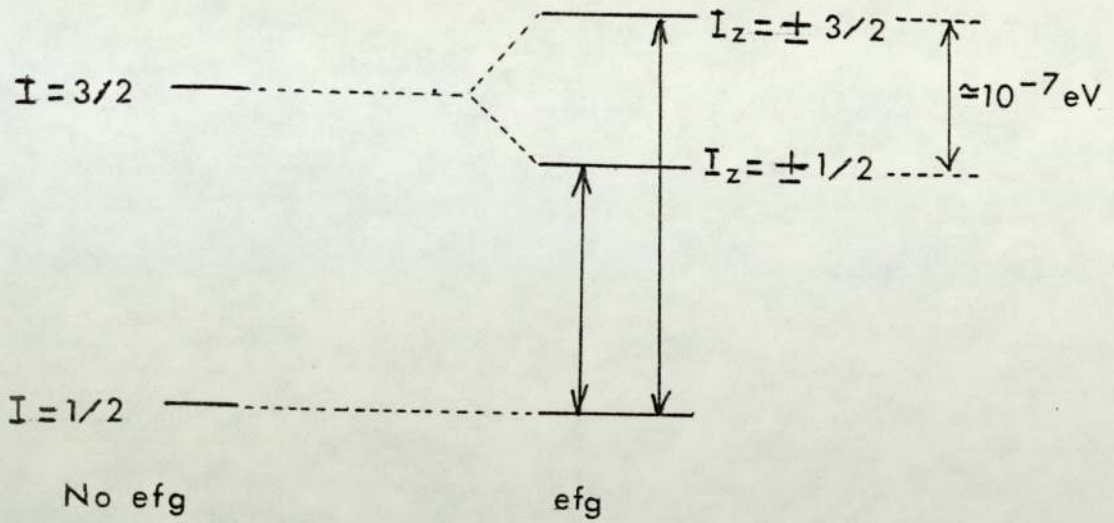
FIGURE 8

Also if a permanent magnetic field is present at the nucleus, then the degeneracy of both ground and excited nuclear states is lifted as indicated in figure 9.
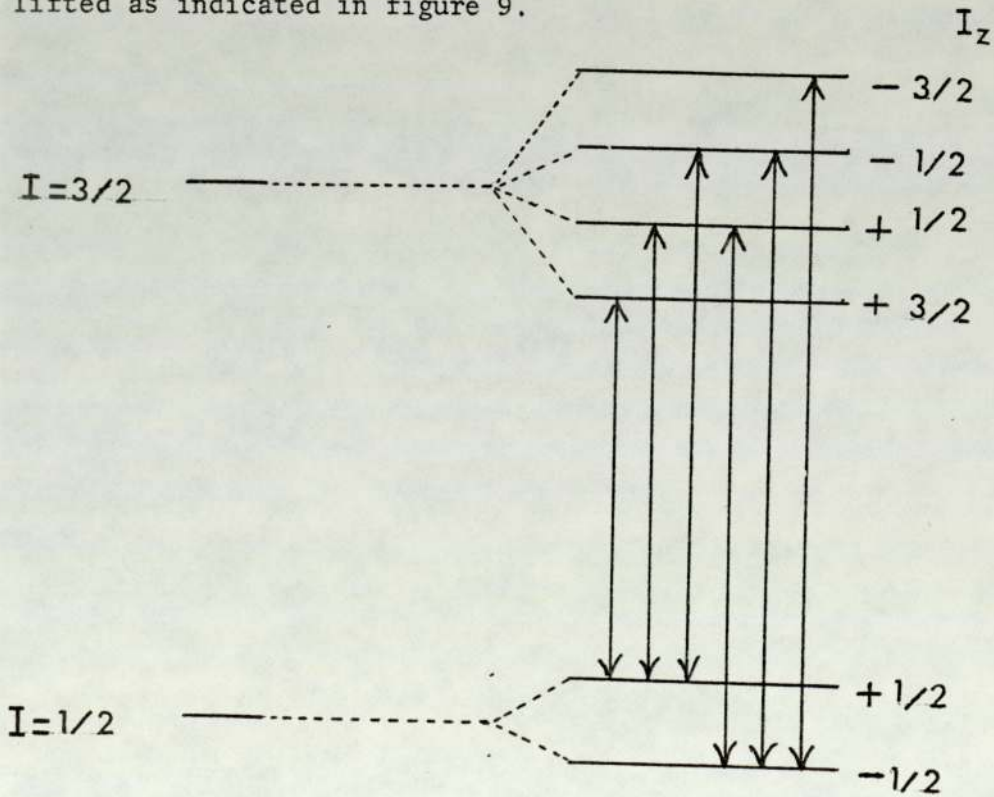
FIGURE 9

The magnetic field may be inherent in the crystal or may be applied during the course of the Mössbauer experiment. The selection rule for M1 radiation states that only transitions for which $\Delta I_z = 0$ or ± 1 are allowed so that in practice a six line magnetic hyperfine spectrum is observed.

In real systems, the Mössbauer spectrum of a single component may be a superimposition of all three interactions described above. Many workers have used Mössbauer spectroscopy to differentiate between different oxides of iron. FeO_{1-x} ($x = .14 \to .10$), Fe_3O_4, bulk α and γ Fe_2O_3 as well as superparamagnetic Fe_2O_3, all give quite characteristic spectra[11]. This has been extensively utilized in the area of mineralogy where iron can be present in any of the above forms as well as being present as a substitute for either Si^{4+} or Al^{3+} ions in the complex silicate structures. A good example of this is the study of the decomposition of kaolinite by [57]Fe Mössbauer spectroscopy although the idealized chemical formula for this mineral contains no iron[12]. Fe^{3+} has been identified in tightly bound sites in an unfired sample. The spectrum changes dramatically after firing to 650 °C when the kaolinite to meta kaolin transformation occurs. The Fe^{3+} ions leave their tightly bound sites and the spectrum obtained after firing to this temperature is due to the presence of many loosely bound Fe^{3+} sites. Changes are also observed after the meta kaolin to spinel transformation at 980 °C and again after the spinel to mullite transformation at 1280 °C although much controversy still exists over the exact structure of the species involved.

Mössbauer spectroscopy has also been used extensively to elucidate problems associated with the nature of iron containing minerals. Bancroft[13] has published centre shift and quadrupole splitting parameter ranges for a large number of compounds and minerals and plotted these against co-ordination number for a variety of oxidation states of iron. This is reproduced in Figure 10. Reference to such data has meant that the structure of a number of iron containing minerals can more clearly be understood. A good example of this is the historical investigation of the structure of tripuhyite, a mixed iron-antimony containing mineral. Hussak[14], as long ago as 1897, determined the chemical formula to be $Fe_2Sb_2O_7$ in which iron is expected to be in the ferrous state whilst antimony is expected to be pentavalent. This formula was confirmed in 1963 by Donnay et al[15] but meanwhile in 1953 Mason et al[16] working both with X-ray diffraction and chemical analysis concluded that the ideal formula of tripuhyite is in fact $FeSbO_4$ so that iron is present totally in the ferric state together with pentavalent antimony. Gakiel et al[17] in 1969 investigated this problem using Mössbauer spectroscopy and found that tripuhyite gives a spectrum with an isomer shift of 0.62 mm s^{-1} with respect to iron metal and a quadrupole splitting of 0.72 mm s^{-1}. These parameters are typical of iron (III) in a site with symmetry less than cubic so that Gakiel concluded that iron is in a trivalent state and that the correct chemical formula is $FeSbO_4$. Another significant result to emerge from Gakiel's work is that although Mössbauer spectroscopy is insensitive to small amounts of impurity (less than 5%), no large amount of substitution of ferric ions by ferrous ions occurs. Such a formulation could be achieved by the presence of antimony in two oxidation states thereby preserving charge balance.

FIGURE 10

Reproduced from Bancroft et al, *Geochim.Cosmochim.Acta.*, 31,2219 (1967).

Isomer Shift

Quadrupole Splitting
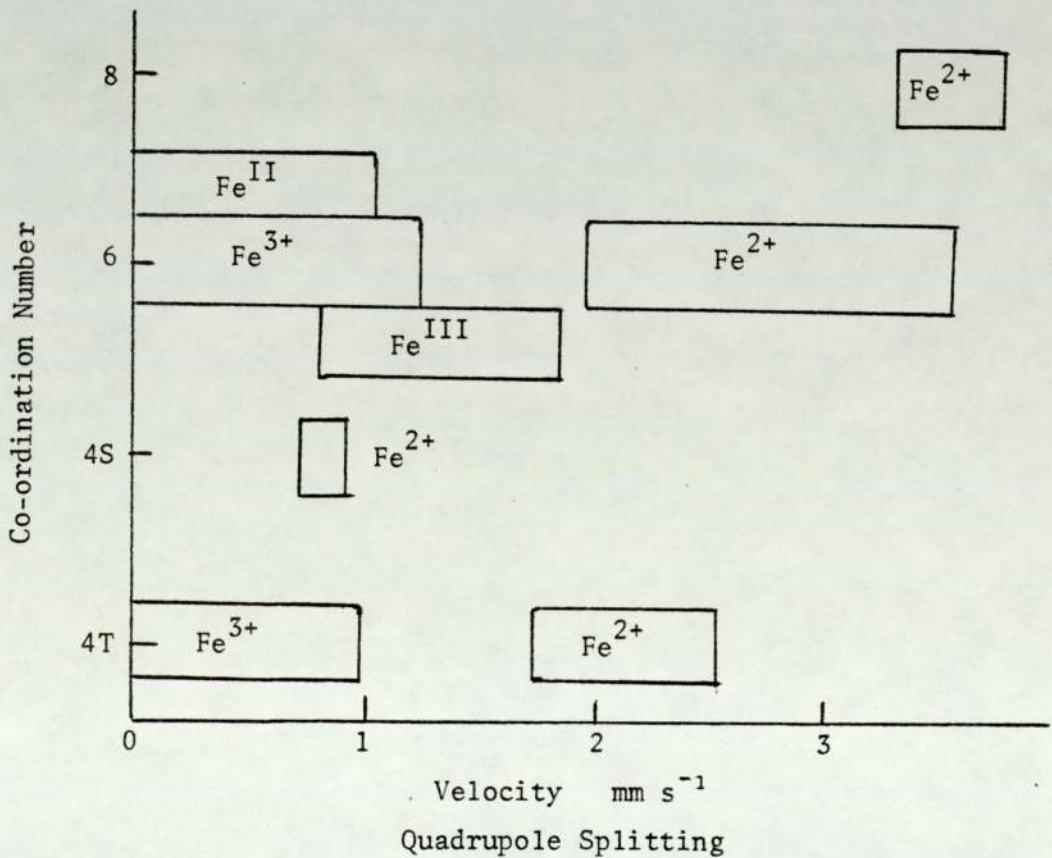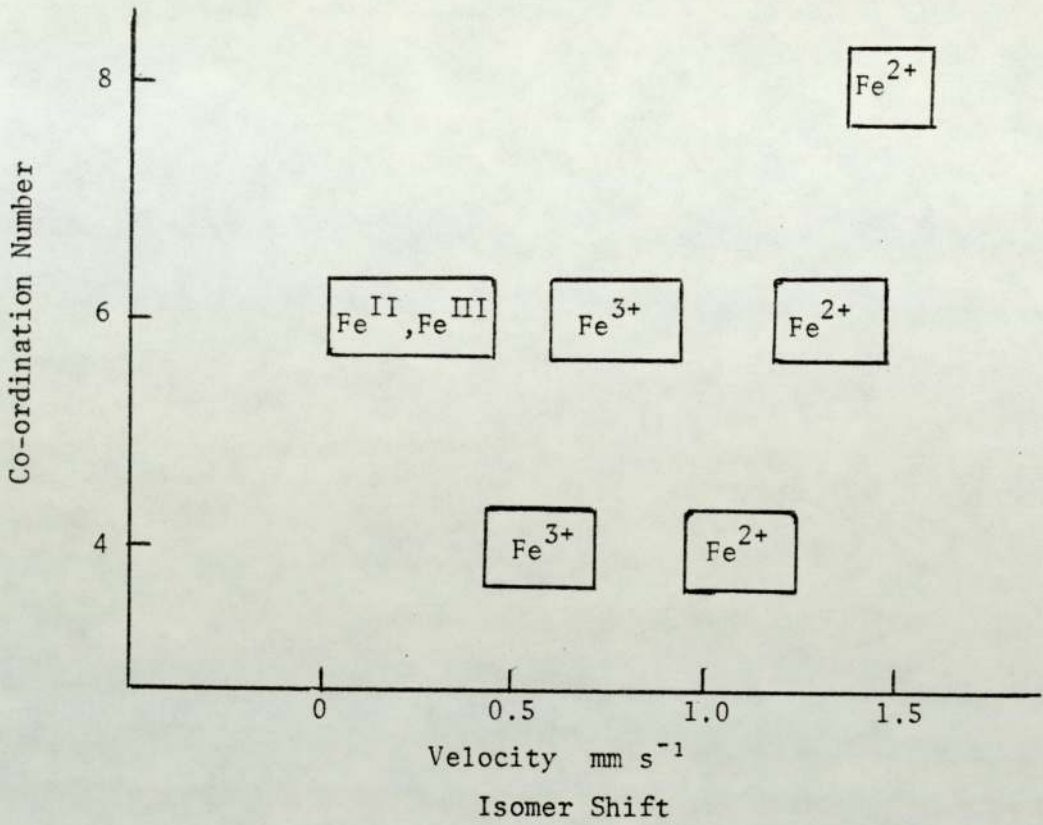
Another example of the application of Mössbauer spectroscopy to minerology is in the study of the mineral neptunite $LiNa_2K$ $(Fe,Mn,Mg)_2 Ti_2O_2(Si_8O_{32})$. This mineral contains titanium in one octahedral site and iron and manganese in another slightly larger octahedral site. Titanium is assigned to the smallest octahedral hole purely on the basis of the fact that it is thought to be present as Ti^{4+} whilst iron is thought to be present as Fe^{2+}, the difference in ionic radii dictating the position of the two ions. However, it could well be the case that iron is present partially as Fe^{3+} with charge balance being achieved by the substitution of Ti^{3+} for Ti^{4+}. The ionic radii of Fe^{3+} and Ti^{4+} are quite similar (0.68 Å and 0.64 Å respectively), so that if such a formulation occurred no longer could titanium be expected to exclusively occupy one type of octahedral site and iron another but a distribution between the two sites is more likely. The Mössbauer spectrum of neptunite resolves this question immediately for Bancroft et al[18] report a single doublet with an isomer shift of 1.42 mm s^{-1} with respect to iron metal and a quadrupole splitting of 2.65 mm s^{-1}. This conclusively proves that the majority of iron is present as Fe^{2+} and therefore titanium is present almost totally at Ti^{4+} so invariably the titanium ions occupy the smaller of the two octahedral sites.

Mössbauer spectroscopy has also been used extensively to monitor solid state reactions, particularly those involved with ferrite formation. Duncan[19] has shown that zinc oxide reacts with iron (III) oxide by a straight forward reaction without the formation of any observable intermediate compounds as follows:

$$ZnO + Fe_2O_3 \longrightarrow ZnFe_2O_4$$

The kinetics of the reaction were studied and the results were compared with those obtained by X-ray diffraction. The two techniques give similar results except in the early stages of the reaction where the agreement is not good. Duncan explains this in terms of the physical differences inherent in the two techniques. Mössbauer spectroscopy is sensitive to the immediate environment of the iron (III) ions and it can therefore record more subtle changes in structure than X-ray diffraction which is sensitive to the inter ionic spacing within the oxygen sublattice.

Similarly, a study of the formation of both $CaFe_2O_4$ and $Ca_2Fe_2O_5$ has been performed [20]. Gallagher and Kurkjian[21] have studied the thermal decomposition of $Fe_2(C_2O_4)_3 6H_2O$, $Ba_3[Fe(C_2O_4)_3]_2 8H_2O$ and $Sr_3[Fe(C_2O_4)_3]_2 2H_2O$ and have followed the change in oxidation state of iron by both isomer shift and quadrupole splitting parameters. On decomposition of the oxalates, the iron (III) is reduced to iron (II). Above 300 °C oxidation of the iron (II) occurs as iron (III) becomes the predominant species. After firing to 700 °C a significant proportion of the iron (III) is further oxidized to iron (IV), although on further increase in firing temperature, the tetravalent species disappears.

Gallagher et al[22] has also shown the presence of iron (IV) during the firing of Barium ferrates in which it is reported that a hexagonal $BaFeO_3-x$ phase with as much as 90% Fe^{4+}, is present with a completely trivalent phase, $Ba_2FeO_2._5$ in which there are an equivalent number of octahedral and tetrahedral sites. Ichida[23] has also followed this system using Mössbauer spectroscopy starting with $BaFeO_4$ in which the

iron is present in the oxidation state VI. Firings were also
performed under different atmospheres as well as under different
oxygen pressures in order to effect varying degrees of reduction.

Mössbauer spectroscopy has also been used extensively in
archaeology to solve problems related to manufacturing techniques
and the dating of ceramic finds. Such information is invaluable in
assessing the technological skill and development of ancient cultures
and can also be used to determine migration patterns of different
races. The high iron content of many ancient pottery samples means
that data can be conveniently accumulated, although the fact that
the results pertain to only one element can be sometimes considered
to be a serious disadvantage when assessing the value of this technique
in comparison with other methods of analysis. One of the first
investigations of this type was undertaken by Cousins et al[24] who
fired a number of clays local to the Cheam area of Surrey and attempted
to review the Mössbauer results in such a way as to both date articles
and describe the kiln firing conditions used in their manufacture.
A uniformly coloured sandy clay was found to give Mössbauer parameters
typical of light coloured sandy bodies found in this area dating back
to mediaeval times. A sample of fired clay from this area gave
Mössbauer parameters which vary regularly with firing temperature so
that an estimate of body firing temperature of ceramic finds was
possible. This effect was particularly noticeable in the variation
of the quadruple splitting parameter. These workers also report the
Mössbauer parameters for a body with a red surface and a black interior.
Results show that the surface colour can always be found whenever
either Fe_2O_3 or Fe_3O_4 is present whereas the internal colour is due

to the predominance of Fe(II) which accounts for 63% of the total iron weight. The almost total oxidation of the surface iron compared to the interior iron is considered to be good evidence for the fact that the firing was performed under oxidizing conditions.

Kostikas et al[25] have examined samples of Mycenean and Minoan pottery and have shown that the quadrupole splitting parameters as well as the total absorption areas can be used to differentiate between the two series. The Mössbauer spectra were measured at a number of different temperatures and a dramatic increase in the ratio of magnetic to total oxides was observed in going from 4.2 °K to 1.4 °K, suggesting that disintegration of the oxide particles has occurred. Comparison of results for pottery samples of different ages indicates that this disintegration is a function of time so that Mössbauer spectroscopy can be used to date pottery finds.

Further work on the determination of firing temperatures by comparison of the quadrupole splitting parameters with those of local clays fired to various temperatures has been performed by Janot et al[26]. These workers studied samples of French pottery from between the tenth and fifteenth centuries and found results similar to those of Cousins et al described above.

The value of Mössbauer spectroscopy in the elucidation of problems where other techniques prove insensitive has been clearly demonstrated by Bouchez et al[27] whilst investigating two types of pottery found in Iranian Turkistan dating from around 3000 BC. The two types of pottery one red and one grey, were found to co-exist in this area about this

time. Archaeologists were particularly curious to find out whether
the appearance of the grey ware was due to migration of people from
other areas or whether it was due to the independent development of
local pottery technology. Mössbauer spectroscopy indicates that the
red and grey ware are different in respect to the ratio of Fe^{III} to
Fe^{II} indicating that one type was fired under reducing conditions
(grey) whilst the other was fired under predominantly oxidizing
conditions. Local soils were fired to various temperatures under
different atmospheres and the Mössbauer results indicate that it was
solely the difference in firing conditions that gave the two types
of pottery ware.

1.7.2 Electron Spin Resonance Spectroscopy

Electron spin resonance[28] can be observed when molecules or ions
containing one or more unpaired electrons are placed in a magnetic
field. In a molecule containing a single unpaired electron in an
S state (i.e. L=0) the applied magnetic field lifts the spin degeneracy
so that the two electronic spin states, $s = +\frac{1}{2}$ and $s = -\frac{1}{2}$, have
different energies. The energy difference is equal to gBH where g
is the gyromagnetic ratio, B is the Bohr magneton and H is the
strength of the magnetic field. For the simple case of an S state as
outlined above, g = 2.0023 as shown in Figure 11.

$s = +\frac{1}{2}$

$s = \pm\frac{1}{2}$

$h\nu = gBH$

$s = -\frac{1}{2}$

zero magnetic field

——increasing field——>
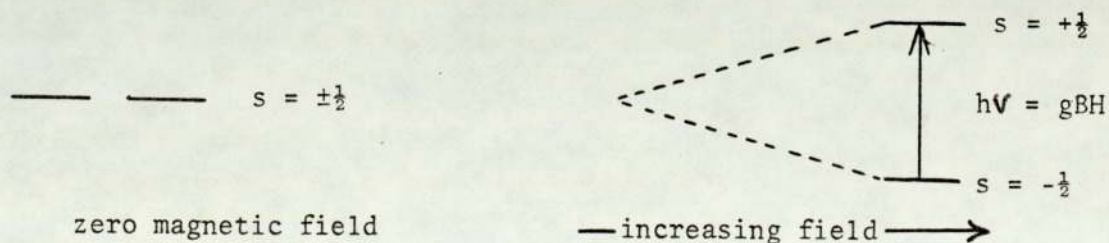
FIGURE 11

The lower energy state is slightly more populated than the upper state at thermal equilibrium so that when radiation of frequency ν is applied, a net absorption occurs as upward absorptive transitions are more numerous than radiative downward transitions. By sweeping the frequency of a microwave oscillator, a frequency of maximum absorption can be obtained. In practice though the reverse procedure is adopted. The frequency of the microwave radiation is fixed whilst the magnetic field is swept so that resonance is observed at a certain field strength. Since the field at which resonance occurs depends upon the operating frequency of the particular instrument, results are not quoted in terms of resonance field strengths but in terms of g values.

The value of electron spin resonance in the study of molecules and crystals is that g value is often modified from the value 2.0023 by orbital contributions to magnetism. These contributions can often be precisely evaluated to give detailed structural information. In polyatomic molecules, the orbital motion of the electron is often quenched because of the electrostatic effect between the negatively charged electron and the positively charged nuclei. It is quite conceivable that the orbital motion can in fact be quenched to a different degree in different directions, this being a direct consequence of the fact that many orbitals contain a direction dependent component. It is therefore quite possible that a molecule will give three different observable g values depending upon whether the magnetic field is applied along the x, y or the z axis.

Much work has been performed on the electron spin resonance of organic solutions[29]. In solution, molecular tumbling averages the effect of the three possible g values and only an average value is experimentally observable. Also a considerable amount of work has been performed on inorganic complexes[30]. The major differences between the spectra of these compounds and organic solution spectra is that the electron spin is often strongly quantized along some molecular axis in the complex so that single crystal experiments along three mutually perpendicular directions can give the three g values, g_x, g_y and g_z. Many cases occur in which two of the g values are the same and these are designated $g_\perp$ and g_{11} where g_{11} is the g value in the unique direction and $g_\perp$ is the value in any direction perpendicular to the unique direction. An example of this type of spectrum is when the metal ion has axial symmetry, many examples of which are found in copper chemistry[31].

Generally speaking, many electron spin resonance transitions depend upon the angle of the applied magnetic field to the system under study so that when single crystal techniques cannot be employed, a certain amount of information is invariably lost through broadening of the resonance signal.

It often happens that an interaction takes place between the nuclear magnetic moment and the electronic spin state so that small hyperfine splitting occurs. This is illustrated for the ^{14}N nucleus in Figure 12 and is responsible for the three line spectrum of an aqueous solution of Fremy's salt, Potassium nitrosyl disulphate.
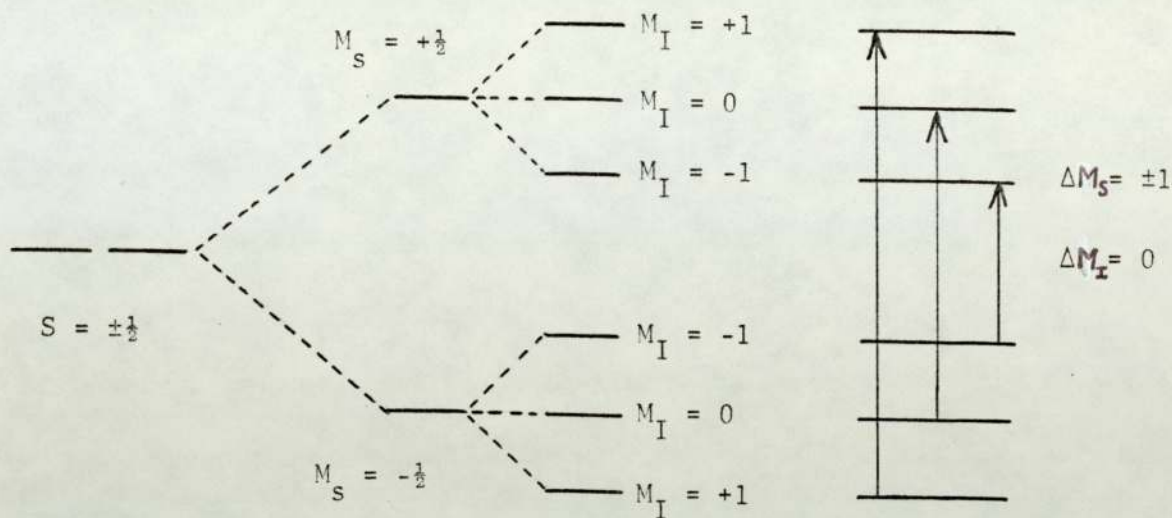
FIGURE 12

The ^{14}N nucleus has a nuclear spin of 1 so in the presence of a magnetic field three orientations (i.e. $2I + 1$) are possible. The selection rules state that $\Delta S = \pm 1$ and that $\Delta I = 0$ so that three absorptions are observed.

Two types of hyperfine interaction can occur. The dipolar hyperfine interaction is concerned with the interaction between an unpaired electron near the nucleus with the nuclear magnetic field, whilst the Fermi interaction is concerned with the contact interaction of an unpaired electron with the nucleus. The anisotropic dipolar interaction is not of great importance for it is often rendered unobservable by molecular tumbling in liquids whilst it is often of negligible comparative magnitude in solids compared to the dipolar hyperfine interaction although it may well be responsible for line broadening.

Contact between the nucleus and an unparied electron can only occur if the electron spends some of its time in an s orbital as only the s orbitals have a finite spin density at the nucleus. The presence of this type of interaction can be used to establish the location of an unpaired electron within a molecule whilst the comparative magnitude of the splitting can be used to deduce information about the nature of the orbital containing the unpaired electron by the relative degree of s character involved in the construction of the hybrid orbital.

One of the chief advantages of electron spin resonance spectroscopy over other spectoscopic techniques is its comparative sensitivity to extremely small concentrations of paramagnetic species. It is possible to detect species with spin concentrations as low as 10^{11} spins per litre. However, one of the serious disadvantages of this technique is that the optimum amount of structural information is obtained only for magnetically dilute systems. If the paramagnetic spin concentration becomes so large that interaction between paramagnetic centres occurs a great deal of information is lost. This limits the use of the technique particularly when ferromagnetic and antiferromagnetic systems are under study.

The success of electron spin resonance in determining the structure of numerous paramagnetic centres led Castner et al[32] to investigate the possibilities of applying electron spin resonance spectroscopy to the study of the structure of glasses. This followed some pioneer work by Sands[33] who had reported some resonances at g values 6.2 and 4.2 of unknown origin in iron containing glasses as well

as a g value of 2.0 with associated hyperfine structure for a sample
of glass containing 0.4% Cu^{2+}. Castner et al concentrated on iron
containing glasses only and showed that g values of 4.27 and 6.2 can
be attributed to the presence of Fe^{3+} in different environments. It
was also pointed out that if the magnitude of the crystal field terms
are small then Fe^{3+}, a d^5 system, can be treated by perturbation theory
as the orbital angular momentum is zero. This treatment shows that
the only observable transition is between the $M_s = +\frac{1}{2}$ and the $M_s = -\frac{1}{2}$
states and that the transition is not perturbed so that a g value of
2.0023 is to be expected. The glasses under study did not give g
values around 2.0 so it was concluded that the crystal electric field
terms in the glass system were not weak. The case where the magnitude
of the crystal field terms and the magnetic terms are comparable was
also considered and it was concluded that a very messy situation
would occur in which no well-defined resonance frequencies would
appear. A broad background was, in fact, observed in most samples
studied and it was concluded that this arose in such a way.

Castner et al then set out to solve the spin Hamiltonian for the
case where the crystal field effects are far greater in magnitude than
the magnetic effects. The spin Hamiltonian is shown below:

$$H = g_o BH S_z + D S_z^2 + E(S_x^2 - S_y^2)$$

D is effectively a term describing the amount of axial distortion
present whereas E describes the degree of rhombohedral distortion.
The energy levels, W, calculated from this Hamiltonian in the absence
of rhombohedral distortion (E = 0) and at zero field were calculated
to be:

$$W = Dm^2$$

where $m = \pm\frac{5}{2}, \pm\frac{3}{2}, \pm\frac{1}{2}$.

The energy levels are shown in Figure 13 for zero field and with an applied magnetic field.
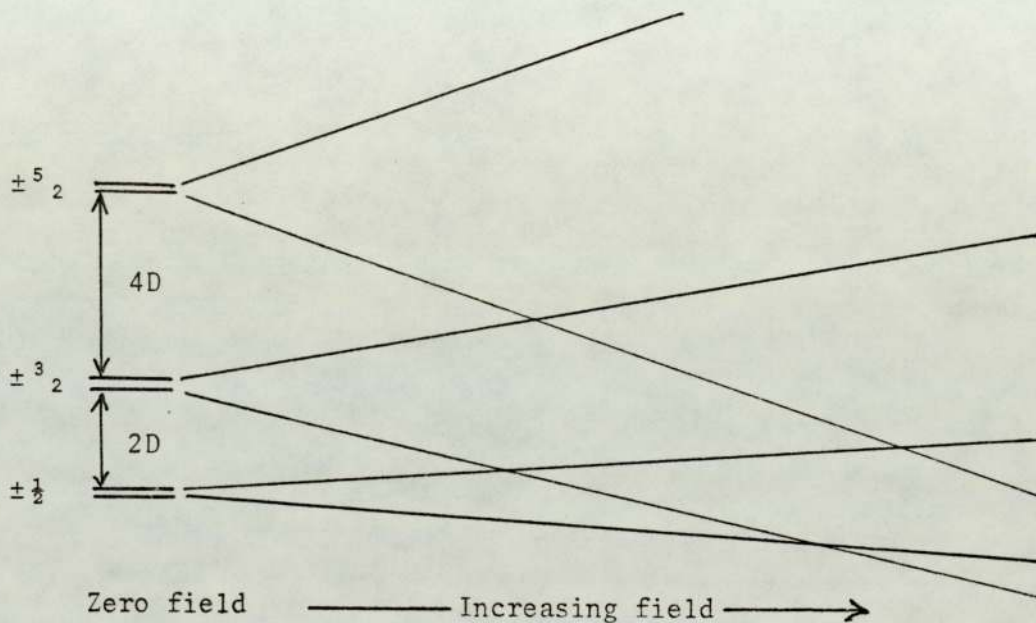
FIGURE 13

All transitions are forbidden except the $m = +\frac{1}{2}$ to $m = -\frac{1}{2}$ transition by the selection rule which states that $\Delta m = \pm 1$ for the case when the z axis is perpendicular to the applied field. It was also shown that when solving the Hamiltonian for the case where the magnetic field is perpendicular to the spin direction, then the expected g value is around 6.0. In a glass the orientation of the z axis with respect to the magnetic field direction is random. However, the probability of the applied field being perpendicular to the spin axis is much greater than it being parallel to it so that although resonance absorptions occur at all values from g = 2.0 to g = 6.0,

the g = 6.0 absorption is very intense and Castner et al conclude
that there is little doubt that this is the origin of one of the
unknown signals reported by Sands.

By similar reasoning and by using exactly the same Hamiltonian
equation, Castner et al have shown that the g value of 4.27 as
reported by Sands is due to the case where the crystal field terms
are large and D = 0 whilst E $\neq$ 0. The significance of g values in
glasses in terms of structure is also discussed. Castner et al consider
that if an iron (III) cation was in a network modifying position
with a co-ordination number of six, both D and E would be of importance
and the resonance pattern would be a broad smear with no sharp well-
defined lines similar to those appearing at g = 4.28 or g = 6.0.
Castner obtained a proportion of background signal spread across a
large range of g values and it was reported that this was due to
iron (III) in a network modifying position, or in other words hexa-
co-ordinated iron (III). It is also quite possible that iron (III)
is present in a tetrahedral position in glass. If an iron (III)
cation is at a centre of a regular tetrahedron surrounded by four
negative charges, then D = 0 and E = 0 and an intense absorption at
g = 2.0 is expected.

However, if one of the four negative charges is not equal to the
other three, then D $\neq$ 0 and E = 0 and an intense absorption at around
g = 6.0 is expected. If on the other hand only two of the four charges
are equal, then D = 0 and E $\neq$ 0 which gives an intense absorption at
g = 4.28, so that the value of electron spin resonance in the study
of iron (III) containing glasses is well illustrated.

1.7.3 X-Ray Diffraction

X-ray diffraction is used in the present work to identify species formed at various temperatures during the firing of ceramic glazes. This technique is useful in two respects in the present work. Firstly it can be used to confirm the Mössbauer results for iron containing species and secondly it has greater versatility than Mössbauer spectroscopy for it can be used to identify a greater variety of crystalline species as it is not restricted to compounds containing iron. The major limitation of the technique is that in multi-component systems the powder diffractogram is very complex and the identification of low concentration species can be a problem. Also although a limited short range order occurs in glass, most glasses are amorphous so that no diffraction pattern can be observed. In the present work species are identified by comparison with reference data from the powder diffraction file which gives powder diffraction data for a large number of compounds and minerals.

CHAPTER TWO

EXPERIMENTAL DETAIL

Chemicals

All chemicals were obtained from commercial sources. Ceramic
mineral samples were obtained from Harrison and Mayer, Stoke-on-Trent.

Magnetic Susceptibility Measurements

Paramagnetic susceptibility measurement were made using the
Gouy method. A semi micro Stantons Instrument balance was used in
conjunction with an electromagnet operating at a current of 10 amps.
Gouy tube constants were determined using $Hg[Co(CNS)_4]$ as a standard
with a known gram susceptibility of 16.44×10^{-6} cgs units at 20 °C.
Susceptibilities were then calculated using the equation:

$$10^6 \ \chi = \frac{\alpha + BF}{W}$$

where F is the force on the sample and W is the sample weight.
Diamagnetic corrections were made from Pascals constants as quoted
by Figgis and Lewis[34].

Electronic Spectra

Electronic spectra of powdered solids were obtained initially
using an SP 700 Unicam instrument. The nujol mull technique described
by Lancaster[35] was followed initially, the face of the quartz cell
being coated with a nujol mull prepared from the finely powdered
sample. However it was found that much improved spectra were obtained
using an SP 800 Unicam spectrometer and coating a Waterman filter
paper with the finely powdered sample in order to obtain the absorption

spectra. In order to facilitate easy balance of the spectrometer, a blank filter paper was positioned in front of the reference beam.

X-Ray Powder Diffractogram Traces

X-ray powder diffractogram traces were obtained as a standard analytical service within the chemistry department of Aston University using Cu K α radiation, wavelength 1.54 $\overset{\circ}{A}$, with nickel filters. Exposure times of up to four hours were necessary and identification of chemical species was achieved through comparison with X-ray diffractogram traces of raw materials and through reference to the powder diffraction file.

Mössbauer Spectra

^{57}Fe Mössbauer spectra were obtained with a centronic Mössbauer spectrometer with a gamma radiation counter and multichannel analyser as described by Fernandopulle[36]. All isomer shift parameters are quoted with reference to natural iron.

Electron Spin Resonance Spectra

Electron spin resonance spectra were obtained using a Joel JES-PE electron spin resonance spectrometer operating in the X band calibrated with a standard Mn^{2+} sample diluted with magnesium oxide.

Sample Preparation

Weighed samples were fired in a platinum crucible in a Carbolyte MFHT furnace with a gas inlet facility. Initially an inert atmosphere of nitrogen was contained in the firing chamber by sealing the door with wet clay in a manner reminiscent of methods employed by craft potters. This was found not to be a particularly successful method as drying and cracking of the clay occurred preventing containment of the inert atmosphere which led to oxidation of the sample on heating. A quartz beaker was therefore commissioned and fitted with a quartz inlet tube and inverted over the platinum crucible to form a sagger as shown in the diagram.
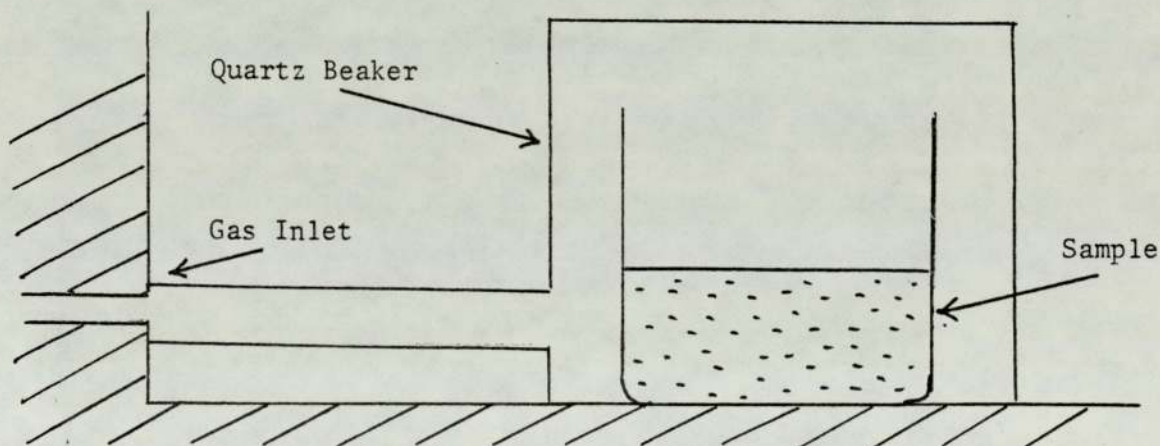
The quartz inlet tube to the sagger was rested against the gas inlet pipe and a positive nitrogen pressure was applied throughout the firing and cooling cycles. This was found to be a very successful method of containing an inert atmosphere in the area around the sample thereby preventing oxidation.

CHAPTER THREE

^{57}Fe MOSSBAUER MEASUREMENTS OF SOME

IRON COMPLEXES IN WEAK LIGAND FIELD ENVIRONMENTS

Introduction

Fernandopulle[36] has investigated the reactions of Iron (III)
salts with various 2 pyridylamines and has reported the synthesis
and physical data including Mössbauer spectra. This work was
performed a few years ago in the chemistry department of Aston
University and as it was left unfinished, it was felt that this
would be a convenient starting point to the present work. The 2
pyridylamine systems are not too far removed, from the Mössbauer
point of view, from the sort of systems that are going to be studied
later in the investigation of iron in glaze systems, as both contain
iron in weak field environments. The ligands used by Fernandopulle
were di(2-pyridyl)amine, tri(2 pyridyl)amine and 5 methyl 2 pyridyl
di(2-pyridyl)amine.
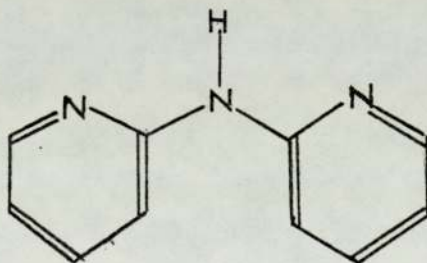
di(2-pyridyl)amine
Abbreviated to Dipyam
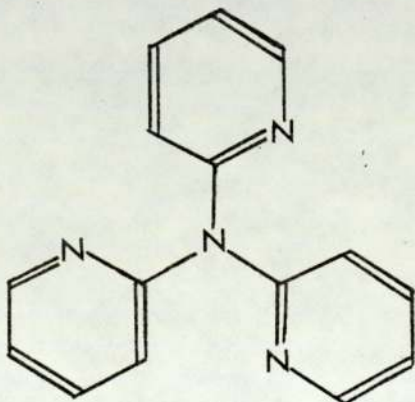
tri(2-pyridyl)amine
Abbreviated to Tripyam
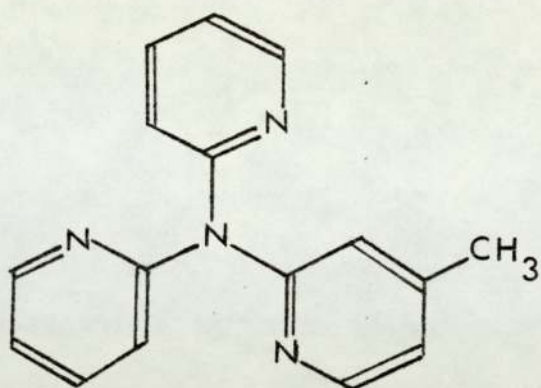
5 methyl 2 pyridyl di
(2-pyridyl) amine
Abbreviated to (5MPT)

Three types of complexes are observed when these ligands are reacted, in alcoholic solutions, with Iron (III) chloride. These three distinct types can be thought of as three distinct stages in the base hydrolysis of the metal ion. Class A complexes are of the general form $[LH^+]_2[Cl_3FeOFeCl_3]^{2-}$, where L is one of the ligands described above. The N-H stretching frequencies observed at around 3320 cm^{-1} are characteristic of unco-ordinated amines whilst electric conductivity measurements in either dimethyl formamide or nitromethane are consistent with values obtained for a 2:1 electrolyte. An infra-red band between 800-890 cm^{-1} is characteristic of $v(FeOFe)$ for a μ oxo bridged complex and this, together with two iron chlorine vibrations, is good evidence for the presence of the anion proposed above. The Mössbauer results confirm this structure for the isomer shift is consistent with a tetrahedral configuration whereas the quadrupole splitting indicates a symmetry less than cubic.

Class B complexes are of the general type $[FeLCl_3]$ and to date examples of these have only been reported when the ligand has been shown to be terdentate[37,38]. The infra-red spectra indicate this

clearly whereas the conductivities, although not negligible, are low and therefore this class seems to be simple monomeric species.

The class C complexes reported by Fernandopulle are the most complex of all the three classes. These give infra-red spectra that confirm the presence of -OH groups and show bands characteristic of v(FeOFe) as well as indicating that terminal halide ligands are present. Extensive analytical data on the chloro derivatives indicates that it has the following stoichiometry, $Fe_2Cl_4O(Dipyam)_35H_2O$.

In the present work, the room temperature Mössbauer measurements of a selection of Fernandopulle's samples are repeated and the agreement with her results is discussed. Mössbauer spectra are also reported at 80 °K for all of these samples as well as some variable temperature magnetic measurements in order to elucidate certain problems arising from the interpretation of the temperature dependence of the Mössbauer parameters of certain samples. Two theoretical models are described and the quadrupole splitting ratios expected for all possible structures are predicted and compared with experimental results in order to try and gain some insight into the type of stereochemistry involved in the structure of the class C chloro derivatives.

RESULTS

Mössbauer Results for Various 2 Pyridylamine Derivatives of Iron III

Class A Complexes

Compound	Fernandopulle's Results Room Temperature		The Present Work Room Temp		80 °K	
	$\delta*$	Δ	$\delta*$	Δ	$\delta*$	Δ
(Dipyam H$^+$)$_2$ [(Cl$_3$Fe)$_2$O]$^{2-}$	0.23	1.20	0.23	1.22	0.34	1.31
(5MPTH$^+$)$_2$ [(Cl$_3$Fe)$_2$O]$^{2-}$	0.23	1.31	0.22	1.25	0.34	1.31

Class B Complexes

Compound	Fernandopulle's Results Room Temperature		The Present Work Room Temp		80 °K	
	$\delta*$	Δ	$\delta*$	Δ	$\delta*$	Δ
[Tripyam FeCl$_3$]	0.33	0.00	0.30	0.00	0.40	0.00
					$T_{\frac{1}{2}} = 0.92$	

Class C Complexes

Compound Fe$_2$(dipyam)$_3$Cl$_4$O5H$_2$O	Fernandopulle's Results Room Temperature		The Present Work Room Temp		80 °K	
	$\delta*$	Δ	$\delta*$	Δ	$\delta*$	Δ
4-year old sample	0.33	0.66	0.44	0.75	0.33	1.42
	0.33	1.36	0.14	0.81	0.18	1.12
Freshly prepared sample	----	----	0.41	0.75	0.43	0.54
			0.25	1.28	0.33	1.33

* wrt Fe metal, all values ±0.03 mms^{-1}

TABLE 1

Mössbauer Results for a Complex of Iron II

Compound	Fernandopulle's Result Room Temperature		The Present Work Room Temp		80 °K	
	$\delta*$	Δ	$\delta*$	Δ	$\delta*$	Δ
$Fe^{II}(5MPT)_2$	0.35	0.20	0.34	0.22	0.41	0.00
$Fe^{II}(NCS)_4$					1.10	2.93

* wrt Fe metal, all values $=0.03$ mms^{-1}

TABLE 2

Room Temperature Magnetic Moment

Compound	μ_{eff} BM
$(DipyamH^+)_2[(Cl_3Fe)_2O]^{2-}$	2.30
$(5MPTH^+)_2[(Cl_3Fe)_2O]^{2-}$	2.20
$[Tripyam\ FeCl_3]$	5.69
$Fe_2(dipyam)_3Cl_4O.5H_2O$ freshly prepared	2.20
$Fe_2(dipyam)_3Cl_4O.5H_2O$ aged sample	3.95
$Fe^{II}(5MPT)_2Fe^{II}(NCS)_4$	5.34

TABLE 3

Electric Field Gradient Tensor Ratios Compared to

Quadrupole Splitting Ratios*

efg Ratios

	Electronegativity Model	Modified Electronegativity Model
Structure I + III	1.07	1.19
Structure I + IV	1.13	1.67
Structure II + III	1.17	1.14
Structure II + IV	1.42	1.64

Δ Ratios

Fernandopulle RT	2.06
The present work aged sample RT	1.08
The present work aged sample 80 °K	1.27
The present work freshly prepared RT	1.71
The present work freshly prepared 80 °K	2.46

* All ratios are calculated in order to give a value greater than unity

TABLE 4

3.1   GENERAL DISCUSSION

Two complexes belonging to class A were investigated,
$(\text{Dipyam H}^+)_2[(\text{Cl}_3\text{Fe})_2\text{O}]^{2-}$ and $(5\text{MPTH}^+)_2[(\text{Cl}_3\text{Fe})_2\text{O}]^{2-}$. Fernandopulle's
room temperature Mössbauer parameters were reproduced within experi-
mental error for both of these complexes, Table 1. The isomer shift
is consistent with a 5/2 spin state for both iron (III) centres which
are shown to be chemically equivalent. The magnetic susceptibility
measurements of 2.2 and 2.3 Bohr Magnetons indicate that the iron
centres in both complexes are antiferromagnetically coupled, Table 3.
The isomer shift data are consistent with a tetrahedral configuration
whilst the quadrupole splitting parameters indicate that the iron
environment is not strictly cubic so that the Mössbauer parameters
are consistent with the proposed formula $(\text{LH}^+)_2[\text{Cl}_3-\text{Fe}-\text{O}-\text{Fe}-\text{Cl}_3]^{2-}$
for these types of complexes, where L = Dipyam or 5MPT in this case.

The small temperature dependence of the isomer shift is expected
due to the second order Doppler effect whilst the quadrupole splitting
parameter is independent within experimental error. A non-zero
electric field gradient can arise from contributions due either to
a non-cubic ligand field or a non-spherical distribution of valence
electrons which tend to polarize the spherical inner core electrons
thereby generating an electric field gradient at the nucleus. The
valence contribution to the electric field gradient is often highly
temperature dependent as the population of the closely spaced electronic
states change. A temperature independent quadrupole splitting indicates
that the valence contribution to the electric field gradient is small

and that the ligand contribution predominates. A 5/2 spin system gives a spherically symmetrical distribution of electrons so that any quadrupole splitting arises from a non-cubic ligand environment. Thus the temperature independent quadrupole splitting is consistent with a 5/2 spin state so that the Mössbauer results provide further evidence for the fact that these systems contain two high spin iron sites antiferromagnetically coupled, and that the low magnetic susceptibility is not due to some unusual low spin electronic configuration.

Similarly, a complex of class B, $Fe(Tripyam)Cl_3$, was studied and the Mössbauer results at room temperature and at 80 °K are compared with Fernandopulle's room temperature result, Table 1. The agreement between the isomer shift parameters in all three cases is good and supports the assignment of a spin 5/2 state, as inferred from the room temperature magnetic moment. No quadrupole splitting was observed although a significant broadening of the Mössbauer peak occurred at 80 °K.

This led to a study of the magnetic properties over a range of temperatures, figures 8 and 17, but the compound was found to be well behaved. The effective magnetic moment was very slightly lower than expected for a 5/2 spin system, but the value remained constant between 300 °K and 80 °K, the Curie-Weiss law being obeyed with a Weiss constant very close to zero, figure 8.

Broadening of Mössbauer resonances at low temperatures if often attributed to the onset of magnetic ordering, but this does not usually occur at temperatures as high as 80 °K. A more likely explanation for

this broadening is that a small quadrupole splitting is present but the higher energy component is broadened to such an extent that it cannot be detected at room temperature. Such behaviour has previously been reported for iron (III) complexes[39][40] and is thought to be due to fast electronic relaxation, involving the lower Kramers' doublet, $M_s = \pm\frac{1}{2}$, which arises from a zero field splitting with positive D, as illustrated in Figure 1.

Zero field splitting for a spin 5/2 state
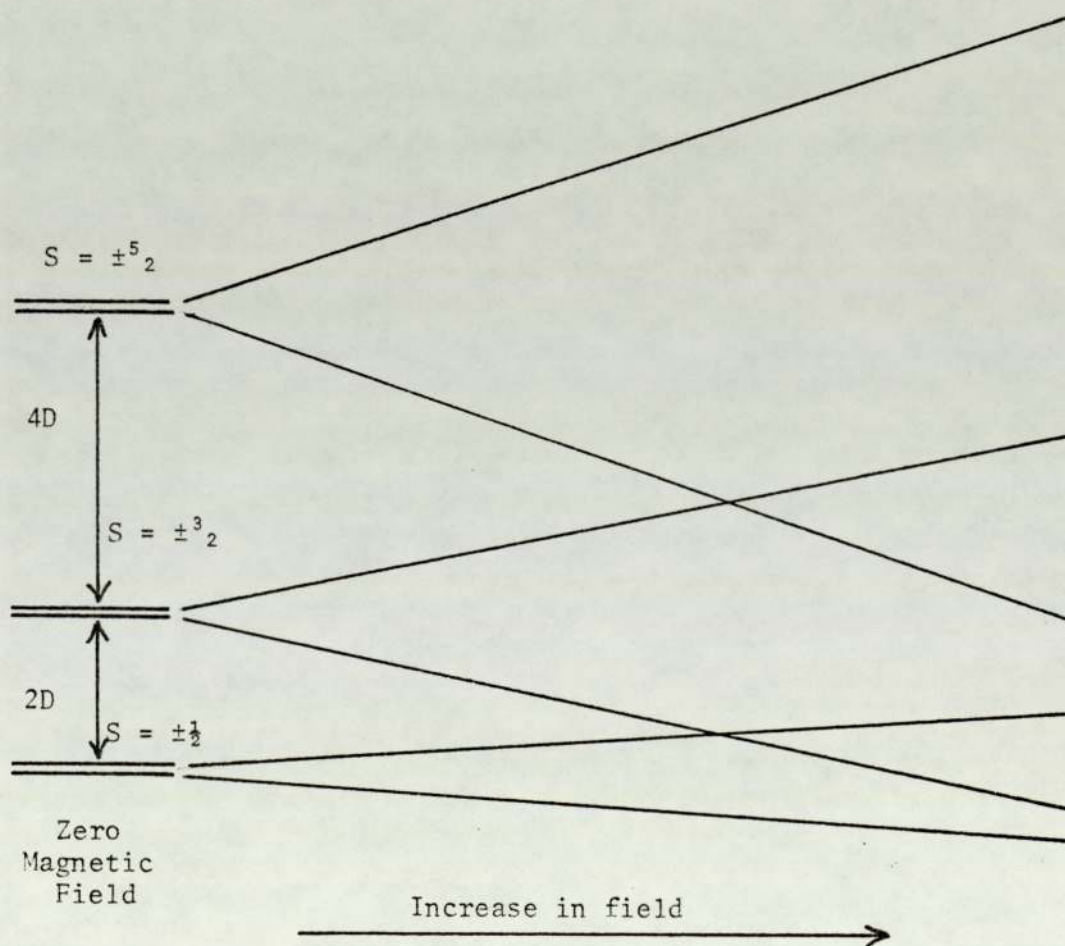
FIGURE 1

The origin of the small quadrupole splitting could be due to the different electronegativities of nitrogen and chlorine giving a small electric field gradient, although a crystal lattice contribution is also a possibility. The lattice contribution could also lead to a distortion from ideal C_{3v} symmetry which would also explain the origin of three infra-red iron-chlorine stretching vibrations as reported by Fernandopulle. Although the behaviour of this compound is not fully understood, the data available supports a simple monomeric structure.

One complex of class C was studied and the Mössbauer results are compared with those of Fernandopulle, Table 1, who reported the presence of two iron sites, both having isomer shift parameters consistent with 5/2 spin states. One site with a quadrupole splitting of 0.66 mm s^{-1}, has parameters consistent with a distorted six co-ordinate environment but the other site has an extremely large quadrupole splitting, 1.36 mm s^{-1}. H. H. Wickman et al[41] have reported examples of iron (III) systems where the structure of the molecule stabilises a spin 3/2 ground state but the quadrupole splittings are unusually large (>2 mm s^{-1}) so this explanation is not really plausible in this case. Also the isomer shift parameter quoted by Fernandopulle is in quite good agreement with the value expected for a 5/2 spin state. Alternatively, the co-ordination number of this iron site may be greater than six as reported by Hall et al[42] for iron (III) in a mixed oxygen-nitrogen environment.

3.2   REMEASUREMENT OF FERNANDOPULLE'S SAMPLE AFTER FOUR YEARS

The Mössbauer parameters of Fernandopulle's sample were measured after a period of four years. The room temperature results indicate that considerable structural change had occurred to the iron environments over that period of time. The elemental analysis of this sample was repeated after four years and was found to be unchanged, the stoichiometrically most simple form being represented by the following formula, $Fe_2Cl_4O(dipyam)_3 5H_2O$.

It is difficult to predict exactly what structural changes have occurred purely from the Mössbauer data, although one iron site does seem to remain in a comparatively constant environment throughout the four year period, as shown in Figure 2.

Mössbauer result for one iron site in $Fe_2Cl_4O(dipyam)_35H_2O$

Freshly Prepared by Fernandopulle   Four Years Old

$$\delta* = 0.33 \text{ mm s}^{-1} \qquad \delta* = 0.44 \text{ mm s}^{-1}$$

$$\Delta = 0.66 \text{ mm s}^{-1} \qquad \Delta = 0.75 \text{ mm s}^{-1}$$

*   wrt Fe metal: experimental error = $\pm 0.03 \text{ mm s}^{-1}$

FIGURE 2

The structural change does seem to be more associated with the other iron site as shown in Figure 3.

Mössbauer Result for the Other Iron Site in $Fe_2Cl_4O(dipyam)_3 5H_2O$

Freshly Prepared by Fernandopulle   Four Years Old

$\delta* = 0.33$ mm s^{-1} $\delta* = 0.14$ mm s^{-1}

$\Delta = 1.36$ mm s^{-1} $\Delta = 0.81$ mm s^{-1}

* wrt Fe metal; experimental error = 0.03 mm s^{-1}

FIGURE 3

3.3 MOSSBAUER RESULTS OF FRESHLY PREPARED
$Fe_2Cl_4O(dipyam)_3 5H_2O$

The unusual behaviour of $Fe_2Cl_4O(dipyam)_3 5H_2O$ led to this complex being remade and a new study of the Mössbauer parameters of a freshly prepared sample was undertaken. The agreement between the Mössbauer parameters of the freshly prepared sample with those of Fernandopulle's freshly prepared sample at room temperature is fairly good, figure 4.

Comparison of Room Temperature Mössbauer Results

for Two Freshly Prepared Samples of $Fe_2Cl_4O(dipyam)_3 5H_2O$

	$\delta*$		Δ
Fernandopulle	Present Work	Fernandopulle	Present Work
0.33	0.41 mm s^{-1}	0.66	0.75 mm s^{-1}
0.33	0.25	1.36	1.28

* wrt Fe metal; experimental error = 0.03 mm s^{-1}

FIGURE 4

It is perhaps worth noting that the agreement between the para-
meters of these two samples is not quite as good as can often be
expected using ^{57}Fe Mössbauer spectroscopy. It may well be the case
that although Fernandopulle's recipe was followed carefully in the
present work, it cannot be guaranteed that all the experimental
conditions were exactly the same in the two preparations. Some
discrepancy might therefore be expected between the two sets of
Mössbauer data indicating some slight structural dependence on the
conditions of preparation.

3.4   LOW TEMPERATURE MOSSBAUER RESULTS FOR
$Fe_2Cl_4O(dipyam)_35H_2O$
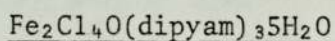
A low temperature study in liquid nitrogen revealed even more
curious behaviour. The sample prepared by Fernandopulle and measured
after four years gave a spectrum in which one iron site had similar
Mössbauer parameters to one of the sites in the room temperature
measurement of Fernandopulle's freshly prepared complex, as shown in
figure 5.

Fernandopulle's Preparation of $Fe_2Cl_4O(dipyam)_35H_2O$: Site 1

Freshly Prepared RT Measurement   4 Years Old 80 °K

$\delta* = 0.33$ mm s^{-1} $\delta* = 0.33$

$\Delta = 1.36$ $\Delta = 1.42$

* wrt Fe metal; experimental error = 0.03 mm s^{-1}

FIGURE 5

The agreement between the Mössbauer parameters of the other iron site is not good so that this rules out the possibility of a phase change in the crystal lattice occurring over a period of time, which can quickly be reversed by cooling to 80 °K, figure 6.

Fernandopulle's Preparation of $Fe_2Cl_4O(dipyam)_35H_2O$: Site 2

Freshly Prepared RT Measurement	4 Years Old 80 °K
$\delta^* = 0.33$ mm s^{-1}	$\delta^* = 0.18$
$\Delta = 0.66$	$\Delta = 1.12$

* wrt Fe metal; experimental error = 0.03 mm s^{-1}

FIGURE 6

The temperature dependence of the Mössbauer parameters of a sample freshly prepared in the present work was not very great and the compound behaved like a normal high spin iron (III) complex, as shown in figure 7.

Mössbauer Parameters of a Freshly Prepared Sample in the Present Work

Room Temperature		80 °K	
$\delta^* = 0.41$ mm s^{-1}	$\delta = 0.25$ mm s^{-1}	$\delta^* = 0.43$ mm s^{-1}	$\delta = 0.33$ mm s^{-1}
$\Delta = 0.75$	$\Delta = 1.28$	$\Delta = 0.54$	$\Delta = 1.33$

* wrt iron metal; experimental error = 0.03 mm s^{-1}

FIGURE 7

The slight increase in isomer shift parameters at the lower temperature is to be expected due to the second order Doppler shift, whilst the temperature dependence of the quadrupole splitting is only

Plot of μ_{eff} against Temperature for Fe(Tripyam)Cl$_3$, Fe(NCS)$_4$Fe(5MPT)$_2$ and for an aged sample of Fe$_2$(dipyam)$_3$Cl$_4$O5H$_2$O
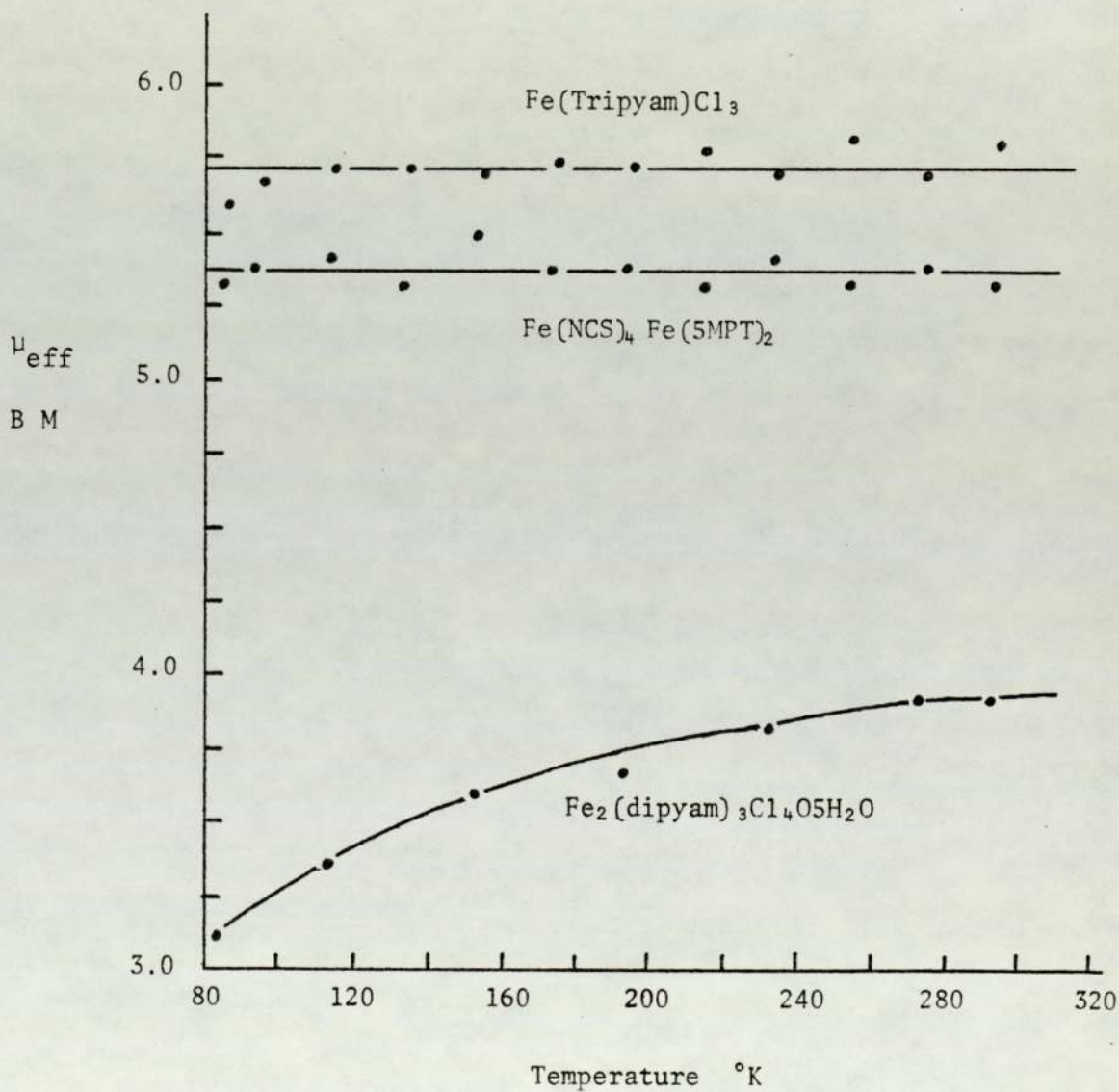
FIGURE 8

slight. This is only to be expected for a singlet electronic state where thermal population of higher electronic states is not important. Hence the magnitude of the electric field gradient is more or less constant over a large temperature range and this is reflected therefore in the near constant quadrupole splitting parameter.

The magnetic moment of the aged sample was found to be 3.95 Bohr magnetons at room temperature compared with 2.20 Bohr magnetons as reported by Fernandopulle and successfully reproduced with a freshly prepared sample in the present work. Figure 8 shows the temperature dependence of the effective magnetic moment of Fernandopulle's aged sample and compares it with the temperature dependence of the magnetic moment of two other samples studied, $FeCl_3(Tripyam)$ and $Fe(NCS)_4Fe(5MTP)_2$.

Figure 9 shows a plot of $1/X_m$ against temperature for $Fe_2Cl_4O(dipyam)_35H_2O$ and shows that it behaves as an antiferromagnet above 80 °K with a Weiss constant of -80 °K. This type of magnetic behaviour is not unexpected for a μ-oxo bridge complex where the metal ions are sufficiently close to each other to have their spins aligned antiparallel with a slight canting of the spins to produce a non-zero effective magnetic moment.

In summary it is clear that two separate effects are being observed in Fernandopulle's sample of $Fe_2Cl_4O(dipyam)_35H_2O$. Firstly an ageing process has occurred over a period of four years associated particularly with one of the iron sites, the Mössbauer parameters of which are greatly modified over this period of time, figures 2 and 3. Secondly, a great temperature dependence of the Mössbauer parameters

- 58 -

Plot of $1/\chi_m$ against T (°K) for a four-year old sample of $Fe_2Cl_4O(dipyam)_3 5H_2O$

Temperature °K

FIGURE 9

$1/\chi_m \times 10^{-1}$
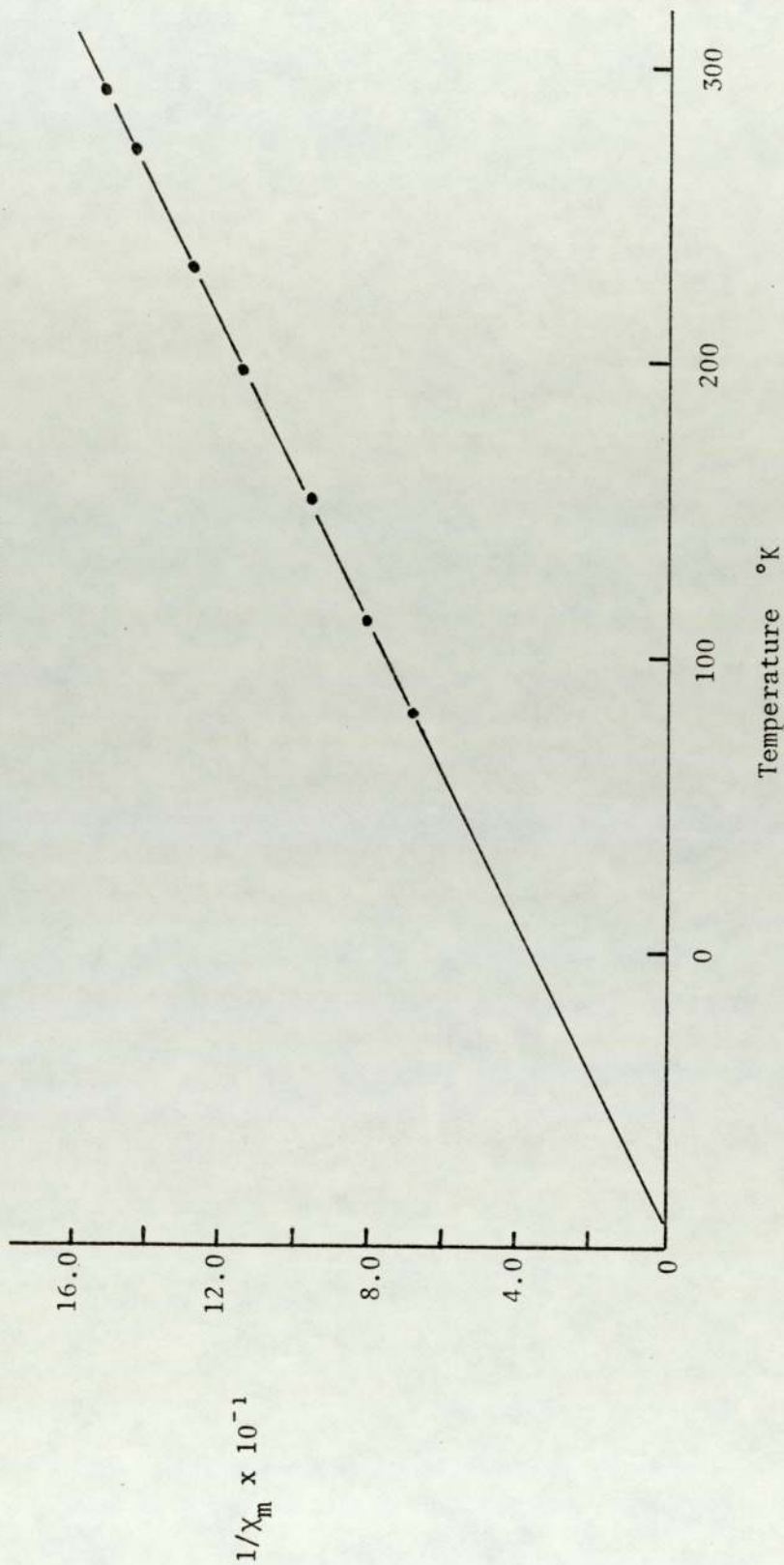
of an aged sample is observed, Table 1. This is in contrast to a freshly prepared sample which by comparison behaves normally over the temperature range 290 °K to 80 °K.

No other spectroscopic information gives any insight into the unusual Mössbauer behaviour that has been recorded for this compound so it is perhaps worthwhile to speculate on the types of structures that may be possible and also to compare the data with theoretical values obtained from a simple point charge model.

3.5   POINT CHARGE MODEL OF $Fe_2Cl_4O(dipyam)_35H_2O$

Bancroft[13] has outlined a point charge model for electric field gradient tensors in which the iron "Mössbauer" atom is assumed to be surrounded by a number of point charges each of which contributes to the overall electric field gradient, the principal component of which interacts with the nuclear quadrupole moment of the excited iron 57 nucleus. This removes some of the degeneracy of the nuclear states, an effect which manifests itself in the form of a quadrupole split spectrum. Generally speaking, there is also a valence contribution as well as a ligand contribution to the electric field gradient tensor although the former is unimportant in the case of high spin iron (III) where the valence shell is spherically symmetrical so that the contributing terms cancel out giving a resultant zero contribution to the overall tensor.

The compound under discussion has the following stoichiometry, $Fe_2Cl_4(dipyam)_3O$, and is known to contain the μ-oxo bridge from the infra-red data, a fact that is supported by the magnetic susceptibility data. Infra-red data also indicate that the di(2-pyridyl)amine ligands are co-ordinated to the iron through the aromatic nitrogen atoms, so that these molecules behave as bidentate ligands. For the sake of simplicity, it will be assumed, when constructing the theoretical model, that both iron (III) cations are six co-ordinated although, at first, no assumptions are going to be made about the exact symmetry of the complex.

The next point to be considered is exactly what structures are possible. One of the ligand sites of both iron (III) ions must be occupied by the μ-oxo group. Remembering the bidentate nature of the nitrogen-containing ligands and taking the stoichiometry into account, all three bidentate ligands cannot be co-ordinated to the same metal ion, if both are to remain hexa-co-ordinated. This means that one di(2-pyridyl)amine ligand is co-ordinated to one metal ion whilst two di(2-pyridyl)amine ligands are co-ordinated to the other. Given this information, the two iron cations are considered separately in order to illustrate what overall structure is possible.

One iron site has the following stoichiometry, $Fe(dipyam)_2Cl.O_{\frac{1}{2}}$, and only two structures are possible within the confines of the model as illustrated in figure 10.
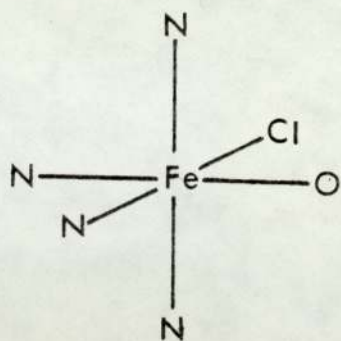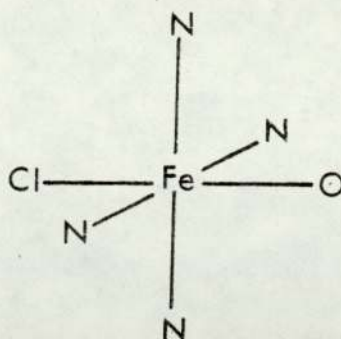
Structure I   Structure II

FIGURE 10

The other iron site has the following possible structures, as illustrated in figure 11.
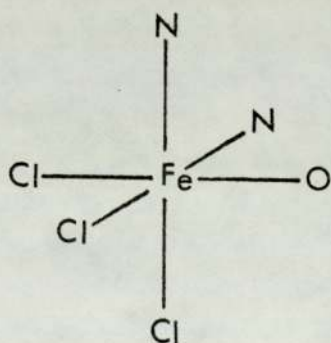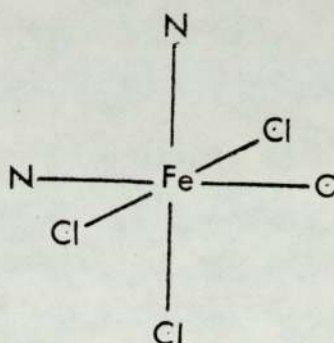
Structure III   Structure IV

FIGURE 11

So overall the complex can be described by one of the following combinations:

(i) I + III   (ii) I + IV   (iii) II + III   (iv) II + IV

Terms describing the three principal components of the electric field gradient tensors for the four structures outlined above have been shown by Bancroft to be as follows:

Structure I

$$V_{11} = (2[O] - [N] - [Cl])e$$
$$V_{22} = (2[Cl] - [N] - [O])e$$
$$V_{33} = (2[N] - [Cl] - [O])e$$

Structure II

$$V_{11} = (2[Cl] + 2[O] - 4[N])e$$
$$V_{22} = V_{33} = (2[N] - [O] - [Cl])e$$

Structure III

$$V_{11} = (2[O] - 2[N])e$$
$$V_{22} = V_{33} = ([N] - [O])e$$

Structure IV

$$V_{11} = (2[O] + [N] - 3[Cl])e$$
$$V_{22} = (3[Cl] - 2[N] - [O])e$$
$$V_{33} = ([N] - [O])e$$

The terms in square brackets are the point charge contributions of the various ligands to the principal components of the electric field gradient. Only the major component is required for each structure as it is this which interacts with the quadrupole moment of the nucleus. To determine which is the major component, the contri-

butions from the various ligands must be estimated in some way so as to assign a numerical value to each.

Two approaches were considered in the assignment of numerical values to these point charge terms. Firstly it was recognised that all the ligands under consideration bond to the metal ion by way of a covalent co-ordination or dative type bond. That is to say that it is not the electrostatic forces between the various ions that hold the complex together, but a bond formed by electron orbital overlap in which the ligand, in the first instance, supplies the electron pair. The electron cloud will be polarized in one direction or the other along the axis of the bond. The degree and direction of polarization depends upon the relative forces of attraction operating upon the electrons between the two nuclei. Differences in the polarization of the electron clouds by the various ligands can give rise to a non-zero electric field gradient at the nucleus. It is this anisotropic polarization that is simulated when the point charge model is set up, the assumption being that such localisation of charge can be adequately described by point charges. The theoretical point charge that should be assigned to a ligand in the electric field gradient point charge model should, therefore, be a function of that ligands attraction for electrons in a covalent bond with iron. Electronegativity is such a quantity for although a quantitative definition is elusive, the original definition as outlined by Pauling is that it is the power of an atom in a molecule to attract electrons to itself. It seems reasonable therefore to substitute ligand electronegativity values for the terms in square brackets as these parameters by definition are a function of the charge distribution in a chemical bond. Further

justification for the use of electronegativity values is that Axtmann et al[43] have demonstrated that at low temperatures, a linear relationship exists between quadrupole splitting and electronegativity of Iron (II) halides. The ratio of the electric field gradient tensors for each of the four possible structures are compared in Table 4 and figure 12 to the experimentally-obtained quadrupole splitting ratios.

Electric Field Gradient Tensor Ratios Compared to
Quadrupole Splitting Ratios*

EFG Ratios		Δ Ratios	
Structure I + III	1.07	Fernandopulle RT	2.06
Structure I + IV	1.13	The Present Work aged sample RT	1.08
Structure II + III	1.17	The Present Work aged sample 80 °K	1.27
Structure II + IV	1.42	The Present Work freshly prepared RT	1.71
		The Present Work freshly prepared 80 °K	2.46

*All ratios are calculated to give a value greater than unity

FIGURE 12

The agreement between experiment and theory is not good although the theoretical value obtained for structure I + III is in good agreement with a room temperature Mössbauer measurement of an aged sample of $Fe_2Cl_4O(dipyam)_3 5H_2O$. When a number of speculative comparisons of this type are made and a certain amount of agreement between theory and experiment is obtained, it should be realised that this may just be coincidental. However, it is interesting to note that structure I + III is one in which the bulky dipyridylamine groups are quite far apart, thereby minimising any steric effects, figure 13.

Structure I + III

trans $Fe_2Cl_4O(dipyam)_3 5H_2O$
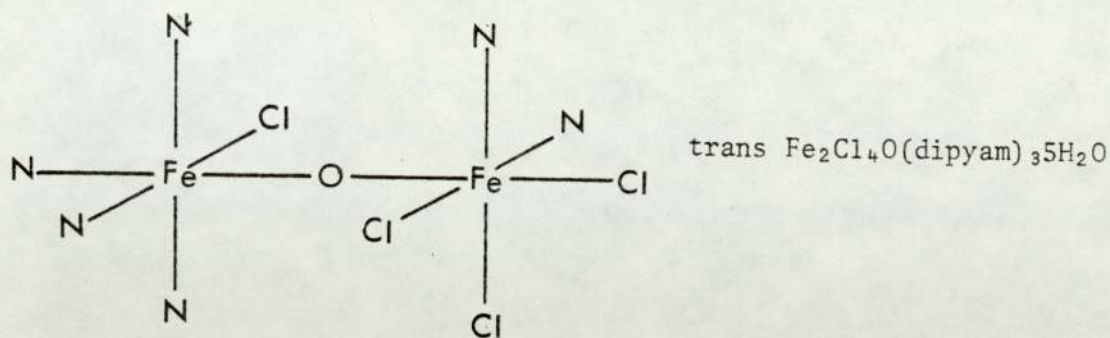
FIGURE 13

The cis configuration may also be favourable but the cis and trans configurations are not distinguishable within the confines of the present model, figure 14.

Structure I + III

cis $Fe_2Cl_4O(dipyam)_3 5H_2O$
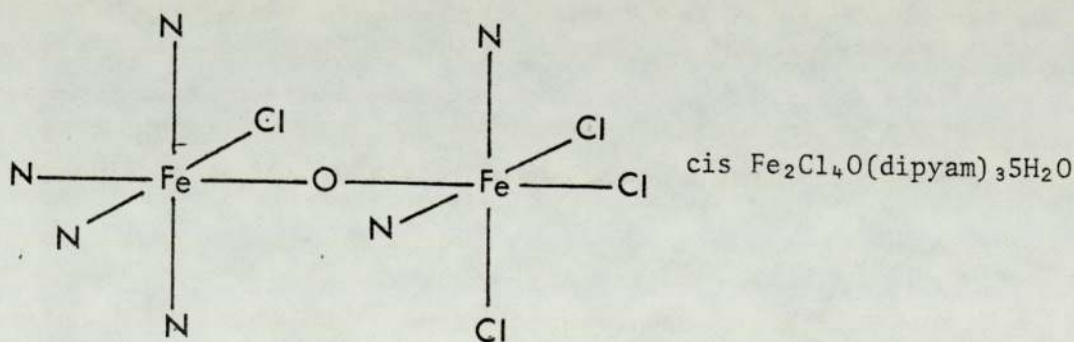
FIGURE 14

The lack of success in comparing theory with experiment is probably due to the simplicity of the theoretical model. A second, more complex, and possibly more realistic approach was considered. One of the limitations of the above model is that the electronegativity values found in the literature are only average values for the particular elements in common oxidation states. It cannot be assumed therefore

that the electronegativity of Cl^- is the same as that of Cl, or O^{2-} the same as that of O.

The second approach surmounts this problem by considering the complex as totally ionic in the first instance and then modifying the ligand contributions to the electric field gradient by estimating the degree of covalency in each of the ligand-metal bonds. If there was no covalent bonding in the system, the formal charge on the 2 pyridylamine nitrogen ligands would be equal to zero and similarly equal to -1 for the chloride ligands and -2 for the μ-oxo bridge anion. The contribution to the electric field gradient from each ligand at the iron nucleus also depends upon the reciprocal of the third power of the distance of the ligand from the iron nucleus. The bond distance of Fe-Cl is assumed to be equal to the sum of the iron (III) radius and the ionic radius of the chloride anion. Similarly, the Fe-O bond distance is assumed to be equal to the sum of the iron (III) radius and the radius of the oxygen anion. The iron-nitrogen bond length is assumed to be equal to the sum of the iron (III) radius and the covalent nitrogen atom radius. Any covalency in the iron-chlorine or the iron-oxygen bonds would be expected to decrease the formal negative charge on the ligands as the ligands in the first instance supply the electrons that form the dative bond. It is assumed that the amount of covalency is a linear function of the electronegativity difference between the two species involved. It is also assumed that the greatest difference in electronegativity between two species is 3.24 in CsF and that this corresponds to a totally ionic bond. The formal charges previously assigned to the ligands are modified by the addition of the term $(+1 - \Delta E/3.24)$ where ΔE is the electronegativity

difference between the ligand and iron (III). This quantity is doubled for the μ-oxo bridge anion which is bonded to two iron (III) ions. The results are given in Table 4 and figure 15 where they are compared with experimentally determined values for the quadrupole splitting ratios.

<u>Electric Field Gradient Tensor Ratios Compared to</u>

<u>Quadrupole Splitting Ratios*</u>

EFG Ratios		Δ Ratios	
Structure I + III	1.19	Fernandopulle RT	2.06
Structure I + IV	1.67	The Present Work aged sample RT	1.08
Structure II + III	1.14	The Present Work aged sample 80 °K	1.27
Structure II + IV	1.64	The Present Work freshly prepared RT	1.71
		The Present Work freshly prepared 80 °K	2.46

*All ratios are calculated to give a value greater than unity

<u>FIGURE 15</u>

Again little agreement between theory and experiment is observed. The possible large source of error in calculating the electric field gradient ratios in the present model is the fact that no account is taken of the modifications of bond length due to covalency. This error could be substantial as the contribution of a ligand to the efg tensor is proportional to the reciprocal of the third power of the bond length. Also the value for the nitrogen ligand-iron (III) bond length may be grossly inaccurate as no account is taken of the possible effects of steric hinderance by the bulky 2-pyridylamine ligands.
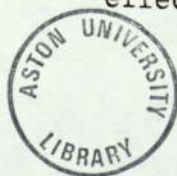
Plot of $1/\chi_m$ against T °K for Fe(NCS)$_4$Fe(5MPT)$_2$
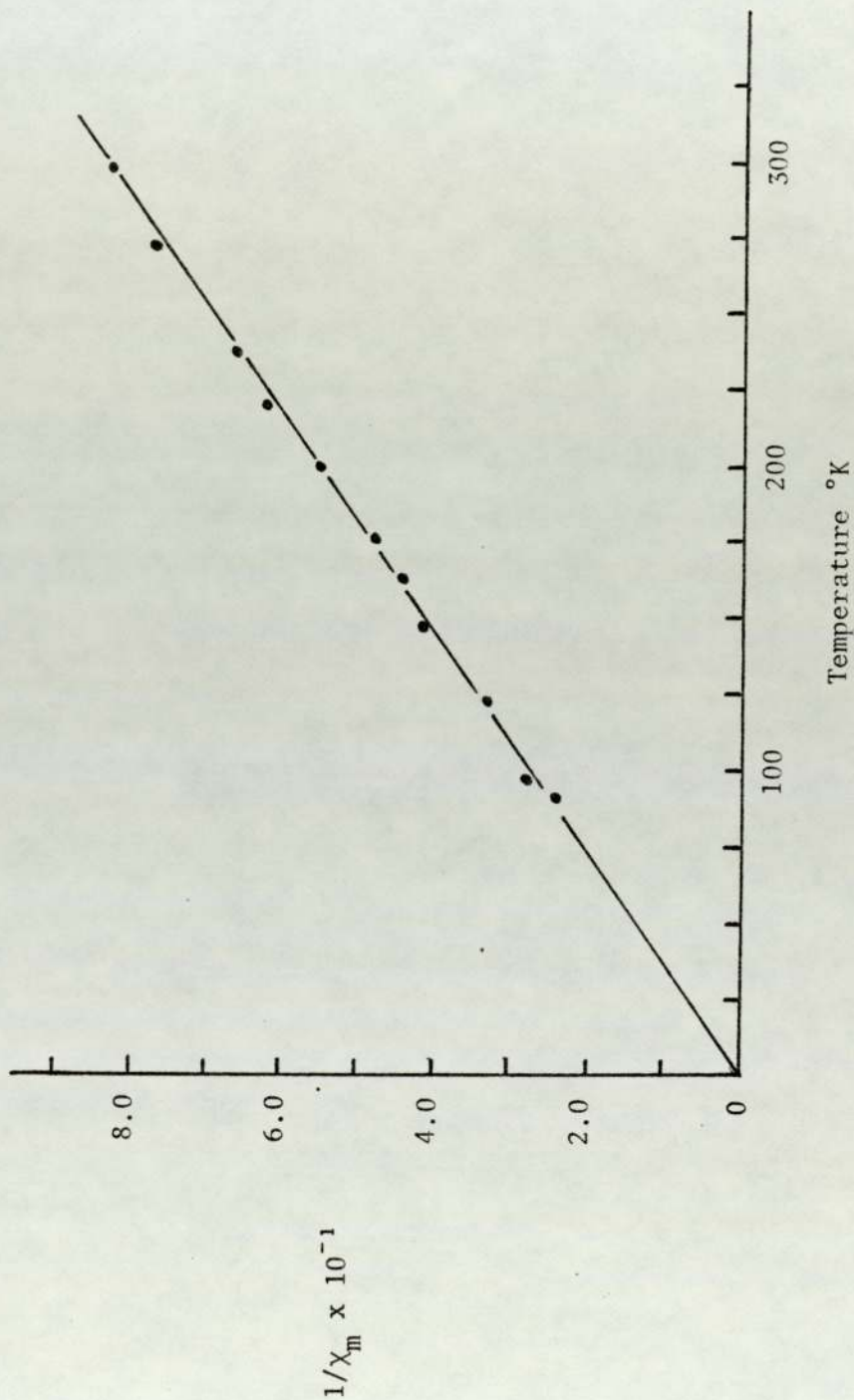
FIGURE 16

However, the electric field gradient ratios obtained for the four structures under the two different models do not cover such a wide range of values as the experimentally determined values for the quadrupole splitting ratios. Both models are based on small distortions from octahedral symmetry. The experimental results tend to suggest that some of the structures in practice have symmetries that deviate to a large extent from regular octahedral symmetry.

3.6   MOSSBAUER PARAMETERS OF $Fe(5MPT)_2 Fe(NCS)_4$

Table 2 gives the room temperature and liquid nitrogen Mössbauer parameters of a sample of $Fe(5MPT)_2 Fe(NCS)_4$ prepared by Fernandopulle. Fernandopulle's room temperature measurements were reproduced within experimental error. Only one iron site was observed with an isomer shift of 0.34 mm s^{-1} and a quadrupole splitting of 0.22 mm s^{-1}. These parameters are consistent with low spin octahedral iron (II) complexes as they are in good agreement with parameters reported by McWhinnie et al[44] and Lancaster et al[38] for FeL_2^{2+} complexes where L = tri-(2-pyridyl)amine and 5 methyl-2-pyridyl di-(2-pyridyl)amine. The very small room temperature quadrupole splitting is not observed at liquid nitrogen temperatures indicating that the iron (II) ion has perfectly octahedral symmetry at this temperature. A second site is evident in the liquid nitrogen temperature spectrum with an isomer shift of 1.10 mm s^{-1} and a quadrupole splitting of 2.93 mm s^{-1}. These parameters are consistent with the presence of high spin iron (II) and they are in good agreement with parameters previously reported for $[Fe(NCS)_4]^{2-}$. The fact that this site cannot be observed in the

Plot of $1/\chi_m$ against T (°K) for $FeCl_3$(Tripyam)

Temperature °K

$1/\chi_m \times 10^{-1}$
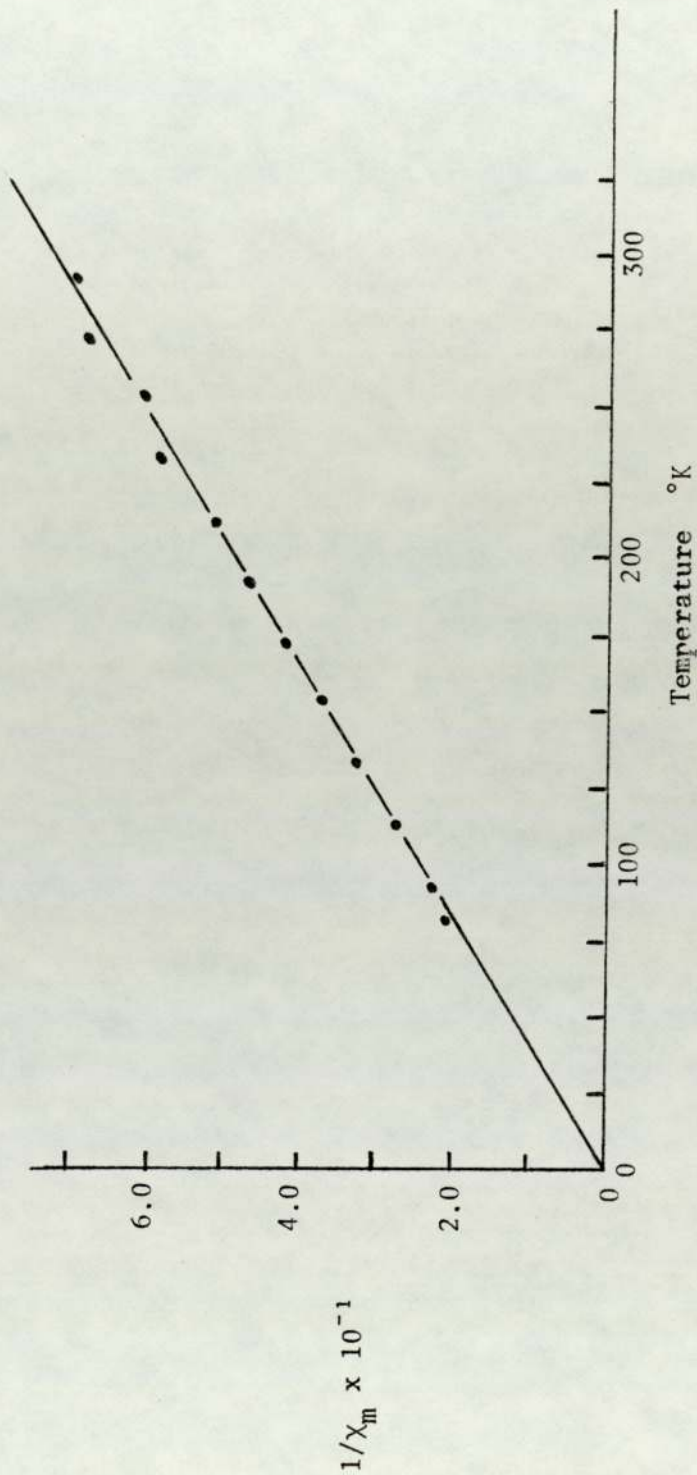
FIGURE 17

room temperature spectrum is not unexpected as tetrahedral species
are often known to give weak room temperature absorption spectra.
The presence of this ion at room temperature is necessary in order
to explain the room temperature magnetic moment of 5.34 Bohr magnetons
as shown in Table 3. The Fe(5MPT)$_2$ site, being low spin, is dia-
magnetic so that the contribution from this site to the overall
magnetic moment is zero.

CHAPTER FOUR

AN INVESTIGATION OF THE ROLE PLAYED BY

TRANSITION METAL IONS IN CERAMIC GLAZES

INTRODUCTION

As stated previously, the general objective of this project is
to provide some scientific information on the reactions that occur
during the firing of ceramic glazes. The work concentrates mainly on
iron glazes which was an idea promoted by the restricted use of lead
in industry. A need for a substitute for lead has, therefore, recently
arisen and iron is considered to be a likely candidate. Iron glazes
are well-known and many examples of both iron (II) and iron (III)
in glaze environments have been studied by Mössbauer spectroscopy.
The usual method of introduction of iron (II) into a glaze is by
reduction of iron (III) which is usually added as haematite. This
work assesses the value of using an inert atmosphere and introducing
the iron as iron (II), thereby preventing oxidation and thereby trapping
iron (II) in glaze environment.

In order to keep more scientific controls over the systems under
study, it was decided at the beginning of the work to use an electric
kiln with a scaled down firing cycle. Although many different types
of kilns and fuels are used throughout Europe, an electric kiln gives
a more controlled heat, which ensures greater reproducibility. The
firing cycle was scaled down largely for convenience as the craft
potter uses cycles which often require 8 to 15 hours heating followed
by slow cooling in order not to damage the article whilst passing
through the various phase transformations of quartz. A three to four
hour heating cycle was found to be convenient as one whole cycle could

be performed easily in a working day. The stoneware glaze firing
temperature range was used which generally speaking is in the region
1,200 °C to 1,280 °C, so that samples were fired at a rate of 400 °C
per hour.

The iron was introduced as iron (II) oxalate dihydrate as this
is a stable iron (II) salt at room temperature which decomposes at
a relatively low temperature, about 300 °C. This salt was preferred
to ferrous chloride or ferrous sulphate which both give unwanted
anions in the fired glaze.

Initially, a soda glass system prepared from reagent grade sodium
carbonate, calcium carbonate and silica was studied. Samples were
fired to various temperatures in air and quickly quenched and Mössbauer
and X-ray results are reported. A more realistic system was then
studied made up from minerals used in the pottery industry. Electron
spin resonance, X-ray diffraction and Mössbauer results are reported
for this system, also fired in air. The mineral system firings were
repeated in an inert atmosphere in order to trap iron (II) in a glaze
environment and the results of these experiments are discussed in the
light of similar systems in which calcium is replaced by strontium.

The investigation was later extended to include copper and chromium
containing glazes in order to see if any further information could be
obtained on the role played by transition metal ions in ceramic glazes.

RESULTS

TABLE I

SUMMARY OF X-RAY DIFFRACTOGRAM RESULTS OF STARTING MATERIALS

Material	Result	Powder Diffraction File Reference
Reagent Grade Silica	Amorphous	--
Reagent Grade Sodium Carbonate	Amorphous	--
Reagent Grade Calcium Carbonate	Calcite + Aragonite	5-0453 17-763
Quartz	α Quartz	5-0490
Potash Feldspar		19-932
Whiting	Calcite	17-763

TABLE II

ATOMIC ABSORPTION RESULTS FOR POTASH FELSDPAR, WHITING AND

REAGENT GRADE CALCIUM CARBONATE

	Potash Feldspar	Calcium Carbonate	Whiting
$\%SiO_2$	64.69	0.00000	0.66000
$\%MnO$	0.00132	0.00148	0.00401
$\%Fe_2O_3$	0.09920	0.00495	0.02005

TABLE III

COMPARISON OF POTASH FELDSPAR SAMPLE WITH POWDER DIFFRACTION DATA CARD 19-932

Potash Feldspar		Card 19-932		Potash Feldspar		Card 19-932	
d value	Intensity	d value	Intensity	d value	Intensity	d value	Intensity
4.21	9	4.22	45	3.29	10	3.29	50
4.02	4			3.24	100	3.24	100
3.96	5	3.96	8	3.18	34		
3.83	6	3.80	20	2.95	6	2.97	14
3.77	5	3.74	14	2.89	6	2.89	8
3.69	5	3.63	6	2.61	3	2.61	6
3.59	3	3.59	4	2.54	4	2.60	14
3.46	10	3.48	16				
		3.47	12				
3.33	13	3.33	14				

TABLE IV

COMPARISON OF QUARTZ SAMPLE WITH POWDER DIFFRACTION DATA CARD 5-0490

Quartz		Card 5-0490	
d value	Intensity	d value	Intensity
6.85	1		
5.00	1		
4.66	2		
4.24	20	4.26	35
3.67	2		
3.55	1		
3.33	100	3.34	100
2.45	8	2.45	12
2.27	7	2.28	12
2.23	3	2.23	6
2.12	1	2.12	9
1.97	11	1.98	6
1.89	3	1.82	17

Quartz		Card 5-0490	
d value	Intensity	d value	Intensity
1.81	1	1.80	1
1.67	8	1.67	7
1.65	1	1.66	3
		1.61	1
1.54	4	1.54	15
1.45	5	1.45	3
		1.42	1
1.38	7	1.38	7
1.37	1	1.37	11
1.37	2	1.37	9

TABLE V

X-RAY DIFFRACTOGRAM RESULTS

Composition	Firing Conditions
10.9% Na_2CO_3	Air
11.1% $CaCO_3$	1,280 °C maximum temperature
58.1% SiO_2	
19.9% $Fe(COO)_2 2H_2O$	

Species Present v Firing Temperature

	Calcite	Aragonite	SiO_2	$Fe(COO)_2 2H_2O$	Other species[a]	
400 °C	√	√	×	×	αFe_2O_3	
600 °C	√	×	×	×	αFe_2O_3	
800 °C	×	×	×	×	αFe_2O_3	
900 °C	×	×	×	×	αFe_2O_3	$CaSiO_3$
1,000 °C	×	×	×	×		$CaSiO_3$
1,200 °C	×	×	×	×		
1,280 °C	×	×	×	×		

[a] CaO could not be detected in any sample. From powder diffraction card 4-0777 it is expected that CaO will give diffraction peaks at d = 2.405, 1.701 and 2.778 with relative intensities of 100%, 45% and 34% respectively.

αFe_2O_3 was identified by diffraction peaks at 2.69, 1.69, 2.51 and 1.83 with relative intensities of 100%, 60%, 50% and 40% (Powder Diffraction Card 13-534).

$CaSiO_3$ was identified by diffraction peaks at d = 3.74, 3.50, 3.30, 2.97 and 2.19 with relative intensities of 80%, 80%, 80%, 100% and 80% respectively.

TABLE VI

X-RAY DIFFRACTOGRAM RESULTS

Composition	Firing Conditions

54.4% Potash Feldspar - $K_2OAl_2O_36SiO_2$ Air   1,280 °C
19.1% Quartz - SiO_2 maximum temperature
10.3% Whiting - $CaCO_3$
16.2% Ferrous Oxalate - $Fe(COO)_22H_2O$

Species Present v Firing Temperature

	Pot.Felds.	Quartz	Calcite	Aragonite	$Fe(COO)_22H_2O$	Other[a]
400 °C	✓	✓	✓	×	×	
500 °C	✓	✓	✓	×	×	αFe_2O_3
600 °C	✓	✓	✓	×	×	αFe_2O_3
700 °C	✓	✓	✓	×	×	αFe_2O_3
800 °C	✓	✓	×	×	×	αFe_2O_3
1,000 °C	✓	✓	×	×	×	αFe_2O_3
1,100 °C	✓	✓	×	×	×	
1,200 °C	✓	✓	×	×	×	
1,280 °C	✓	✓	×	×	×	

[a]   CaO could not be detected in any sample.

TABLE VII

X-RAY DIFFRACTOGRAM RESULTS

Composition   Firing Conditions

(1)   49.2% Reagent Grade $CaCO_3$ 1,000 °C soaked
       50.8% Silica (amorphous)   for 2 hours
                                   in air

(2)   49.2% Reagent Grade $CaCO_3$
       50.8% Quartz

Species Identified	(1) Calcium Carbonate + α Quartz	(2) Calcium Carbonate + Silica
Calcium Carbonate	×	×
Calcium Oxide	✓	×
α Quartz	✓	×
Calcium Silicate	×	✓
Other Species	×	×

TABLE VIII

MOSSBAUER SPECTROSCOPY RESULTS

Composition	Firing Conditions
10.9% Na_2CO_3	Air
11.1% $CaCO_3$	1,280 °C maximum
58.1% SiO_2	temperature
19.9% $Fe(COO)_2 2H_2O$	

Species Identified v Firing Temperature

	Haematite	Unresolved Central Region	Other Components	
400 °C	√	×		
600 °C	√	×		
800 °C	√	√		
900 °C	√	√		
1,000 °C	√	√		
1,100 °C	√	√		
1,280 °C	×	×	δ [a] Δ	
			0.32 0.95	
			0.03 0.97	

[a] δ values with respect to iron metal. Error in δ and Δ 0.03 mm s^{-1}

TABLE IX

MOSSBAUER SPECTROSCOPY RESULTS

Composition	Firing Conditions

54.4% Potash Feldspar - $K_2OAl_2O_36SiO_2$ Air

19.1% Quartz - SiO_2 1,280 °C maximum

10.3% Whiting - $CaCO_3$ temperature

16.2% Ferrous Oxalate - $Fe(COO)_2 2H_2O$

Species Identified v Firing Temperature

	Haematite	Unresolved Components	Other Components	
400 °C	✓	×		
600 °C	✓	×		
800 °C	✓	×		
900 °C	✓	×		
1,000 °C	✓	×	δ [a]	Δ
1,100 °C	✓	×	0.26	0.91
1,280 °C		×	0.28	0.91

[a]   All values in mm s^{-1}, δ with reference to natural iron metal. Error in δ and Δ = 0.03 mm s^{-1}.

TABLE X

Composition of Iron Glaze Recipes

	(a)	(b)	(c)
Potash Feldspar - $K_2OAl_2O_36SiO_2$	54.4	64.2	64.8
Quartz - SiO_2	19.1	22.5	22.7
Whiting - $CaCO_3$	10.3	12.3	12.4
Ferrous Oxalate - $Fe(COO)_2 2H_2O$	16.2	1.9	0.1

Firing Conditions

air, 1,280 °C

Electron spin resonance of these fully matured glazes are given in Figure 2.

TABLE XI

ELECTRON SPIN RESONANCE RESULTS

Composition	Firing Conditions
54.4% Potash Feldspar - $K_2OAl_2O_36SiO_2$	Air
19.1% Quartz - SiO_2	1,280 °C maximum
10.3% Whiting - $CaCO_3$	temperature
16.2% Ferrous Oxalate - $Fe(COO)_22H_2O$	

Type of Resonance Observed v Firing Temperature

	Broad Absorption	Magnetic Hyperfine Absorption
400 °C	✓	✓
500 °C	✓	✓
600 °C	✓	✓
700 °C	✓	✓
800 °C	✓	✗
900 °C	✓	✗
1,000 °C	✓	✗
1,280 °C	✓	✗

TABLE XII

X-RAY DIFFRACTION RESULTS

Composition	Firing Conditions
CaO formed on decomposition[a] of Whiting CaCO₃	900 °C in air

Comparison of X-Ray Diffractogram with Data Card 4-0777 CaO

Product of Whiting Decomposition		Powder Diffraction Card 4-0777	
d value	% relative intensity	d value	% relative intensity
2.79	60	2.778	34
2.40	100	2.405	100
1.70	40	1.701	45
1.44	25	1.451	10
1.39	7	1.390	5
		1.203	4
		1.1036	4
		1.0755	9

[a] Thermal Gravimetric Analysis is illustrated in Figure 6
Electron spin resonance spectrum is illustrated in Figure 7

TABLE XIII

MOSSBAUER AND X-RAY DIFFRACTION RESULTS

Composition

54.4% Potash Feldspar - $K_2OAl_2O_36SiO_2$
19.1% Quartz - SiO_2
10.3% Whiting - $CaCO_3$
16.2% Ferrous Oxalate - $Fe(COO)_22H_2O$

Firing Conditions

Nitrogen Atmosphere
1000 °C
Chamber door sealed
with china clay

X-Ray Result: Species Identified

Potash Feldspar	✓
Quartz	✓
Calcite	✕
Calcium Oxide	✕
Haematite	✓
FeO	✕
Fe_3O_4	✕
Other Species	✕

Mössbauer Result

Magnetic hyperfine spectrum
Six lines at the following
positions:

+ 8.28 mm s^{-1}
+ 5.01
+ 1.60
- 0.91
- 4.39
- 8.01

TABLE XIV

X-RAY DIFFRACTOGRAM RESULTS

Composition	Firing Conditions

55.0% Potash Feldspar - $K_2OAl_2O_36SiO_2$ Nitrogen Atmosphere
18.8% Quartz - SiO_2 with Quartz sagger
10.7% Whiting - $CaCO_3$ 1,280 °C maximum
15.5% Ferrous Oxalate - $Fe(COO)_2 2H_2O$ temperature

Species Present v Firing Temperature

	Pot.Felds.	Quartz	Calcite	Ferrous Ox.	Other Species
400 °C	✓	✓	✓	×	×
600 °C	✓	✓	✓	×	×
800 °C	✓	✓	×	×	×
1,000 °C	✓	✓	×	×	×
1,280 °C	✓	✓	×	×	×

TABLE XV

MOSSBAUER SPECTROSCOPY RESULTS

Composition	Firing Conditions

55.0% Potash Feldspar - $K_2OAl_2O_36SiO_2$
18.8% Quartz - SiO_2
10.7% Whiting - $CaCO_3$
15.5% Ferrous Oxalate - $Fe(COO)_2 2H_2O$

Nitrogen Atmosphere
with Quartz sagger
1,280 °C maximum
temperature

Species Present v Firing Temperature

	Haematite Fe_2O_3	Magnetite Fe_3O_4	Unresolved Components	Other Resolved Components
400 °C	×	✓	×	
600 °C	×	✓	×	
800 °C	×	✓	×	
1,000 °C	×	✓	×	
1,200 °C	×	✓	×	
1,280 °C	×	×	×	$\delta=0.29$ $\Delta=1.16$: $\delta=1.06$ $\Delta=1.99$*

* δ with respect to iron metal.   Error = ±0.03 mm s^{-1}

TABLE XVI

MOSSBAUER SPECTROSCOPY RESULTS

Composition	Firing Conditions

60.5% Potash Feldspar - $K_2OAl_2O_36SiO_2$ Nitrogen Atmosphere in a
21.2% Quartz - SiO_2 Quartz sagger 1,280 °C
11.6% Whiting - $CaCO_3$ maximum temperature
5.0 % Haematite - αFe_2O_3
1.7 % Iron metal - Fe

Species Present v Firing Temperature

	Haematite αFe_2O_3	Iron Metal	Other Components
400 °C	✓	✓	
600 °C	✓	✓	
800 °C	✓	✓	
1,000 °C	×	×	
1,200 °C	×	×	
1,280 °C	×	×	$\delta=1.05$ $\Delta=2.36*$

* δ with respect to iron metal. Error = 0.03 mm s^{-1}
Mössbauer spectra of samples of this glaze recipe
are shown in Figure 10.

TABLE XVII

X-RAY DIFFRACTOGRAM RESULTS

Composition   Firing Conditions

60.5% Potash Feldspar - $K_2OAl_2O_36SiO_2$ Nitrogen Atmosphere in a
21.2% Quartz - SiO_2 Quartz sagger 1,280 °C
11.6% Whiting - $CaCO_3$ maximum temperature
5.0 % Haematite - αFe_2O_3
1.7 % Iron - Fe

Species Present v Firing Temperature

	Potash Feldspar	Quartz	Calcite	αFe_2O_3	Fe	Other Species
400 °C	✓	✓	✓	✓	✓	×
600 °C	✓	✓	✓	✓	✓	×
800 °C	✓	✓	×	✓	✓	×
1,000 °C	✓	✓	Χ	×	×	×
1,280 °C	✓	✓	×	×	×	×

TABLE XVIII

MOSSBAUER SPECTROSCOPY RESULTS

Composition

61.3% Potash Feldspar - $K_2OAl_2O_36SiO_2$
21.5% Quartz - SiO_2
11.7% Whiting - $CaCO_3$
5.4 % Iron - Fe

Mössbauer Parameters v Firing Conditions

Temperature	Atmosphere	Magnetic Component	δ* mm s^{-1}	Δ mm s^{-1}
1,000 °C	Air	Haematite	×	×
1,000 °C	Nitrogen	Iron metal	×	×
1,280 °C	Air	×	0.26	0.91
1,280 °C	Nitrogen	×	0.99	1.78

* with respect to Iron metal. Error = ±0.03 mm s^{-1}

TABLE XIX

MOSSBAUER SPECTROSCOPY RESULTS

Compositions   Firing Conditions

a   b

55.0%   55.0% Potash Feldspar - $K_2OAl_2O_36SiO_2$ 1,280 °C in atmospheres
18.8%   18.8% Quartz - SiO_2 of air or nitrogen
 7.2%   3.6% Whiting - $CaCO_3$
 3.6%   7.2% Strontium Oxalate - $Sr(COO)_2$
15.4%   15.4% Ferrous Oxalate - $Fe(COO)_22H_2O$

Mössbauer Parameters v Firing Conditions

Composition	Atmosphere	δ*	Δ
a	Air	0.32	1.01
a	Nitrogen	0.22 0.96	1.01 1.77
b	Air	0.26	1.09
b	Nitrogen	0.21 0.96	1.00 1.75

* with respect to iron metal.
Error = ± 0.03 mm s^{-1}

TABLE XX

ELECTRON SPIN RESONANCE RESULTS

Composition   Firing Conditions

59.9% Potash Feldspar - $K_2OAl_2O_36SiO_2$ 1,200 °C Maximum
21.0% Quartz - SiO_2 Temperature
11.5% Whiting - $CaCO_3$ Air
 7.5% Copper Oxide - CuO

Types of Signal Obtained v Firing Temperature

	Broad Resonance Width $\simeq$ 1,000 G	Magnetic Hyperfine Spectrum g = 2.006	Cu Glass Resonance
400 °C	✓	✓	×
600 °C	✓	✓	×
800 °C	✓	×	×
1,000 °C	✓	×	×
1,200 °C	×	×	✓

TABLE XXI

X-RAY DIFFRACTION RESULTS

<u>Composition</u>   <u>Firing Conditions</u>

59.9% Potash Feldspar - $K_2OAl_2O_36SiO_2$ 1,200 °C maximum
21.0% Quartz - SiO_2 temperature
11.5% Whiting - $CaCO_3$ Air
 7.5% Copper Oxide - CuO

<u>Species Present v Firing Temperature</u>

	Pot.Felds.	Quartz	Calcite	CuO	Others
400 °C	✓	✓	✓	✓	×
600 °C	✓	✓	✓	✓	×
800 °C	✓	✓	×	✓	×
1,000 °C	✓	✓	×	✓	×
1,200 °C	✓	✓	×	×	×

TABLE XXII

LOW COPPER CONCENTRATION RECIPES

	a	b
Potash Feldspar - $K_2OAl_2O_36SiO_2$	64.2%	64.8%
Quartz - SiO_2	22.5%	22.7%
Whiting - $CaCO_3$	12.3%	12.4%
Copper Oxide - CuO	0.9%	0.1%

TABLE XXIII

X-RAY DIFFRACTION RESULTS

Composition	Firing Conditions

60.1% Potash Feldspar - $K_2OAl_2O_36SiO_2$
20.9% Quartz - SiO_2
12.8% Whiting - $CaCO_3$
 6.2% Copper Oxide - Cu_2O

Air
1,200 °C maximum
firing temperature

Species Present v Firing Temperature

	Pot.Felds.	Quartz	Calcite	Cu_2O	CuO	Others
400 °C	✓	✓	✓	×	✓	×
600 °C	✓	✓	✓	×	✓	×
800 °C	✓	✓	×	×	✓	×
1,000 °C	✓	✓	×	×	✓	×
1,200 °C	✓	✓	×	×	×	×

TABLE XXIV

X-RAY DIFFRACTOGRAM RESULTS

Composition	Firing Conditions

60.1% Potash Feldspar - $K_2OAl_2O_36SiO_2$ Nitrogen Atmosphere
20.9% Quartz - SiO_2 with quartz sagger
12.8% Whiting - $CaCO_3$ Maximum temperature
  6.2% Copper Oxide - Cu_2O 1,200 °C

Species Present v Firing Temperature

	Pot.Felds.	Quartz	Calcite	Cu_2O	Others
400 °C	✓	✓	✓	✓	CuO
600 °C	✓	✓	✓	✓	CuO
800 °C	✓	✓	×	✓	CuO
1,000 °C	✓	✓	×	✓	CuO
1,200 °C	✓	✓	×	×	×

TABLE XXV

X-RAY DIFFRACTOGRAM RESULTS

Composition	Firing Conditions

60.1% Potash Feldspar - $K_2OAl_2O_36SiO_2$ Nitrogen Atmosphere
20.8% Quartz - SiO_2 with quartz sagger
12.7% Whiting - $CaCO_3$ 1,200 °C maximum
 3.7% Copper Oxide - CuO   temperature
 2.7% Copper - Cu

Species Present v Firing Temperature

	Pot.Felds.	Quartz	Calcite	CuO	Cu	Others
400 °C	✓	✓	✓	✓	✓	Cu_2O
600 °C	✓	✓	✓	✓	✓	Cu_2O
800 °C	✓	✓	×	✓	✓	Cu_2O
1,000 °C	✓	✓	×	✓	✓	Cu_2O
1,200 °C	✓	✓	×	×	×	×

TABLE XXVI

X-RAY DIFFRACTOGRAM RESULTS

Composition	Firing Conditions

59.8% Potash Feldspar - $K_2OAl_2O_36SiO_2$

20.8% Quartz - SiO_2

13.0% Whiting - $CaCO_3$

 6.4% Copper - Cu

Nitrogen Atmosphere
with quartz sagger
1,200 °C maximum
temperature

Species Present v Firing Temperature

	Pot.Felds.	Quartz	Calcite	Copper	Others
400 °C	✓	✓	✓	✓	Cu_2O CuO
600 °C	✓	✓	✓	✓	Cu_2O CuO
800 °C	✓	✓	✗	✓	Cu_2O CuO
1,000 °C	✓	✓	✗	✓	Cu_2O CuO
1,200 °C	✓	✓	✗	✗	✗

Composition of Cu(II)-Sr Glazes

	(a)	(b)	(c)
Potash Feldspar - $K_2OAl_2O_36SiO_2$	59.9%	59.9%	59.9%
Quartz - SiO_2	21.0%	21.0%	21.0%
Whiting - $CaCO_3$	7.5%	5.1%	3.4%
Copper Oxide - CuO	7.5%	7.5%	7.5%
Strontium Oxalate - $Sr(COO)_2$	4.0%	6.4%	8.1%

TABLE XXVII

COMPOSITION OF SOME CHROMIUM-STRONTIUM CONTAINING GLAZES

	a	b	c	d
Potash Feldspar - $K_2OAl_2O_36SiO_2$	56.8%	56.8%	56.8%	56.8%
Quartz - SiO_2	22.0%	22.0%	22.0%	22.0%
Whiting - $CaCO_3$	9.1%	6.9%	3.4%	1.2%
Strontium Oxalate - $Sr(COO)_2$	1.3%	3.5%	7.0%	9.2%
Chromium Trioxide - CrO_3	10.8%	10.8%	10.8%	10.8%

Visible spectra of samples a and d firing in air to 1,200 °C are given in Figure 28.

	e
Potash Feldspar - $K_2OAl_2O_36SiO_2$	59.9%
Quartz - SiO_2	22.1%
Strontium-Chromium Oxide - Sr_2CrO_4	17.9%

Visible spectrum of sample e fired to 1,200 °C is compared to some acidic Cr(III) solution spectra in Figure 24.

4.1 X-RAY ANALYSIS OF GLAZE SYSTEMS FIRED IN AIR

Simple glaze recipes were prepared and fired as outlined in the experimental section and X-ray powder diffractogram traces were obtained for all the starting materials as well as for samples at different stages of firing. Table I summarises the results obtained for the starting materials. Diffraction patterns could not be obtained for samples of the reagent grade sodium carbonate and silica used in the preparation of the soda glass, indicating that these samples are amorphous. The reagent grade calcium carbonate was shown to be a mixture of two common crystallographic forms of calcium carbonate, calcite and aragonite. Whiting on the other hand was shown to consist only of one of the crystallographic forms, calcite, although elemental analysis shows that it also contains some silica impurity, Table II. No silica could be detected by X-ray diffraction probably due to the low concentration of this impurity.

X-ray powder diffractogram traces of potash feldspar and quartz were analysed and compared with similar samples reported in the powder diffraction file. Table III indicates that the potash feldspar used in the present work is similar to the sample reported in the diffraction file, card 19-932, whilst Table IV indicates that the quartz used in the present work is clearly the alpha form.

The diffractogram results for samples of the soda glass recipe fired to different temperatures in air are summarised in Table V. Ferrous oxalate could not be detected in a sample fired to 400 °C,

indicating that thermal decomposition is complete by this temperature.
Haematite diffraction peaks can be detected in all samples heated
from 400 °C to 900 °C indicating that this is the major iron containing
species throughout this stage of the firing. In samples fired above
900 °C, the haematite peaks are no longer evident, indicating that
interaction of haematite with other components of the system has
occurred. Careful analysis has shown, however, that no other iron
containing crystalline species, such as ferrates, can be detected in
samples heated above 900 °C. This may only reflect the fact that the
average particle size of such species is small, rather than the fact
that they are amorphous.

The aragonite to calcite phase transformation was seen to occur
between 400 °C and 600 °C which is in agreement with published[45] data
which reports that it occurs at 510 °C. The decomposition of calcite
is shown to occur between 600 °C and 800 °C, although in a sample
fired to 800 °C, no calcium containing species can be detected.
Samples heated to 900 °C and 1,000 °C did nevertheless contain a small
amount of calcium silicate, $CaSiO_3$, but the fully matured green glass
formed at 1,280 °C was shown to be totally amorphous.

Samples of the mineral glaze recipe fired to various temperatures
show a marked contrast to those of the soda glass system so far as the
X-ray data is concerned , Table VI. The decomposition of ferrous
oxalate dihydrate is seen to occur as previously reported below 400 °C
although with this system, haematite could not be identified in a
mineral glaze sample fired to 400 °C. The intensity of X-ray diffraction
peaks is dependent on particle size as reported by Gallagher et al[21],

so it is to be expected that haematite, freshly formed on the decomposition of ferrous oxalate, will give low intensity reflections. The total amount of crystalline material in the mineral glaze system is far greater than the amount in the soda glass system which contains an appreciable amorphous content. The fact that haematite can be identified in a soda glass recipe heated to 400 °C and not in the mineral recipe heated to the same temperature is considered to be purely a matter of resolution. The small haematite diffraction peaks in the diffractogram trace of the highly crystalline mineral glaze recipe cannot be resolved, whereas this is possible in the largely amorphous soda glass system. This problem does not occur with samples fired to 500 °C and above, presumably because the average particle size increases due to a sintering process and the more intense diffraction peaks can therefore be resolved.

The mineral glaze sample heated to 1,000 °C gives a diffractogram trace which indicates that haematite is still present. This is in contrast to the soda glass system for which no iron containing species could be identified in a sample heated to this temperature, indicating that haematite interacts with other components in the soda glass system at a lower temperature than in the mineral glaze system.

The decomposition of whiting in the mineral glaze system occurs between 700 °C and 800 °C although no other calcium containing species, such as calcium oxide or calcium silicate, could be identified in samples heated to any higher temperature. Again this is in contrast to the soda glass system, results for which indicate that small amounts of calcium silicate are present in samples fired to 900 °C and

1,000 °C.

There does, therefore, appear to be a difference in the mode of interaction of the quartz-whiting containing recipe compared to the silica-calcium carbonate containing recipe, not only in the way that these two sets of components interact with each other, but also in the way that haematite interacts with the two systems.

4.2   X-RAY ANALYSIS OF CALCIUM CARBONATE-SILICA SYSTEMS

The above results led to a separate investigation being undertaken in order to shed some light on this problem. Calcium carbonate (i.e. reagent grade) was mixed in a 1:1 ratio with firstly quartz and then silica and both samples were fired for two hours at 1,000 °C. The X-ray diffractogram results are given in Table VII.

Little crystalline structure could be detected in the calcium carbonate-silica mixture. No calcium oxide could be found and the small diffractions recorded were identified as being due to the presence of a small amount of calcium silicate. In contrast to this the diffractogram trace of the calcium carbonate-quartz mixture showed the presence of a number of sharp diffraction peaks which were found to be due to a mixture of calcium oxide and α quartz. No silicate species were detected.

This result is important for two reasons. Firstly, calcium oxide could not be detected during either the firing of the soda glass recipe or the mineral glaze recipe suggesting that either it does not crystallize in large enough particles to be detected, after its formation from the thermal decomposition of calcium carbonate, or that it interacts with other species in the system. The fact that calcium oxide can be detected in a heated mixture of calcium carbonate and quartz at 1,000 °C indicates that it is not its small particle size that prevents its detection in these systems. This is considered to be strong evidence for the fact that it interacts with other species in the glaze recipe systems. Secondly, this result indicates a marked difference in behaviour between amorphous silica and quartz at elevated temperatures with respect to their reaction with calcium oxide. These conclusions may be significant in view of the observation reported above that haematite interacts with the soda glass system at a lower temperature than it interacts with the mineral glaze system. On the other hand, this result is not conclusive as the different behaviour of haematite in the two systems may be due to the fact that sodium carbonate is present in the soda glass sytem and not in the mineral glaze system. A powder diffractogram trace could not be obtained for the reagent grade sodium carbonate so no information could be obtained by this technique on any possible sodium carbonate-haematite interactions.

4.3 MOSSBAUER RESULTS OF GLAZE SYSTEMS FIRED IN AIR

Mössbauer spectra were obtained for samples of the soda glass system fired in air to various temperatures and the results are given in Table VIII. The decomposition of ferrous oxalate is complete on firing to 400 °C. Ferrous oxalate gives a single quadrupole split spectrum with an isomer shift of 1.24 mm s^{-1} with respect to natural iron and a quadrupole splitting of 1.70 mm s^{-1}. The characteristic six line magnetic hyperfine spectrum obtained for a sample fired to 400 °C confirms the X-ray diffraction result that ferrous oxalate decomposes in air to form haematite. This is the only iron containing species that can be identified in any sample fired up to 800 °C. Samples fired to 800 °C and above in air give spectra that contain a very messy central region in which the distribution of the counts recorded in these particular channels was significantly greater than in the baseline. Computation of the Mössbauer data could not successfully resolve any structure in this region which is presumably due to a superimposition of many spectra due to the presence of iron (III) in many different environments. The area of this central region, which it should be noted obscured the two innermost magnetic hyperfine lines, increases at the expense of the outer four magnetic hyperfine lines of haematite as the firing temperature is increased from 800 °C to 1,100 °C. These results are interpreted as being due to haematite interacting with other components in the system above 800 °C so that the iron (III) ions slowly enter their glass sites, although this process is not complete until 1,280 °C. The Mössbauer parameters

of the fully matured soda glass formed on firing to 1,280 °C indicate that the iron (III) cations occupy two sites. The isomer shift data 0.32 mm s^{-1} and 0.03 mm s^{-1} are consistent with iron (III) in octahedral and tetrahedral environments. Generally, tetrahedral iron (III) compounds have less positive isomer shifts than octahedral iron (III) compounds and it is thought that this is the case here also. The most likely explanation for this is that there is a degree of overlap of electronic orbitals between the iron (III) cations and the oxygen anions. In an octahedral environment the donation of ligand p electrons into metal orbitals that are effectively sp^3d^2 hybridised, so that six ligands donate electrons into orbitals that have one sixth s character. In a tetrahedral environment, the metal orbitals involved in any overlap are sp^3 hybridised so that four ligands donate electrons into orbitals that have one quarter s character. The degree of donation into the metal s orbitals so far is equal in both the octahedral and the tetrahedral case. The difference occurs when the metal ligand distance is considered. The metal cations effectively occupy octahedral and tetrahedral holes respectively. In a close packed array of spheres the tetrahedral holes are considerably smaller than the octahedral holes so that the degree of overlap of the orbitals is greater in the tetrahedral case. This means that the s electron density at the iron nucleus is greater in the tetrahedral case, due to a greater contribution from the 4s orbital, than in the octahedral case. A greater electron density in ^{57}Fe Mössbauer spectroscopy is reflected in a more negative isomer shift due to the negative sign of $\delta R/R$.

The Mössbauer results for samples of the mineral glaze system are different to the results obtained for the soda glass system for the iron (III) cations appear to enter their glass sites at different temperatures, Table IX. A sample fired to 400 °C gave a characteristic six line hyperfine spectrum indicating the presence of haematite. This was found to be the only iron containing species that could be detected in the mineral glaze system even in samples fired up to 1,000 °C. A sample fired to 1,100 °C gave a six line magnetic hyperfine spectrum superimposed upon a two line central doublet for which the isomer shift parameter was found to be 0.26 mm s^{-1} with respect to iron metal and the quadrupole splitting parameter was found to be 0.91 mm s^{-1}. A sample fired to 1,280 °C formed a fully mature green glass which gave a Mössbauer spectrum containing no magnetic component but only a quadrupole split doublet. (δ = 0.28 mm s^{-1}, Δ = 0.91 mm s^{-1}) This is interpreted as being due to iron (III) in an octahedral environment. So in contrast to the Mössbauer parameters obtained for the soda glass system, it appears that haematite does not interact with any part of the system until the temperature of firing is above 1,000 °C and that the iron (III) in the fully matured glaze obtained on firing to 1,280 °C occupies octahedral positions only with no tetrahedral component. It is interesting to note that the temperature at which potash feldspar melts has been reported to be 1,100 °C[46], so it may be that the haematite has to wait for the potash feldspar to melt before it can interact with any component of this system. Further justification for this conclusion is that there are no tetrahedral iron sites in the fully matured glaze. Feldspars have very rigid three dimensional ring structures comprising silica tetrahedra in which every fourth silicon cation is replaced by an

aluminium cation. The silicon and aluminium cations are therefore in tetrahedral sites. Potassium cations in this case (i.e. potash feldspar) and oxygen anions fill interstitial sites between the ring structures in six co-ordinated positions. X-ray studies of the fully matured mineral glaze indicate that most of the diffraction peaks associated with potash feldspar are still present and that it does not interact sufficiently with the other components of the system either to render it totally amorphous or to significantly alter its crystalline structure. Presumably the initial step in the melting process of potash feldspar is the migration of the six co-ordinated cations and anions rather than the breakdown of the strong silicate structure. It is these six co-ordinated positions that are taken up by the iron (III) cations. The temperature of firing of this system is not so high as to lead to a complete break-down of the feldspar lattice as indicated by X-ray work, Table VI, so that substitution of iron (III) for silicon or aluminium is not possible and there are therefore no tetrahedral sites.

The fact that tetrahedral iron (III) sites are present in the soda glass system as well as the fact that haematite interacts with the soda glass system at much lower temperatures than in the mineral glaze system could be taken to be due to the different reactivity of amorphous silica compared to quartz, although no X-ray evidence for any haematite-silica species can be found, such as Fe_2SiO_5. Although such interactions are possible, it should also be remembered, as stated previously, that one important difference between the two glaze recipes is that the soda glass recipe contains sodium carbonate whilst the mineral glaze recipe does not. The presence of sodium

carbonate may well affect the melting points of other components making the soda glass recipe a much less refractory system.

Comparison of the Mössbauer parameters of the octahedral site for the mineral glaze, δ = 0.28 mm s^{-1}, Δ = 0.91 mm s^{-1} with the octahedral site for the soda glass, δ = 0.32 mm s^{-1}, Δ = 0.95 mm s^{-1}, shows that within experimental error ($\pm$ 0.03 mm s^{-1}), the parameters are not significantly different. The isomer shifts are both well within the range expected for octahedral iron (III) and the quadrupole splitting parameters indicate that the ligand environment is distorted from perfect octahedral symmetry. Generally there are two contributions to the electric field gradient, one from the valence shell and one from the ligand environment. High spin iron (III) has a spherically symmetrical electronic environment so that there is no valence contribution to the electric field gradient. The quadrupole splitting is generated therefore by a distortion of the ligand field environment from regular octahedral symmetry.

4.4 ELECTRON SPIN RESONANCE OF GLAZE SYSTEMS FIRED IN AIR

Electron spin resonance studies of the two glaze systems were undertaken in order to see if any useful information could be obtained as octahedral iron (III) in a magnetically dilute environment under certain circumstances can be expected to give sharp resonance absorption signals. The exact position and shape of the derivative

form of the electron spin resonance signal can give information on
the discreet environment of the cation. The electron spin resonance
spectra obtained for a fully matured mineral glaze and a fully
matured soda glass are shown in Figure 1, together with a spectrum
of a sample of haematite. No sharp signals were obtained in any of
these three cases. This is to be expected for haematite in which
the iron (III) cations are not in a magnetically dilute environment.
The magnetic moment of each ion is incapable of interacting independ-
ently with an applied magnetic field as interaction of neighbouring
moments with each other occur to form a system of complex magnetic
behaviour. Haem atite acts as an antiferromagnet below 263 °K as
does $Fe_2Cl_4(dipyam)_3O5H_2O$ at room temperature as reported in chapter
three.

The overall iron concentration in the soda glass and in the
mineral glaze is much lower than in pure haematite, around 10%
compared with 69.8% and such internal magnetic behaviour as described
above is not expected. It was expected that each iron (III) cation
would act independently as a simple paramagnet and that the spectra
obtained would be similar to those reported by Castner et al[32] in a
study of iron (III) in glass systems. It was thought that perhaps
an iron (III) concentration of around 10% was a little high in order
for the ions to interact independently so glasses were prepared with
around 1% Fe(III) and 0.1% Fe(III), Table X. The electron spin
resonance spectra of these samples are shown in Figure 2. These
spectra were similar to the 10% iron concentration glaze spectrum
and little improvement in resolution could be obtained even when
going down to iron concentrations so low that the mineral glaze

ESR Spectra of (a) mineral glaze (b) soda glass, both fired to 1,280 °C, compared to esr of a sample of haematite (c)
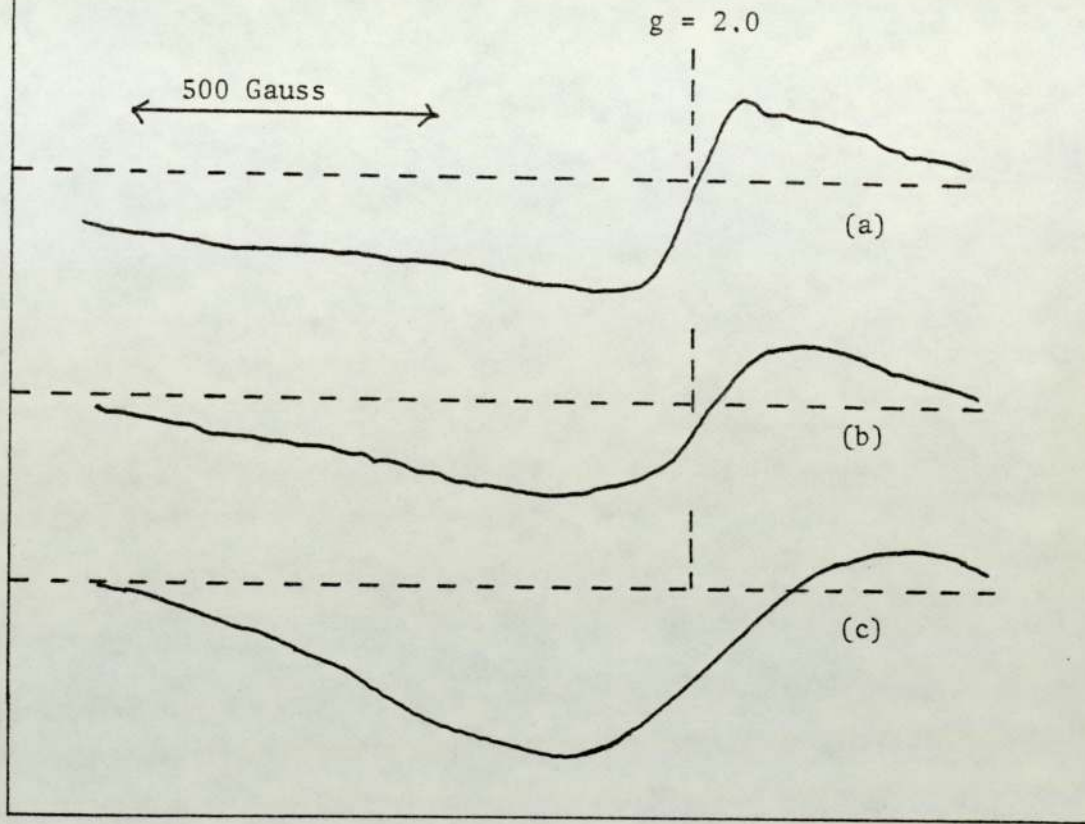

g = 2.0

500 Gauss

(a)

(b)

(c)

FIGURE 1

ESR Spectra of mineral glazes containing (a) 1%, (b) 0.1% Fe(III)
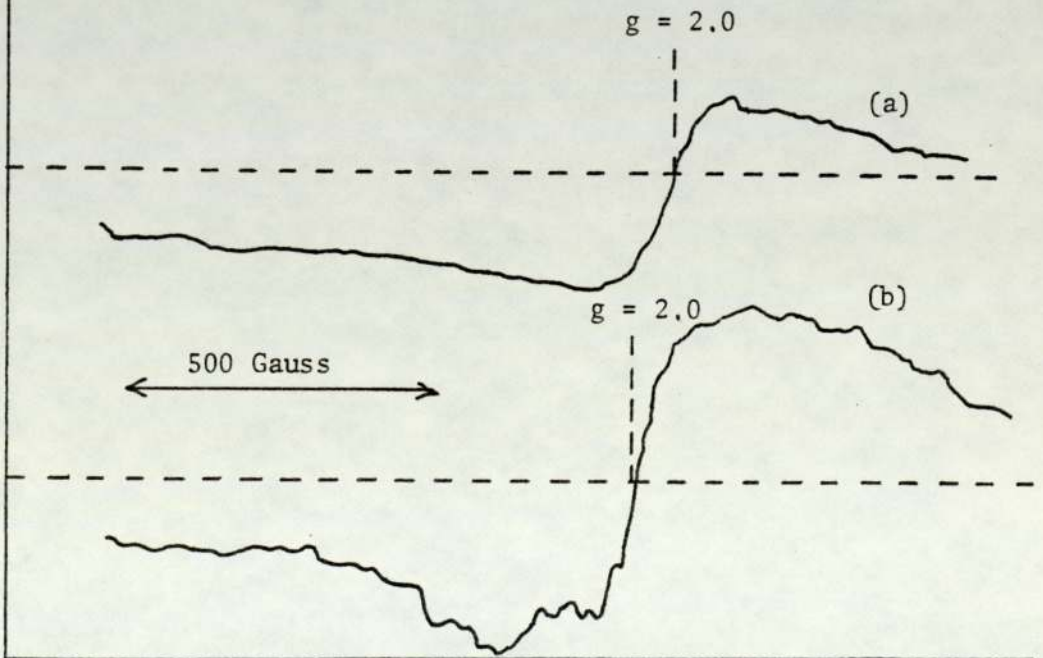

g = 2.0

(a)

g = 2.0

(b)

500 Gauss

FIGURE 2

appeared white to the naked eye as opposed to the dark green appear-
ance of the 10% iron containing glaze. It could well be the case that
when the concentration of iron is reduced the effective average metal-
metal interionic distance is not altered to any significant degree.
If this is the case, then this indicates that the fully matured glaze
is by no means a completely homogeneous mixture but consists of areas
of either crystalline or non-crystalline iron containing components
embedded in the overall glass matrix. However there are other reasons
why no sharp signals can be observed in the electron spin resonance
of iron containing glasses, as outlined by Castner et al. The most
likely explanations are that, firstly, the crystal field terms are
comparable in magnitude to the magnetic terms and with random
orientation, the spectrum is spread over many g values and secondly
that the values of D and E are both large in which case the same
sort of effect occurs. This is considered likely to be the case when
iron (III) is in a network modifying position, however it is still
interesting to note that no signal could be obtained from the soda
glass even though the Mössbauer result unambiguously identified the
presence of a tetrahedral site.

The electron spin resonance of samples of the mineral glaze
system and the soda glass sytem fired to a number of different
temperatures were also studied, initially to see if the difference
in the behaviour of haematite in the two systems could be monitored
by this technique. The broad resonance obtained at higher firing
temperatures was observed in all cases but with samples of the
mineral glaze system, a complex multiline resonance was obtained in
certain samples superimposed upon the former absorption as indicated

g = 2.006

100 gauss
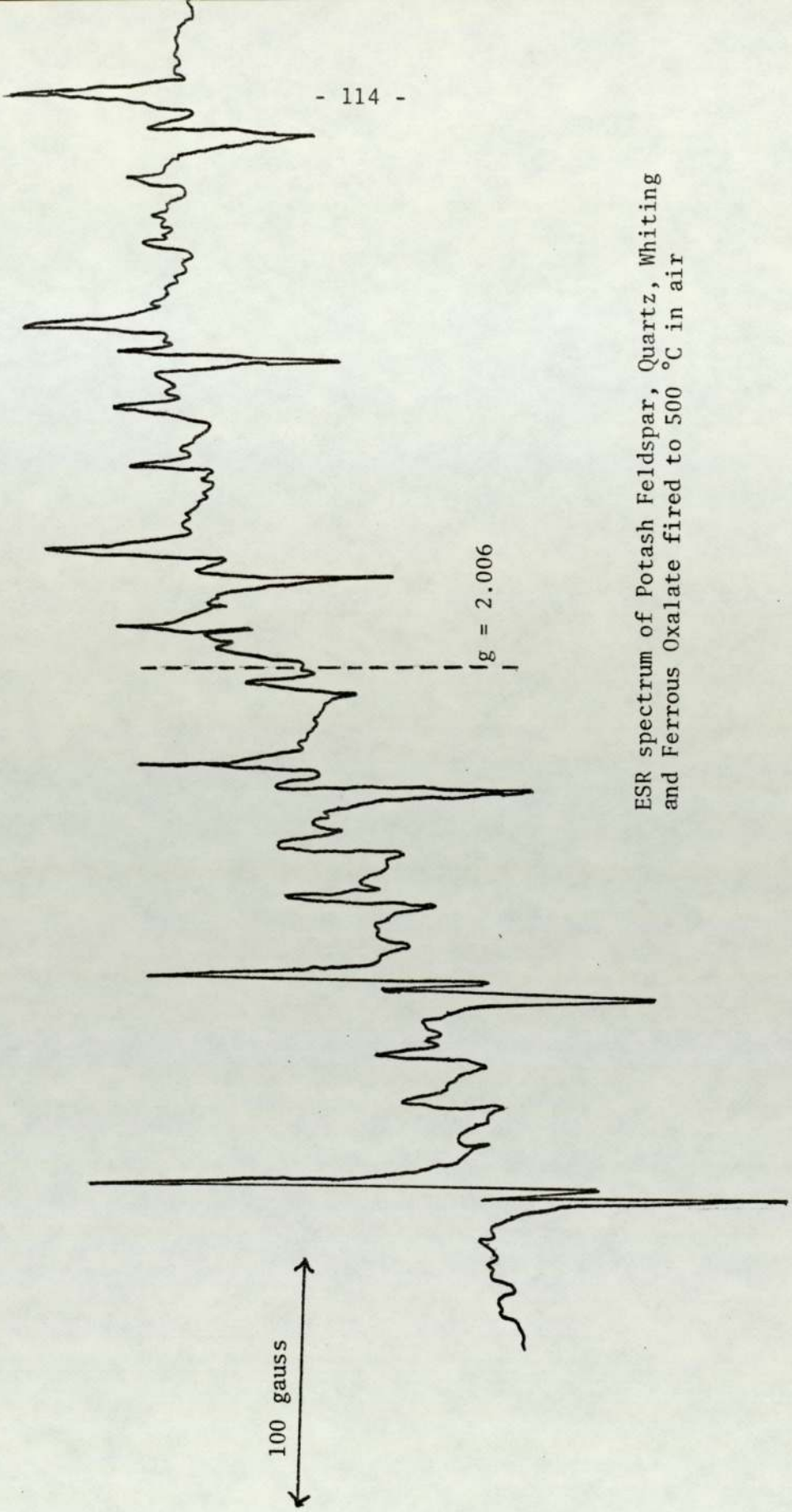
ESR spectrum of Potash Feldspar, Quartz, Whiting
and Ferrous Oxalate fired to 500 °C in air

FIGURE 3

in Table XI and illustrated in Figure 3. The multiline resonance could not be observed in any sample fired above 700 °C. Electron spin resonance spectra of the starting materials indicated that this signal comes from the mineral form of calcium carbonate, whiting.

The reagent grade calcium carbonate gave an extremely weak signal which could not be observed when the compound is diluted to the extent that it is in the soda glass recipe. Atomic absorption results for samples of the two sources of calcium carbonate are given in Table II. Whiting is shown to contain a small amount of silica as well as a much higher concentration of manganese than reagent grade calcium carbonate. The multiline electron spin resonance is attributed to the presence of manganese (II) which substitutes for some of the calcium cations in the crystal lattice. The nuclear spin of ^{55}Mn, which is present to 100 percent in naturally abundant manganese, is 5/2. The nuclear spin couples with the ground and excited electronic states to give six hyperfine lines of equal intensity. The electronic spin multiplicity of manganese (II) is 6, but under the influence of a crystal field, the degeneracy is partially lifted so that it splits into three sets of Kramers doublets, Figure 4. The degeneracy of the three sets of doublets is lifted only by the application of a magnetic field and it is the $M_S = +\frac{1}{2}$ to $M_S = -\frac{1}{2}$ transition that is normally observed at $g = 2.0$ as indicated in Figure 5. Coupling of the nuclear spin with the ground state Kramers doublets gives six hyperfine lines as indicated for $\Delta M = \pm 1$, $\Delta I = 0$. The weaker intensity lines are due to spin forbidden transitions where the nuclear spin quantum number changes simultaneously with the resonance absorption.

FIGURE 4

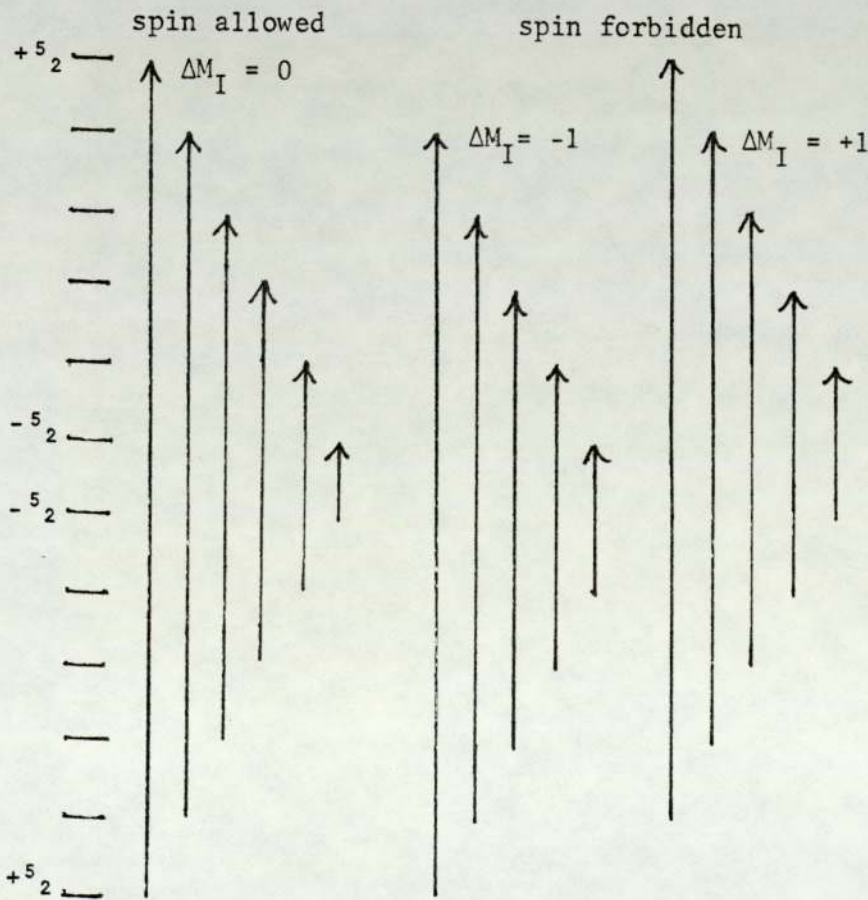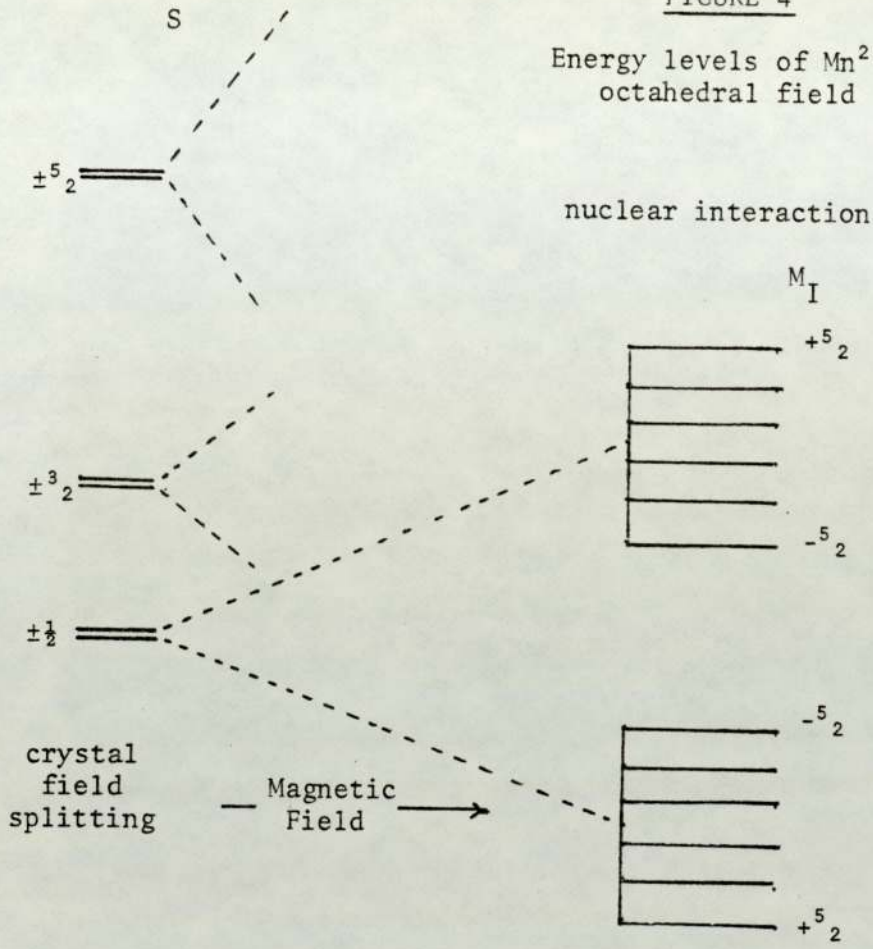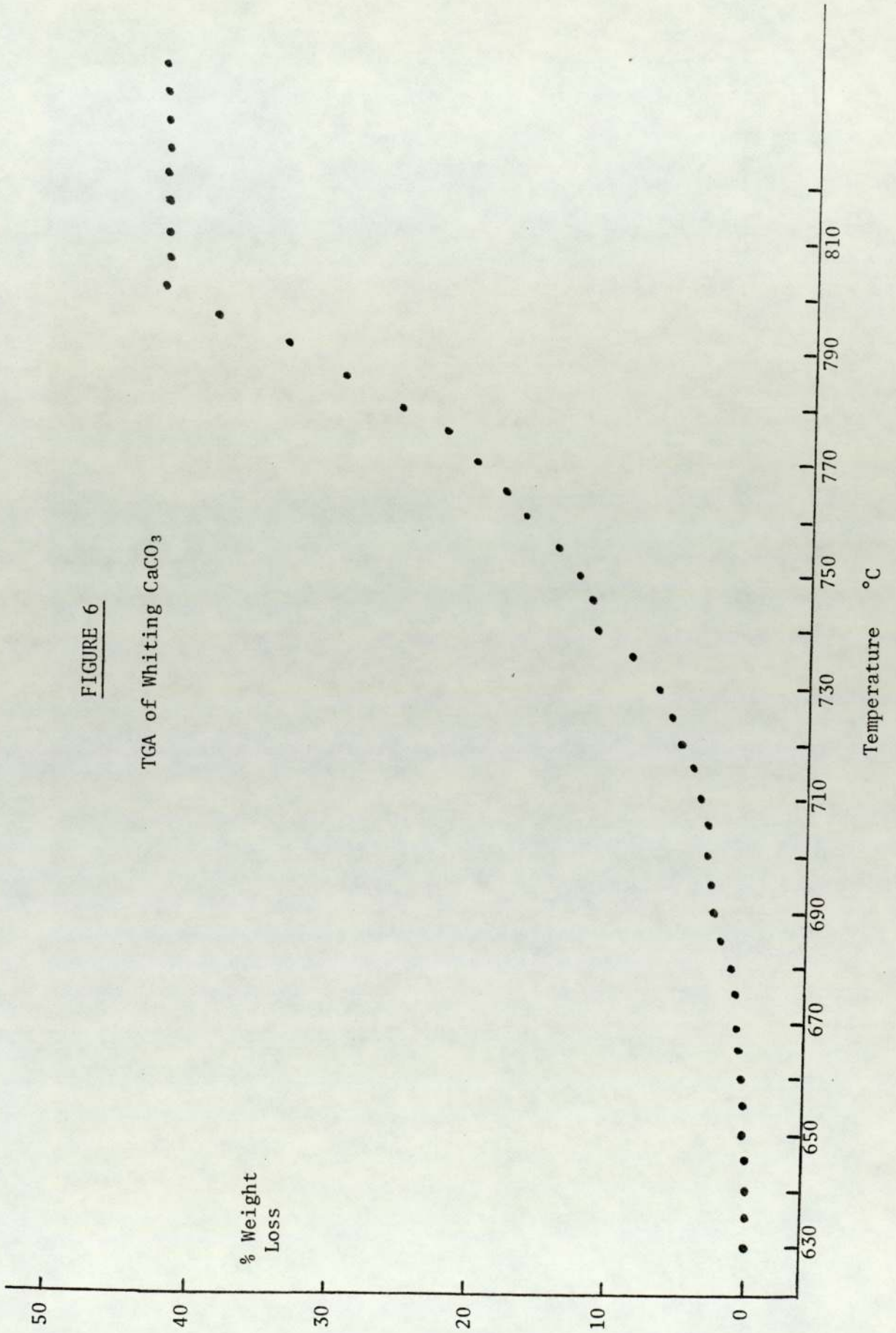Energy levels of Mn^{2+} in
octahedral field

nuclear interaction

M_I

S

$\pm^5_2$

$+^5_2$

$\pm^3_2$

$-^5_2$

$\pm\frac{1}{2}$

$-^5_2$

crystal
field
splitting

— Magnetic
Field →

$+^5_2$

spin allowed   spin forbidden

$+^5_2$

$\Delta M_I = 0$ FIGURE 5

$\Delta M_I = -1$ $\Delta M_I = +1$

$-^5_2$

$-^5_2$

$+^5_2$

FIGURE 6

TGA of Whiting $CaCO_3$

% Weight Loss

Temperature °C

The disappearance of the electron spin resonance signal in samples fired to above 700 °C was thought at first to be due to thermal oxidation of manganese (II) to manganese (IV). Thermal gravimetric analysis of whiting, however, showed that thermal decomposition of calcite occurs between 650-800 °C as shown in Figure 6, and that the calcium oxide formed on the decomposition gave a characteristic six line electron spin resonance spectrum with very weak forbidden transitions, Figure 7. Also a clearly identifiable X-ray powder diffractogram was obtained as outlined in Table XII. The non-appearance of the calcium oxide resonance signal in the firing of the mineral glaze recipe further confirms the X-ray result that calcium oxide does not crystallise out in this system. The calcium ions in some way interact with other components of the system such that no X-ray information can be obtained and such that the environment of the calcium ions, and therefore the manganese ions, if they are assumed to undergo the same chemistry, is modified so that no electron spin resonance spectrum can be obtained.

4.5 METHODS OF PREVENTION OF OXIDATION OF FERROUS OXALATE

The mineral glaze recipe was fired in an inert atmosphere to a number of different temperatures to evaluate the possibility of trapping ferrous ions from the ferrous oxalate in a glass matrix. This method is not usually used by craft potters or technologists who prefer to introduce iron in the trivalent form and reduce to the ferrous state

ESR of Whiting
CaCO₃ containing
an Mn²⁺ impurity

g = 2.006

ESR of CaO
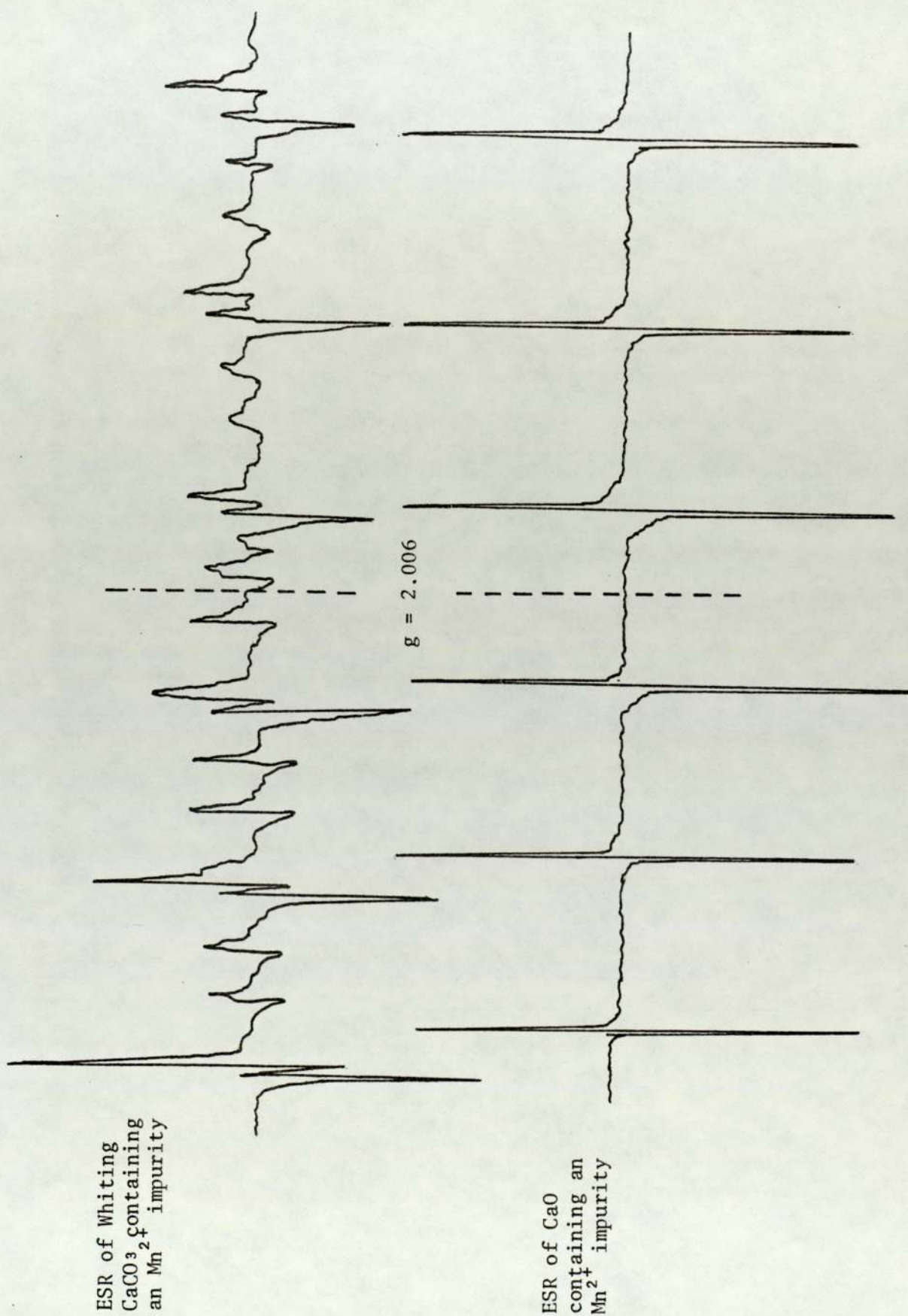containing an
Mn²⁺ impurity

FIGURE 7

by changing the kiln atmosphere at a specific stage in the firing cycle. The chamber of the Carbolite furnace used throughout the course of this work was flushed with a steady stream of nitrogen gas as outlined in chapter two. To minimise leakages and in order to reduce the quantity of nitrogen being used, the furnace door was sealed with wet china clay in a manner similar to methods used by some craft potters to confine a reducing atmosphere and prevent any 'contamination' by air. A positive nitrogen pressure was applied throughout the duration of the firing cycles. Although this procedure represented quite a realistic model in comparison to the potters full scale firings in which the door is generally sealed with cement, it was not very practical as the clay cracked frequently , which meant that the furnace had to be monitored throughout the whole of the firing cycle and some of the cooling cycle. Samples of the mineral glaze system were fired to a number of different temperatures and the light red colour of the quenched samples in all cases indicated that haematite was probably present. This was confirmed by both X-ray diffraction and Mössbauer spectroscopy as indicated by a typical sample in Table XIII.

It was found therefore that the firing technique had to be modified if any success was to be achieved. To further minimise leakages a small quartz beaker was commissioned and was fitted with a quartz tube in such a way as to provide an inner chamber as indicated in Figure 8.

This technique appeared to be successful as a black glaze maturing below 1,280 °C was produced. Samples fired to lower temp-
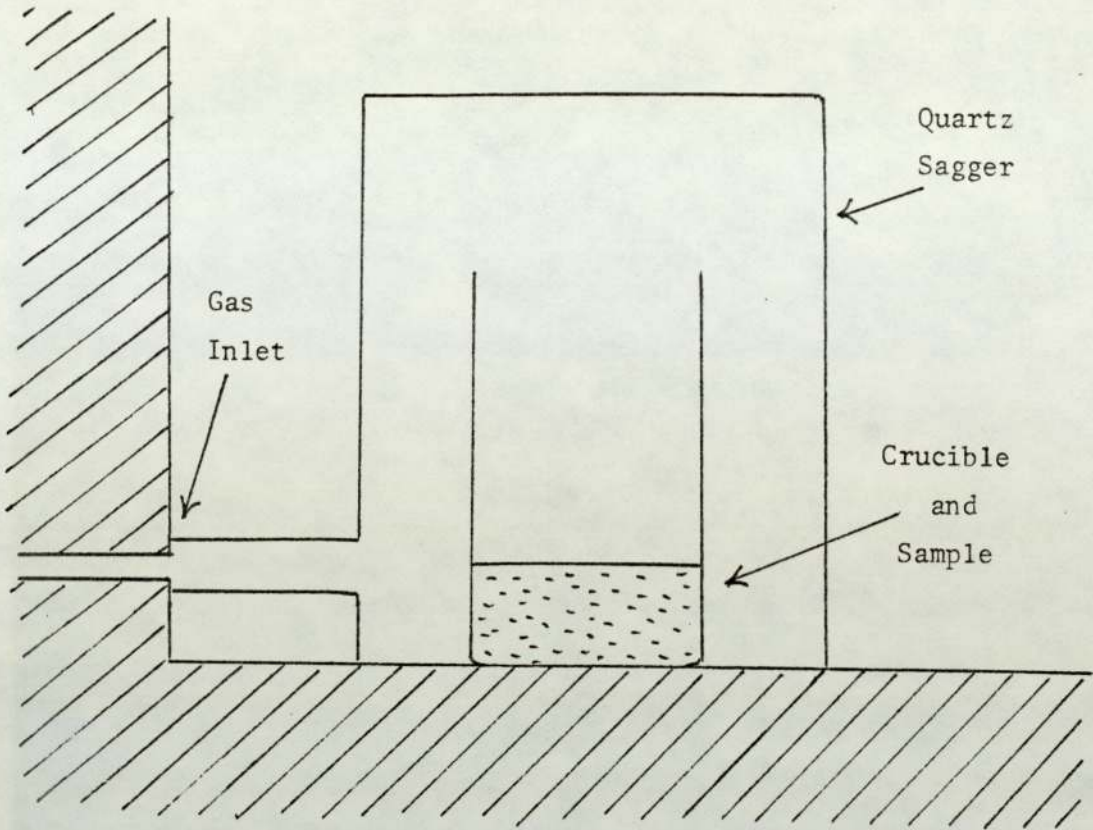
FIGURE 8

eratures were grey in colour indicating that oxidation of ferrous oxalate to haematite probably did not occur. Samples fired to 1,200 °C in nitrogen did not form a fully matured glaze but formed hard dull black solids. After a number of firings, it was noted that a surprisingly small amount of nitrogen could produce the same results, a large BOC cylinder at 2,200 psi pressure lasting for approximately three firings to 1,280 °C.

4.6 X-RAY ANALYSIS OF MINERAL GLAZE RECIPE FIRED IN NITROGEN

X-ray diffraction results for a series of samples of the mineral glaze recipe fired in a nitrogen atmosphere are given in Table XIV. The potash feldspar and quartz diffraction patterns were again evident in the fully matured glaze, formed on firing to 1,280 °C, as they were also in a sample fired to the same temperature in air. The decomposition of calcite was found to occur between 600 °C and 800 °C as expected and no calcium containing species could be detected in samples fired above 800 °C as is the case when the same recipe is fired in air. But maybe rather surprisingly, no other crystalline species could be detected in samples fired above this temperature. The diffraction peaks due to haematite usually found at d values 2.69, 2.51 and 1.69, were all absent in samples fired under nitrogen which were light grey in colour compared with light red when fired in air. The powder diffraction file reports that ferrous oxide gives diffraction peaks at d = 1.52, 1.51 and 1.29 with relative respective intensities of 100%, 100% and 60% or can give a diffraction pattern with peaks at d = 2.15, 2.49 and 1.52 with relative intensities of 100%, 80% and 60% respectively. No evidence of either of these two forms of ferrous oxide could be detected in any of the samples fired under a nitrogen atmosphere. Similarly, two forms of magnetite, Fe_3O_4, are reported in the powder diffraction file. One form is reported to give diffraction peaks at d = 2.53, 1.49 and 2.97 with relative intensities of 100%, 40% and 30%, whilst another form is reported to give diffraction peaks at d = 2.44, 1.43 and 1.56 with relative respective intensities of 100%, 50% and 40%. Again no evidence of

either of these two forms of magnetite could be detected. The diffraction traces were carefully analysed and no other unidentified peaks were observed in any of the diffractogram traces of samples belonging to this system. As stated previously, the non-appearance of diffraction peaks is due either to the very small crystal particle size of the species formed after the decomposition of ferrous oxalate or is due to the fact that amorphous phases are being encountered with no long range order.

4.7 MOSSBAUER SPECTRA OF THE MINERAL GLAZE RECIPE FIRED IN NITROGEN

Mössbauer spectra were obtained for samples of the mineral glaze system fired to various temperatures up to 1,280 °C under nitrogen. The position of the absorption peaks in the multiline magnetic hyperfine spectra obtained for all samples fired to 1,200 °C indicate conclusively the presence of magnetite, Fe_3O_4. Haematite gives a characteristic six line spectrum at room temperature provided that the average particle size is greater than 13 Å . The six lines are due to the magnetic hyperfine interaction and in careful measurements a small quadrupole splitting can also be observed. Ferrous oxide gives a broad doublet which can be resolved into a number of quadrupole split components, although the exact result depends upon the stoichiometry of the particular sample. Magnetite, on the other hand, has previously been reported[47] to give a multiline magnetic hyperfine spectrum although this is not so well understood as the six line

hyperfine spectrum obtained from bulk samples of haematite. The
magnetite spectrum has traditionally been interpreted in terms of
two distinct magnetic hyperfine interactions due to iron in two
distinct crystallographic sites. More recent work has indicated that
the system is not so simple as the widths of the two sets of
absorption peaks have been shown to be significantly different.
This was thought to be due to an electron hopping process between
iron (III) and iron (II) sites, although other workers using electric
conductivity measurements[48] report that this is not possible. It has
more recently been suggested that the larger widths are due to two
possible values of the electric field gradient with possibly some
magnetic anistropy.

It is clear that the Mössbauer spectrum of magnetite is not well
understood, however Mössbauer spectroscopy is being used in the present
work purely to identify the iron containing species involved in the
firing of ceramic glazes and in this respect it is far superior to
X-ray crystallography which is only able to indicate the presence or
absence of haematite.

It is interesting to note, as shown in Table XV, that magnetite
is still present in a mineral glaze sample fired to 1,200 °C in an
atmosphere of nitrogen, but is completely absent in a sample fired to
1,280 °C which forms a fully matured black glaze. The Mössbauer
parameters for this sample are $\delta_1 = 0.29$ mm s^{-1}, $\Delta_1 = 1.16$ mm s^{-1},
$\delta_2 = 1.06$ mm s^{-1}, $\Delta_2 = 1.99$ mm s^{-1}. These results are interpreted as
being due to iron in two sites, both octahedral, the site with the
larger isomer shift and quadrupole splitting being Iron (II) and the

other being Iron (III). It appears therefore that the decomposition of ferrous oxalate occurs below 400 °C under nitrogen to give small particles of magnetite which do not interact with any other component in the system until the temperature has exceeded 1,200 °C, when it then interacts and becomes trapped in a glass environment on cooling.

Hedges[10] has published data on the Mössbauer parameters of a number of old Chinese glazes and the Mössbauer parameters for the mineral glaze system fired under nitrogen are compared in Figure 9 with data for a mirror black Chinese glaze which Hedges also inter- prets as being consistant with the presence of both octahedral iron (II) and octahedral iron (III). The agreement between these two sets of parameters is quite good considering that there is no way of knowing exactly the nature of the raw materials used by the Chinese. These could adventitiously have been quite similar to the materials used in the present work although the two sets of Mössbauer results may indicate that the exact nature of the glass forming matrix is un- important and that the environment of the iron cations is determined by the nature of the iron oxide.

Comparison of Mössbauer Data with a Mirror Black Chinese Glaze

| Mineral glaze recipe fired under nitrogen 1,280 °C		Mirror Black reported by R.E.M. Hedges	
$\delta*$	Δ	$\delta*$	Δ
0.29 ± 0.03	1.16 ± 0.03	0.30	1.29
1.06 ± 0.03	1.99 ± 0.03	1.08	2.02

* with respect to iron metal

FIGURE 9

Other evidence for this is that the Mössbauer parameters of the octahedral iron site in the chemical glaze system described previously are quite similar to those for the octahedral iron (III) site in the mineral glaze system, even though the nature of the glass forming matrix in the two examples is quite clearly different. It may well be the case that instead of the iron (II) and iron (III) cations migrating to suitably sized holes in the network former and becoming entrapped on cooling, that the fluid glass matrix is able to accommodate an ion of any size by being a fairly open structure when molten, fairly permeable to ion migration, which closes up on cooling to an extent determined to some degree by the size of the entering ion.

4.8 $Fe^{o}-Fe^{III}$ CONTAINING RECIPES

The black colour of the glaze formed when the mineral glaze system is fired in a nitrogen atmosphere is to be expected, considering that iron is present in two oxidation states, charge transfer resulting in the absorption of a large portion of the visible region of light. Black glazes are highly valued from an aesthetic point of view in the ceramic world although iron (II) is also noted for giving aesthetically pleasing rich blue glazes. Ferrous oxalate does not appear to be a good starting material for obtaining a blue glaze in view of the fact that under nitrogen it decomposes to give an oxide containing iron in two oxidation states which are subsequently both trapped within a glass environment.

Bhatt[49] has reported a method of introducing iron (II) into glass by the action of iron metal on iron (III) already present in the glass. The following equilibrium is set up:

$$Fe^{o} + 2Fe^{III} \rightleftharpoons 3Fe^{II}$$
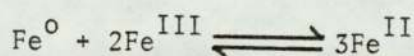
In view of this, stoichiometric amounts of iron metal and haematite were mixed together with whiting, potash feldspar and quartz in the usual proportions to see if the Bhatt equilibrium could be set up in a glaze whilst firing under a nitrogen atmosphere. Samples were fired to various temperatures between 400 °C and 1,280 °C and the Mössbauer results are given in Table XVI. Figure 10 shows the Mössbauer spectra for samples of this system fired to different temperatures. All samples fired to 800 °C and below were red powders suggesting the presence of haematite. The sample fired to 1,000 °C was found to be a grey powder whilst a very dark blue solid was formed on firing to 1,200 °C and a rich blue fully matured glaze was formed on firing to 1,280 °C. The similarity in the Mössbauer parameters of the sample fired to 1,000 °C with the sample fired to 1,280 °C is striking considering that the former is a grey powder and the latter a rich blue fully matured glaze. Both samples give Mössbauer parameters consistent with iron (II) in an octahedral environment. No Iron (III) could be detected in this system in samples fired to 1,000 °C or above so that the reaction of iron metal with a stoichiometric amount of haematite appears to go to completion between 800 °C and 1,000 °C. The rate of temperature increase during the firing process is about 400 °C per hour so that this reaction in fact goes to completion in less than half an hour in the furnace. The similarity of the spectrum
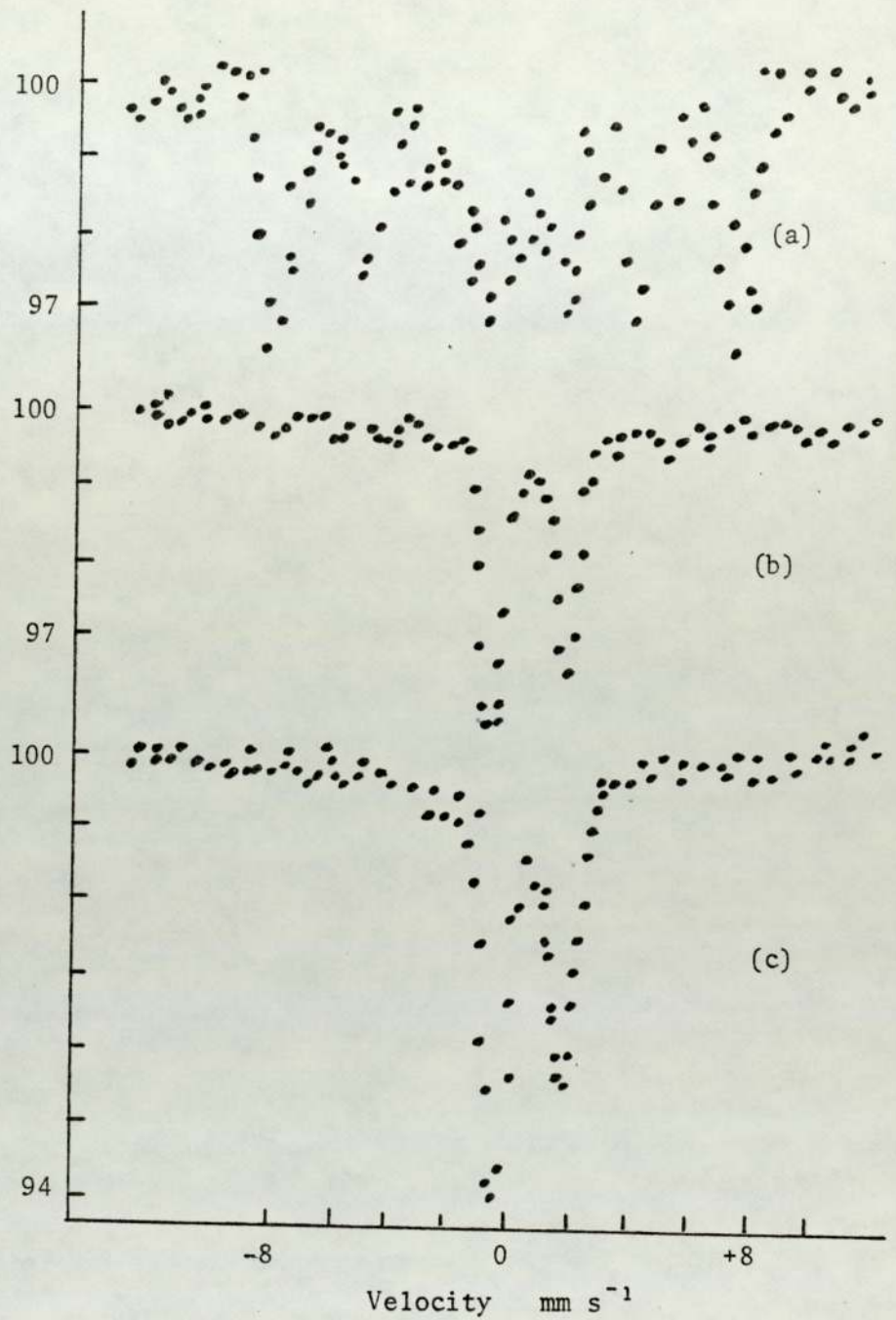
Mössbauer spectra of glaze recipes containing Fe metal
and Fe_2O_3 fired under nitrogen to (a) 800 °C, (b) 1000 °C
and (c) 1,280 °C

FIGURE 10

of a sample fired to 1,280 °C with a sample fired to 1,000 °C indicates that the immediate local environment of the iron (II) ions in the glaze is determined a long time before glass formation occurs. The potash feldspar may have no other role than that of physically trapping the iron (II) species in a glassy environment, or on the other hand, migration of the anions and cations that are situated between the three dimensional ring structure of the feldspar may occur and these then could facilitate the interaction between the iron metal and the haematite. Quartz is unlikely to play any role in the electron transfer process as not only has its lack of reactivity already been demonstrated at these temperatures when considering the interaction between it and calcium carbonate, but crystalline quartz is present to a large extent in the fully matured glaze, Table XVII. The only other species present in the system is calcium oxide formed upon the decomposition of whiting. As in all the glaze recipe systems considered so far, no calcium oxide could be detected either by X-ray diffraction or electron spin resonance techniques after the decomposition of whiting. It might well be the case, therefore, that the iron metal-haematite interaction occurs indirectly through a reaction with small particles of calcium oxide and that the Mössbauer spectra obtained after firing to 1,000 °C and above are due to a form of calcium iron (II) oxide. Nevertheless, no X-ray diffraction data can be obtained for any such species and no electron spin resonance signal can be obtained for the manganese impurity in calcium carbonate which would presumably become entrapped in any calcium ferrate structure.

Figure 11 compares Mössbauer parameters for the iron (II) site in the mineral glaze recipe fired to 1,280 °C, using ferrous

oxalate as a means of introduction of iron, with the iron (II) site in the mineral glaze fired under the same conditions, but with a stoichiometric amount of iron metal and haematite in place of the ferrous oxalate.

Comparison of Mössbauer Parameters of Iron (II) Sites in Glazes

Method of Iron Introduction	δ*	Δ
Ferrous Oxalate	1.06 ± 0.03	1.99 ± 0.03
Haematite + Iron Metal	1.05 ± 0.03	2.36 ± 0.03

* with respect to iron metal

FIGURE 11

The isomer shifts of the two sites are identical within experimental error, but the quadrupole splitting parameters, although both within the range expected for Iron (II), are significantly different. In both glaze systems, the nature and percentage composition of the glass former are the same although the environments of the ions are different indicating that structurally there is definitely some dependence upon the form of introduction of iron into the system.

Iron metal was added to a mineral glaze recipe and fired both under nitrogen and in air to 1,000 °C and 1,280 °C. The Mössbauer results for these four samples are given in Table XVIII.

There is no difference in the Mössbauer parameters of the resultant glaze when iron is introduced as ferrous oxalate and fired

in air compared to when it is introduced as iron metal and then fired in air. This is to be expected as ferrous oxalate has already been shown to decompose below 400 °C in air to form haematite. Iron metal oxidizes when heated in air to form haematite so that in both these cases, iron (III) is being introduced into the glaze as haematite. In contrast to this is the Mössbauer result obtained when iron is introduced in the metallic form under an atmosphere of nitrogen. Iron metal can be detected in a sample fired under nitrogen to 1,000 °C by its distinct six line hyperfine spectrum which is immediately distinguishable from the six line magnetic hyperfine spectrum of haematite. But, on the other hand, a sample fired under nitrogen to 1,280 °C gave a spectrum which indicated that all the iron was present in the glaze in the ferrous state. The Mössbauer results for the pale green glaze are similar to those reported by Hedges for a pale green Celadon glaze as indicated in Figure 12.

Comparison of Mössbauer Data with a Pale Green Celadon Glaze

	$\delta*$	Δ
Pale Green Celadon	1.12 mm s^{-1}	1.81 mm s^{-1}
Iron metal fired in Nitrogen to 1,280 °C	0.99 ± 0.03 mm s^{-1}	1.78 ± 0.03 mm s^{-1}

* with respect to iron metal

FIGURE 12

Hedges also reports the presence of a tetrahedral site with Mössbauer parameters $\delta = 0.69$ mm s^{-1} and $\Delta = 1.38$ mm s^{-1}, however no tetrahedral site could be detected in the present work.

Comparison of the Mössbauer results obtained when iron metal is introduced under nitrogen into the glaze with the two cases considered previously (i.e. haematite and iron metal under nitrogen, and ferrous oxalate under nitrogen), provides further evidence for the fact that the method of introduction of the transition metal ion is of great importance in determining its environment in the fully matured glaze. This is illustrated in Figure 13.

Comparison of Mössbauer Parameters of Iron Containing

Glaze Recipes Fired Under Nitrogen to 1,280 °C as a

Function of Method of Introduction

Method of Introduction	δ*	Δ
Ferrous Oxalate	0.29 ± 0.03 mm s^{-1}	1.16 ± 0.03 mm s^{-1}
	1.06 ± 0.03 mm s^{-1}	1.99 ± 0.03 mm s^{-1}
Haematite and Iron metal	1.05 ± 0.03 mm s^{-1}	2.36 ± 0.03 mm s^{-1}
Iron metal	0.99 ± 0.03 mm s^{-1}	1.78 ± 0.03 mm s^{-1}

* with respect to iron metal

FIGURE 13

However, the non-appearance of crystalline calcium oxide suggests that this species may have an active role in determining the final glaze structure. There is some evidence to suggest that calcium containing species can be formed at high firing temperatures as $CaSiO_3$ has been identified in samples of the soda glass system fired to 900 °C and 1,000 °C, whilst there is some Mössbauer evidence for haematite interaction with the mineral glaze recipe when samples are fired in

air to a temperature just below the glass formation temperature.
Also the system containing a stoichiometric amount of Iron metal and
haematite shows curious behaviour in that the iron (II) environment
is determined between 800 °C and 1,000 °C even though samples fired
to this temperature are fine powders showing little sign of glass
formation. This glaze does not fully mature until it has been fired
up to 1,280 °C. This evidence strongly implies that calcium oxide
formed on the decomposition of calcium carbonate has some role in
structure determination. No calcium iron containing intermediate
species in mineral recipes could be detected by any spectroscopic
technique but that is not to say such species do not form even if
only immediately prior to glass formation. The different environments
of Iron observed when it is introduced in different forms may there-
fore be due not to a difference in the way that the original iron
containing species interact with the glass matrix, but due to a
difference in the way that the original iron species react with
calcium oxide, the products of which subsequently dissolve in the
glass matrix.

4.9 STRONTIUM-IRON CONTAINING GLAZES

Shteinberg[4] has suggested that the structure determining species
in glazes and glasses are the group (II) metal cations and not, as
is conventionally thought to be the case, the silicate species. It
was decided to see if any evidence could be obtained for this in the

present work. Also this is of particular interest in respect to the conclusion made in the previous section that calcium ions may have an important structure determining role. Iron was introduced into the glaze recipes as before in the form of ferrous oxalate and firings were performed in both air and nitrogen with different ratios of calcium to strontium to see if the Mössbauer parameters could reflect any changes in structure. The results are given in Table XIX and these indicate that in the systems studied, no differences in structure could be observed, indicating that the immediate environment of iron (II) and iron (III) in the glaze systems studied is not affected by the presence of different group (II) metal cations. This is not be say, however, that the overall structure of the glazes are the same. The transition metal ions in ceramic glazes are invariably surrounded by an environment of oxygen anions. The chemical isomer shift is a measure of the s electron density at the iron nucleus so is sensitive to the nature of the chemical bonds between the iron cations and their surrounding anions. It is not to be expected that an iron cation would have a group (II) cation as one of its nearest neighbours. Neither is it to be expected that an ion that is not a nearest neighbour could affect the s electron density at the iron nucleus so the fact that the chemical isomer shift does not appear to be sensitive to strontium and calcium concentration is not, therefore, too surprising.

The quadrupole splitting parameter is a measure of the principal component of the electric field gradient tensor which interacts with the quadrupole moment of the iron nucleus. For an iron (III) cation which has a spherically symmetrical electronic ground state, the

sign, magnitude and direction of the electric field gradient tensor is determined purely by contributions from ligands. In a glaze environment in which it is to be expected that the ferric ion is surrounded by oxygen anions only, there is only an electric field gradient if the symmetry is lower than cubic. Hence a ferric ion in a cubic environment would not be expected to give a quadrupole split spectrum. If on the other hand a departure from cubic symmetry occurs, then a quadrupole splitting is to be expected due to the different contributions from ligands situated at different average distances. This is illustrated for the case of axial symmetry in Figure 14. This situation is typical of those encountered for iron (III) in an octahedral glass site. If some of the oxygen anions that contribute towards the electric field gradient are situated adjacent to group (II) cations, then it is reasonable to suppose that the distortion in the iron environment is generated by the group (II) cations. If this is so, then changing the group (II) cation should purely from steric considerations alter the distortion of the iron environment. Under these circumstances, then, the substitution of strontium for calcium should be reflected in the magnitude of the quadrupole splitting.

Iron (II) presents a more complex problem so far as the quadrupole splitting parameter is concerned, for as well as a ligand contribution to the electric field gradient, there is also an electronic contribution. In a cubic environment, Iron (II) exhibits no quadrupole splitting as the t_{2g} orbitals are degenerate and are equally populated, so the electronic contribution averages to zero. But under axial symmetry for example, some of the degeneracy of the t_{2g} orbitals is removed and the electronic population of the three t_{2g} orbitals is

cubic symmetry   axial symmetry
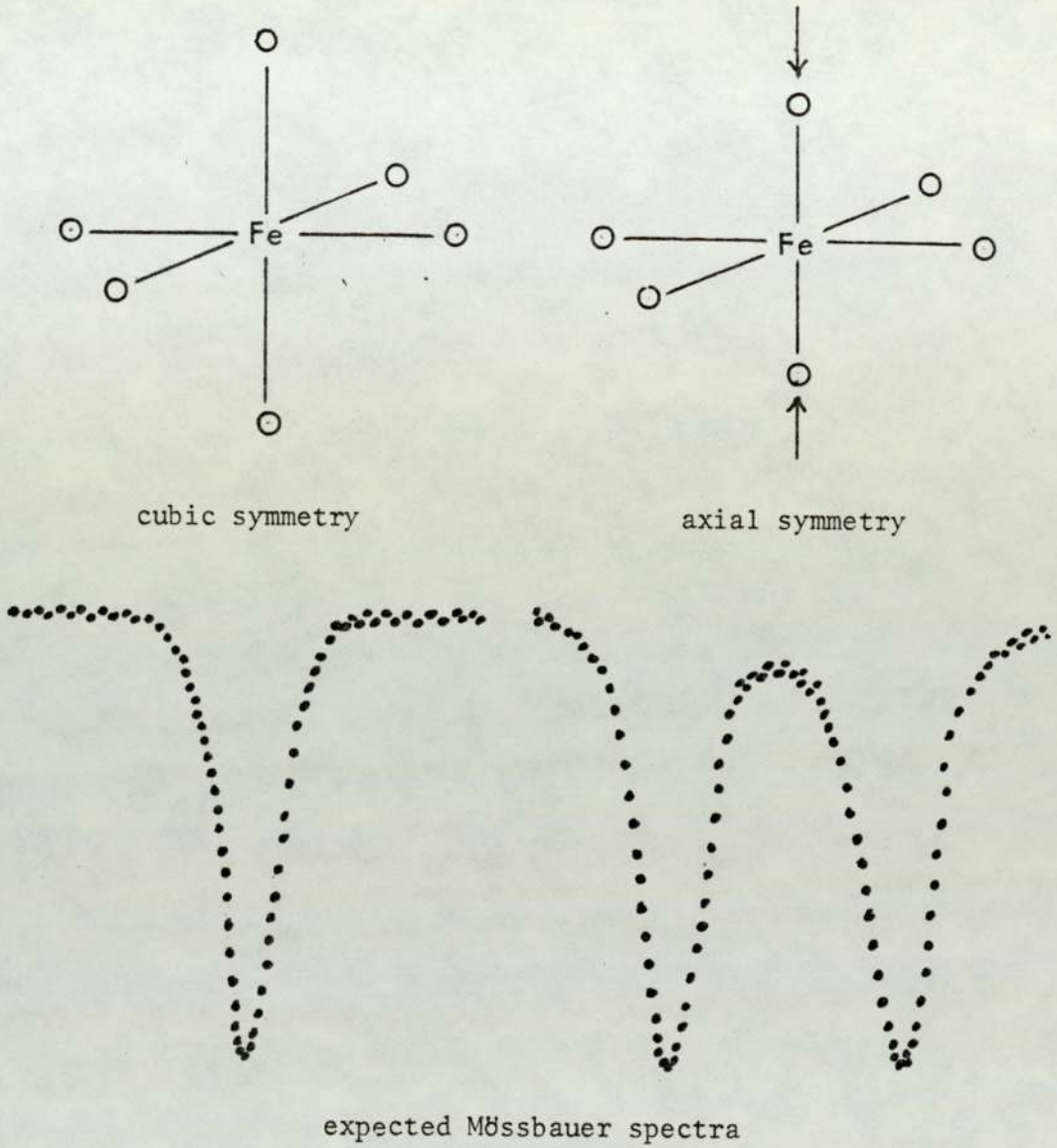
expected Mössbauer spectra

FIGURE 14

unequal. This generates an electronic contribution to the electric
field gradient, as illustrated in Figure 15.

This electronic contribution to the electric field gradient is
highly temperature and structure dependent but there is no reason to
suppose that it has the same sign or direction as the ligand contri-
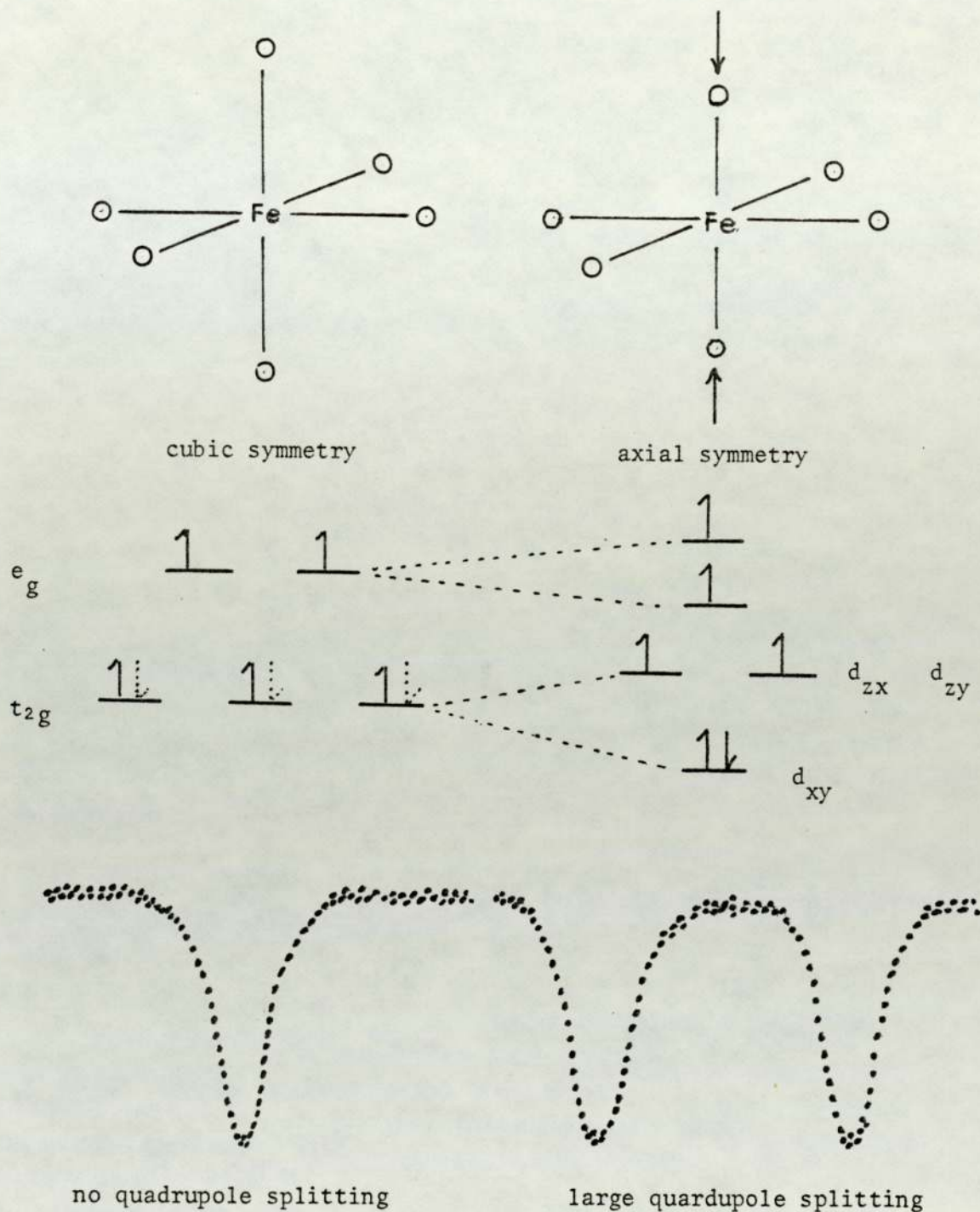
cubic symmetry   axial symmetry

no quadrupole splitting   large quardupole splitting

FIGURE 15

bution so that the behaviour of Iron (II) is not so easy to predict
as that of Iron (III). But as is the case with iron (III), if the
group (II) cations are adjacent to the oxygen anions that surround
the Mössbauer atom, then changing the composition of the group (II)

component should have a considerable effect upon the quadrupole splitting.

The Mössbauer results for strontium containing glazes are given in Table XIX and can be compared to the results in Tables IX and XV for samples containing no strontium. The quadrupole splitting parameter, Δ, for samples fired in air show a small increase on increase in strontium concentration; 0.91 mm s^{-1} for the strontium free glaze recipe to 1.01 mm s^{-1} for the 3.6% strontium oxalate containing recipe and 1.09 mm s^{-1} for the 7.2% strontium oxalate containing recipe. The quadrupole splitting parameter of the Iron (II) site in samples fired under nitrogen differ from 1.99 mm s^{-1} for the strontium free case to 1.77 and 1.75 mm s^{-1} in the strontium containing glazes, the last two parameters being the same within experimental error. Similarly the quadrupole splitting parameters of the iron (III) sites in glaze samples fired under a nitrogen atmosphere are slightly reduced on the addition of strontium.

The isomer shift parameters of samples fired in air are the same within experimental error whilst they just fall outside the experimental error ranges for samples fired under nitrogen. The dependence of the Mössbauer parameters of the samples studied on strontium concentration is extremely small. No marked changes were observed on the addition of strontium and little significance is placed upon the small variation in the quadrupole splitting parameters.

The fact that the quadrupole splitting is independent of the relative concentrations of either calcium or strontium suggests that

the sort of system oulined above does not occur in glazes prepared from ferrous oxalate in the present work, in either an atmosphere of air or an atmosphere of nitrogen. This tends to suggest that the iron containing component of the glaze does not become entrapped in the glass matrix in the form of small crystallites in which the iron cations are preferentially situated adjacent to group (II) metal cations.

The Mössbauer results do not necessarily contradict Shteinberg's results for, firstly, it may well be the case that the group (II) cations do modify the silicate structure. The Mössbauer results indicate that the group (II) cations do not directly modify the environment of either the iron (II) or iron (III) sites in the final glass. Secondly, the result of the present work does not eliminate an indirect effect in which the group (II) oxides interact with different iron oxides to form a variety of intermediates depending upon the nature of the iron oxide. However, in the systems studied, no differences in any such interaction could be observed by substituting strontium for calcium.
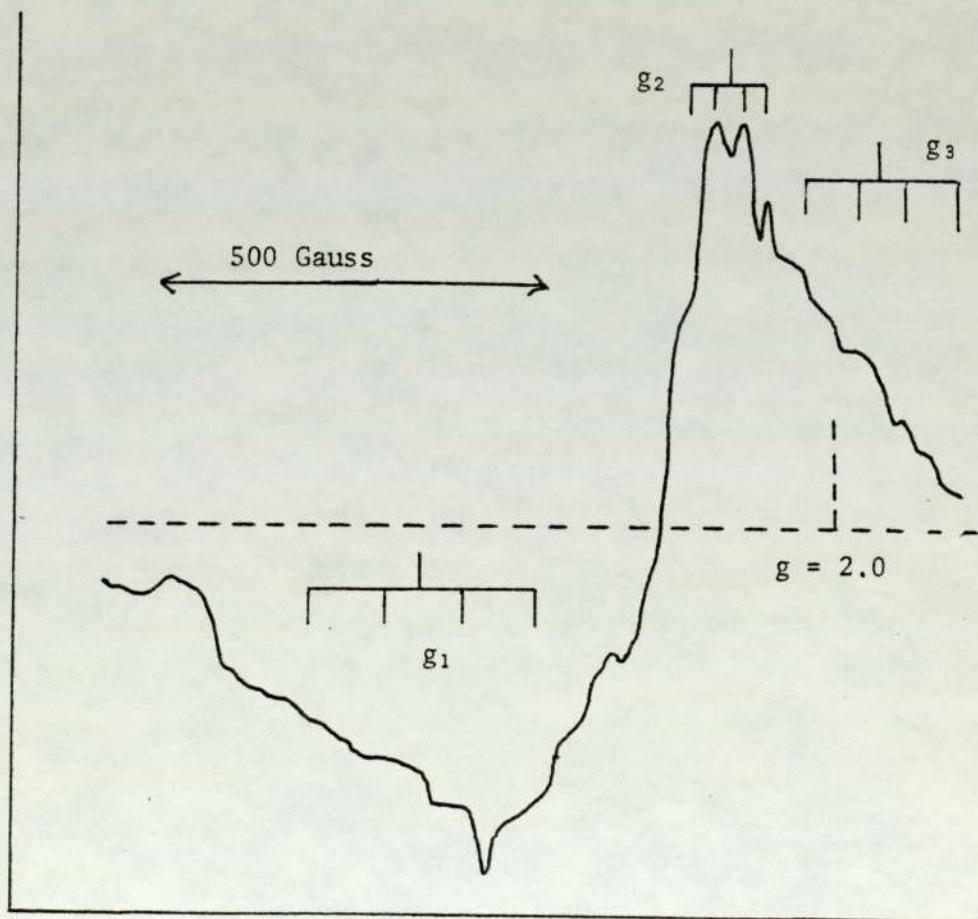
4.10 COPPER CONTAINING GLAZES

4.10.1 Copper (II) Glazes

The investigation of the role of transition metal ions in ceramic glazes was extended to include copper. Copper (II) oxide was added to a mixture of potash feldspar, quartz and whiting as shown in Table XX. All samples fired to 1,000 °C and below in air resulted in black powders, whereas a sample fired in air to 1,200 °C formed a dark green fully matured glaze. Electron spin resonance spectra were obtained for a series of samples fired to various temperatures up to 1,200 °C and the results are summarised in Table XX. Samples fired to 400 °C and 600 °C gave a broad absorption about 1000 gauss in width, which was superimposed upon the hyperfine spectrum associated previously with the manganese impurity in whiting. As with samples of the iron glaze recipe, this nuclear hyperfine component was found to be absent after the firing temperature exceeds the decomposition temperature of calcite. A summary of the X-ray diffraction results obtained for this system is given in Table XXI. Copper (II) oxide was identified by X-ray diffraction peaks of d values 2.53, 2.32, 2.53 and 2.31 with respective relative intensities of 100%, 96%, 49% and 30%. The broad electron spin resonance absorption peak obtained for all samples heated to 1,000 °C is consistent with the presence of an antiferro-magnetic species such as copper (II) oxide. The fully matured glass formed on firing this system in air to 1,200 °C gave an electron spin resonance signal centred around $g \simeq 2.0$ as shown in Figure 16. The exact position of this peak is difficult to measure as it is quite broad, about 400 gauss in width, and it is also quite asymmetric.

500 Gauss

g = 2.0
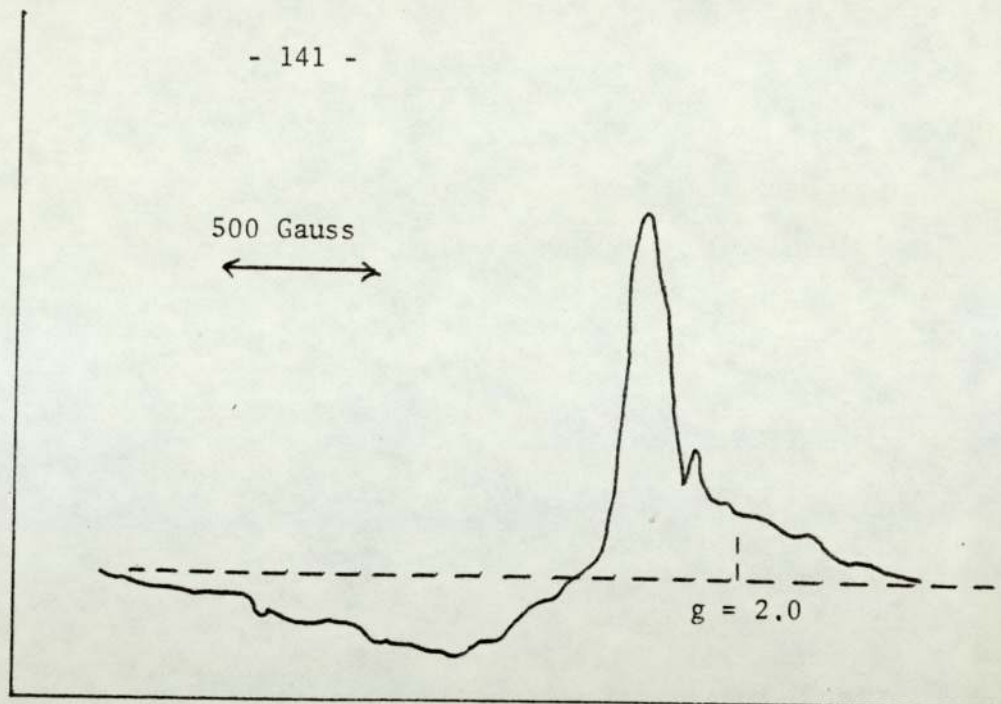
ESR of glass containing around 10% Cu^{II}

FIGURE 16

500 Gauss

g$_2$

g$_3$

g = 2.0

g$_1$

ESR of glass containing 0.1% Cu^{II}

FIGURE 17

Similar glaze recipes were prepared and fired with lower copper concentrations as indicated in Table XXII. The electron spin resonance spectrum of the fully matured light green glaze formed on firing a sample containing 1% copper (II) oxide gave much better resolution than the spectrum of the 10% copper (II) oxide containing glaze. The colourless glaze formed from firing a .1% copper (II) oxide glaze recipe again gave a well resolved electron spin resonance spectrum as shown in Figure 17. Both samples containing reduced amounts of copper (II) oxide formed glazes that gave electron spin resonance spectra in which three g values could be resolved. The 10% copper (II) oxide containing glaze is thought not to give such well resolved electron spin resonance signals because the copper (II) ions are sufficiently close together to interact with each other, so that they cannot interact independently with the applied magnetic field as magnetic exchange interactions predominate. Lowering the initial concentration of copper in the glaze recipes increases the average copper (II)-copper (II) cation distance allowing each cation to inter-act independently with the applied field. This is in contrast to the iron glaze system in which not much better resolution in the electron spin resonance system could be obtained by lowering the initial concentration of iron in the system. This result is probably not significant in terms of the way that either copper (II) oxide or haematite interact with the other glaze components, but serves to outline the fact that the iron cations seem to occupy a site in which sharp resonance peaks are not expected to be observed, even in a magnetically dilute system when the iron species are randomly orientated with respect to the applied field as they are in a glass sample. Such a situation can arise by iron (III) being in a network modifying

position as discussed in section 4.4. However, Sands[33] has shown that copper (II) in glass can be expected to give an asymmetric absorption around g = 2.0 as is the case in the present work. This is also attributed to copper (II) being present in a network modifying position so that the electron spin resonance results indicate that there is no difference in the roles played by iron (III) and copper (II) in the glass systems studied.

The actual shape of the signal obtained for Cu(II) in a glaze environment is accounted for by the presence of an anisotropic g tensor. Two g values are observed by Sands, $g_{||}$ and $g_\perp$. The less intense g value has been shown by Sands to be g_{11} which also more often gives observable nuclear hyperfine interaction from the ^{63}Cu and ^{65}Cu nuclei, natural abundance 69.1% and 30.9% respectively, both of which have a nuclear spin of $\frac{3}{2}$. The nuclear magnetic moments of ^{65}Cu and ^{63}Cu are quite similar, 2.3790 Bohr magnetons and 2.2206 Bohr magnetons respectively, so that resolution of the hyperfine interaction into the individual components from the two copper isotopes is not possible. The absorption due to g_{11} is split by the nuclear spin of the copper nuclei into four lines (i.e. 2I + 1) so that the nuclear coupling constant can be calculated.

The electron spin of transition metal ions in complexes is usually strongly quantized along one of the major crystal axes so that the geometry of the complex introduces an anisotropy into the electron spin resonance spectrum. A copper (II) cation, which has a d^9 electronic configuration, in a perfectly octahedral environment, gives a single g value spectrum as shown in Figure 18.

Perfectly octahedral symmetry   Isotropic g value
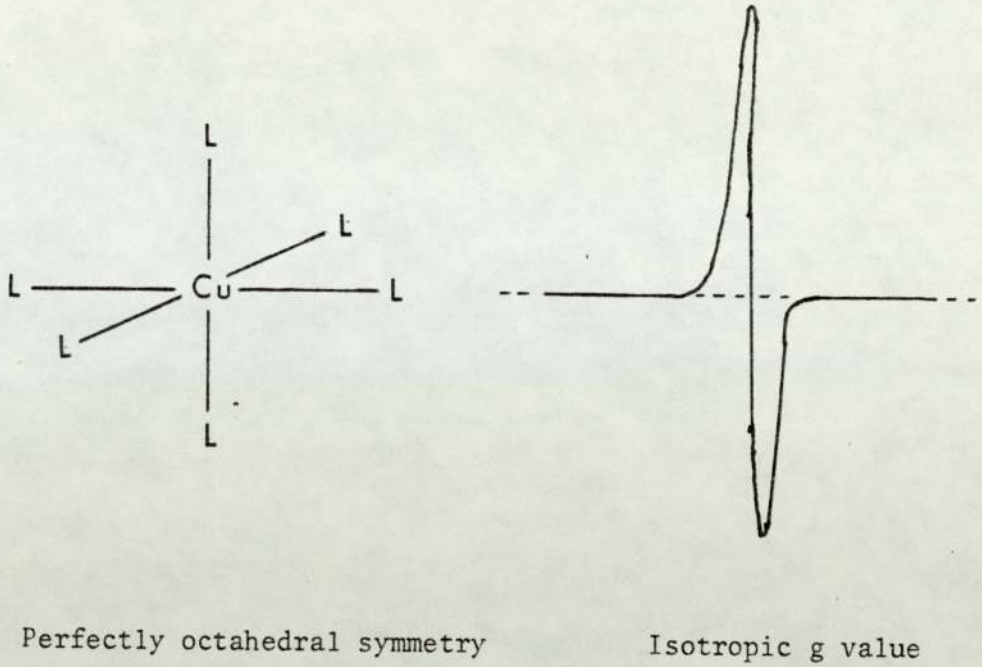
FIGURE 18

Such a situation in practice does not exist due to the presence of
Jahn-Teller distortions. Each of the three axes would be equivalent
in the case of octahedral symmetry so that a totally isotropic g
value is observed. If a distortion from octahedral symmetry occurs
such that the complex is still axially symmetrical, then the three g
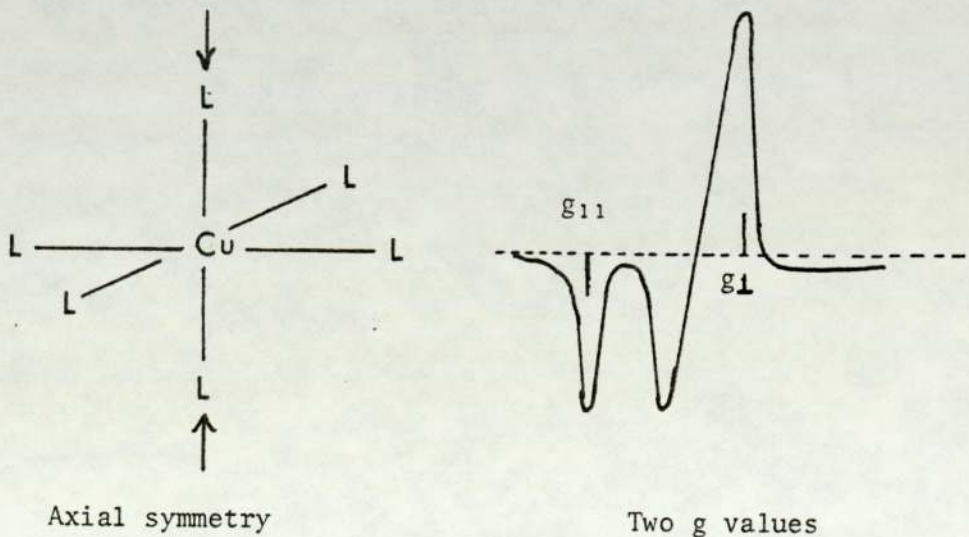values are not all equivalent as shown in Figure 19, and a two g
value spectrum is obtained.

Axial symmetry   Two g values

FIGURE 19

This is the type of spectrum obtained experimentally by Sands when copper (II) oxide is introduced into a glaze system, except that the g_{11} resonance absorption is resolved by the nuclear hyperfine magnetic interaction of copper to give four resolvable absorption peaks.

It is also possible that the three axes are all inequivalent as in the case of rhombohedral symmetry. In this case, three g values are normally observed. Various absorption line shapes can result from such a system as shown in Figure 20. It was tempting at first to interpret the electron spin resonance signal obtained from a 0.1% copper (II) containing glaze as being due to two g values, g_{11} and $g_{\perp}$ with nuclear hyperfine splitting being observed as reported by Sands. However, this means that the nuclear hyperfine coupling constant for the g_{11} would give a splitting of well over 1000 gauss. Nuclear coupling constants of this magnitude for Cu(II) are not normally encountered. An alternative explanation for this spectrum is that the low field absorption is not part of the nuclear hyperfine splitting of g_{11} but is in fact a third g value indicating that the copper (II) ions are in a rhombohedrally distorted environment rather than one that has axial symmetry. Castner considers that if a transition metal ion is in a rhombohedrally distorted environment, then the parameters D and E, used to describe the deviation from cubic symmetry, are both large and comparable in magnitude. Solving the spin Hamiltonian for d^5 and d^9 systems, he concludes that if D and E are large in a d^5 system, then in a powdered spectrum, where random orientation occurs, the electron spin resonance signal is spread over a large range of g values and no sharp signal is observed. However, for a d^9 system under the same conditions, sharp d values around g = 2.0 are to be

expected. The electron spin resonance results obtained in the present work for iron (III) and Cu(II) ions in glass indicate therefore that these ions occupy the same sort of sites. The shape of the electron spin resonance signal for a d^9 system such as copper (II) can, in fact, provide more detailed information on the symmetry of the metal ion than can the ^{57}Fe Mössbauer resonance spectrum of octahedral iron (III) discussed in section 4.9. As illustrated here, the electron spin resonance spectrum can differentiate between axial and rhombohedral symmetries purely by the shape of the signal obtained. The ^{57}Fe Mössbauer spectrum of octahedral iron (III) can differentiate between perfectly octahedral symmetry, in which no quadrupole splitting is observed, and distorted octahedral symmetry in which the ligand contribution to the electric field gradient is non-zero and a quad- rupole splitting occurs. Although for the right sort of systems the presence of an increasing or decreasing rhombohedral distortion could possibly be observed over a series of compounds, Mössbauer spectroscopy is not normally used to differentiate between such differences in symmetry.
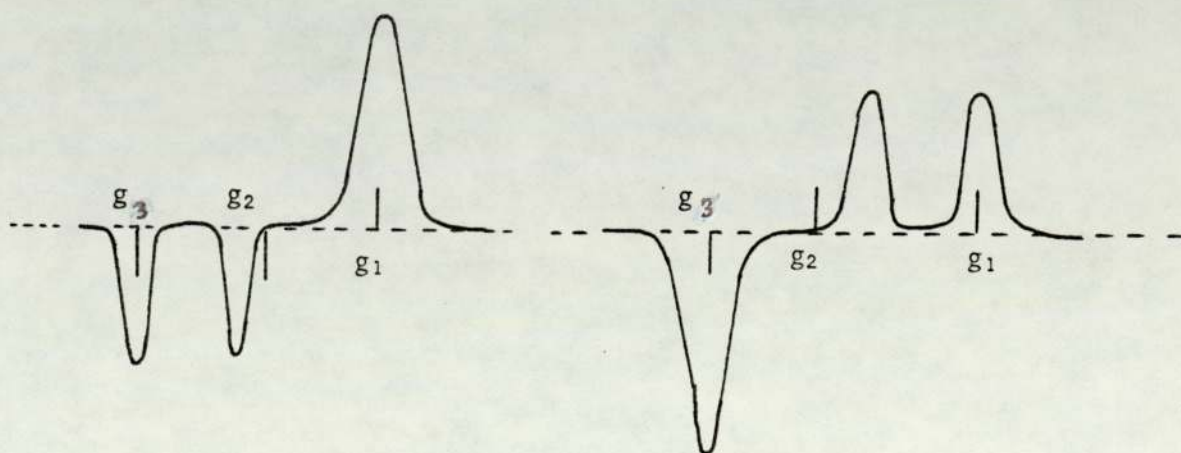
Examples of three g value esr line shapes

FIGURE 20

FIGURE 21

Visible spectrum of Cu^{II} glaze
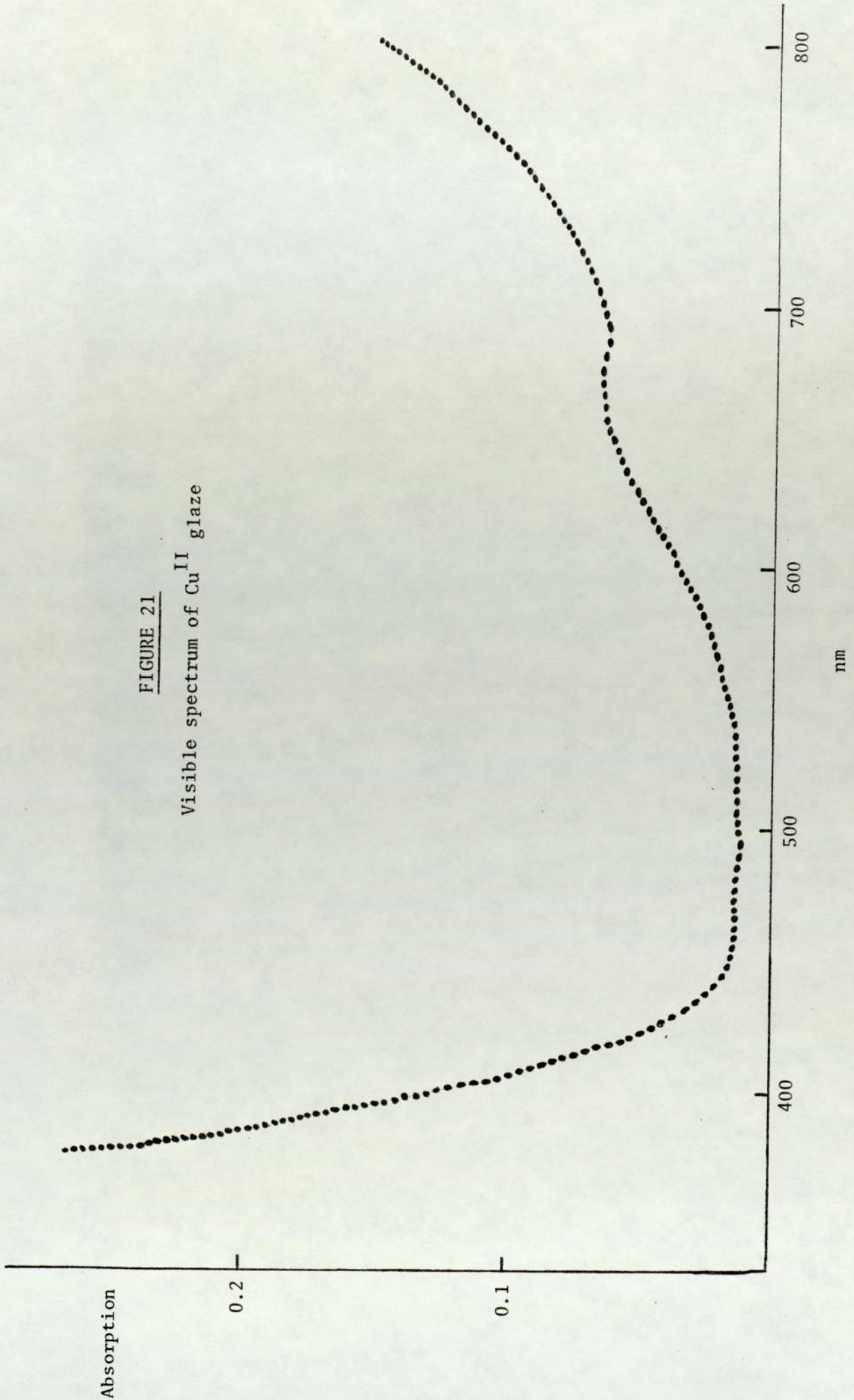
The visible spectrum of a finely powdered sample of the fully matured copper glaze fired to 1,200 °C was obtained using the filter paper technique outlined in chapter 2. The spectrum is shown in Figure 21. Cu(II) systems usually give absorptions centred somewhere around 850-900 nm due to the promotion of a t_{2g} electron to the e_g level as shown in Figure 22 for a perfectly octahedral site.
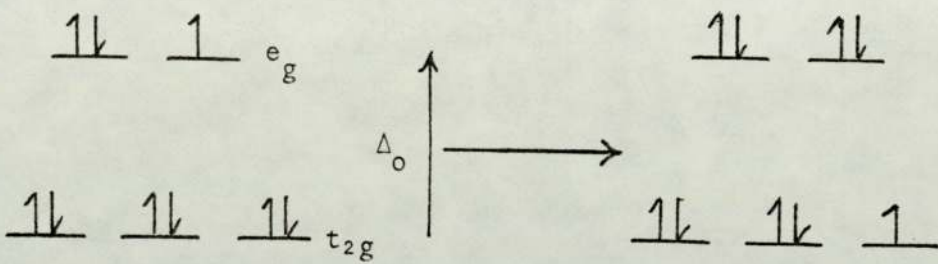

FIGURE 22

Δ_o is the crystal field splitting energy and the transition is observed by the absorption of light having a frequency equal to v where $v = \Delta/h$ and h is Planck's constant. But if the system is not perfectly octahedral, the t_{2g} and e_g states are no longer degenerate and three absorptions are expected as indicated in Figure 23.
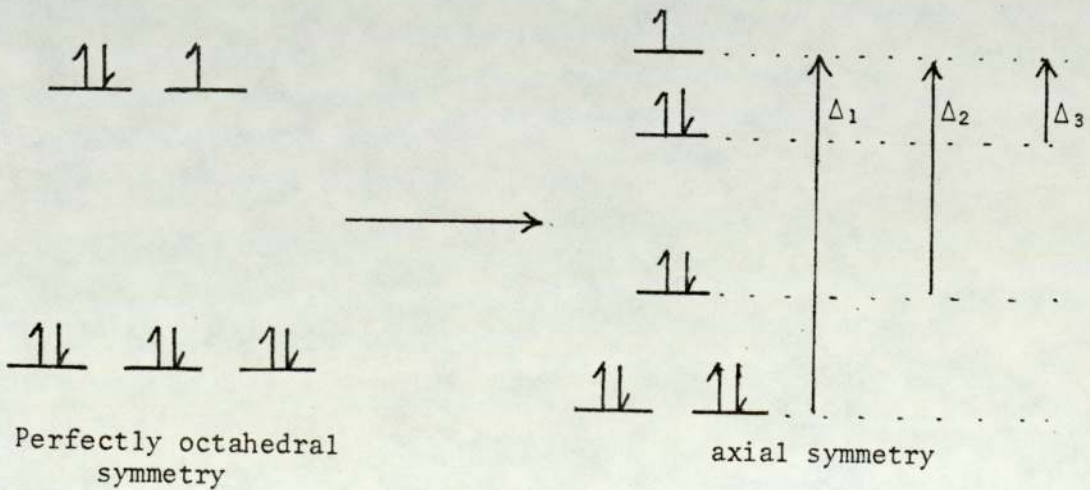

Perfectly octahedral
symmetry

axial symmetry

FIGURE 23

Three possible absorptions can occur in the case of axial symmetry. The crystal field splitting energy, Δ_o, shown in Figure 22 is split into two absorptions, Δ_1 and Δ_2, and this manifests itself in the form of an asymmetric absorption. The shelf at 600 nm in the visible spectrum of a powdered copper (II) glaze sample is therefore thought to be due to a distortion from perfectly octahedral to axial or perhaps rhombohedral symmetry which agrees with the esr results. Such a distortion for Cu(II) is not only normal but is actually predicted by the Jahn-Teller theorem for any non-linear molecular system with a degenerate electronic state.

4.10.2 Copper (I) Glazes

Copper (I) oxide was added to potash feldspar, quartz and whiting in the proportions shown in Table XXIII. This recipe was fired in air to various temperatures up to 1,200 °C. All samples fired up to 1,000 °C formed grey powders whereas samples fired to 1,200 °C formed fully matured dark green glazes. X-ray powder diffraction results indicate that oxidation of copper (I) to copper (II) occurs at a very early stage in the firing process. Electron spin resonance of the fully matured glaze also confirms the presence of copper (II).

The same glaze recipe was then fired in a nitrogen atmosphere as outlined previously using a quartz sagger as an inner chamber to ensure that a blanket of nitrogen surrounds the glaze samples throughout the firing and cooling cycles. X-ray diffraction results are summarised in Table XXIV and these show that both copper (I) oxide

and copper (II) oxide are present in all samples fired to a variety of different temperatures. Copper (I) oxide was identified by the presence of diffraction peaks at d values 2.46, 2.13 and 1.51 with respective relative intensities of 100%, 37% and 27%. All samples fired up to 1,000 °C formed light green powders, whilst the fully matured glaze formed on firing to 1,200 °C was multicoloured, green and yellow predominating although small areas of blue and red could also be observed. The electron spin resonance spectrum clearly showed the presence of copper (II). Three possible mechanisms of oxidation of copper (I) are possible, oxidation by leakages in the nitrogen blanket, oxidation by another glaze component or disproportionation. It is highly unlikely that copper (I) oxide can interact with either quartz or potash feldspar. However it could be possible that some transition metal impurities are present in the glaze recipe raw materials and that these interact with copper (I) causing partial oxidation to copper (II). Although such interactions are possible, it is thought to be unlikely due to the low temperature at which such an interaction would have to take place (i.e. below 400 °C) in what is quite a refractory system as well as the fact that it would require a very high proportion of transition metal ion impurity to be present in order to oxidize approximately 10% by weight copper (I) oxide.

Disproportionation can occur as follows:

$$Cu_2O \rightarrow CuO + Cu$$
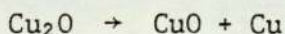
X-ray diffraction should be able to distinguish between disproportionation and oxidation by the presence or absence of diffraction peaks due to copper metal. These have d values of 2.09 and 1.81 with

relative respective intensities of 100% and 46%. But these peaks
cannot be observed in any of the samples investigated so that no
evidence for disproportionation could be obtained.

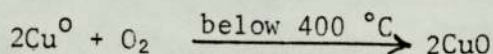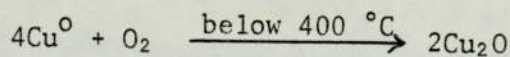### 4.10.3 Copper (II)-Copper Metal Glaze Recipes

It is known that copper (II)-copper metal $\rightleftharpoons$ copper (I)
equilibria[50] can readily be displaced in solution in either direction
by varying the nature of the ligand. A mixture of copper (II) oxide
and copper metal was fired in a nitrogen atmosphere with potash felds-
par, quartz and whiting and the X-ray powder diffractogram results for
samples fired to various temperatures are summarised in Table XXV.
Copper metal, copper (I) oxide and copper (II) oxide were found in
all samples indicating that the interaction between copper (II) oxide
and copper metal proceeds below 400 °C to form copper (I) oxide.
Samples fired to 1,000 °C clearly contained copper metal whilst a
fully matured red glaze was formed on firing to 1,200 °C. Electron
spin resonance spectroscopy indicates that no copper (II) was present
in samples of the fully matured glaze so it appears that the copper (II)
-copper metal interaction proceeds to completion between 1,000 °C and
1,200 °C. The red colour of the fully matured glaze is therefore due
to the exclusive presence of copper (I) which becomes trapped in the
glass matrix. It is interesting to note that the most successful way
of trapping copper (I) in a glaze environment is to add a stoichiometric
amount of copper (II) oxide to copper metal and fire in an inert
atmosphere. Attempts to fire copper (I) oxide in an inert atmosphere
result in oxidation to copper (II) oxide and are therefore more or

less totally unsuccessful in producing a copper (I) containing glaze. These results are analogous to the iron containing glaze recipe results in which ferrous oxalate fired in an inert atmosphere to 1,280 °C gave a glaze containing a mixture of iron in two oxidation states, iron (II) and iron (III). A stoichiometric amount of iron metal and iron (III) when fired with potash feldspar, whiting and quartz in an inert atmosphere to 1,280 °C gave a rich blue glaze due to the exclusive presence of iron (II), as shown by Mössbauer spectroscopy.
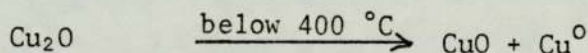
4.10.4 Copper Metal Glaze Recipes

Copper metal was added to a mixture of potash feldspar, quartz and whiting as shown in Table XXVI and samples were fired to a variety of temperatures under a nitrogen atmosphere. X-ray diffraction results clearly show the presence of copper metal in samples fired to 1,000 °C as well as significant amounts of both copper (II) oxide and copper (I) oxide. The fully matured glaze formed on firing to 1,200 °C was bright red in colour. Electron spin resonance spectroscopy indicates that no copper (II) was present in this glaze. This system appears to be quite complex in behaviour. Partial oxidation of copper metal is seen to occur at quite low temperatures. It is likely that this is a two stage process with some of the copper metal first of all oxidizing to copper (I) oxide and a proportion of this then oxidizing to copper (II) oxide. As is the case when copper (I) oxide is fired in a glaze recipe in an inert atmosphere, it is difficult to envisage which species in the glaze recipe is responsible for oxidation. It could well be the case that small amounts of residual oxygen in the system oxidize

some of the copper metal to copper (I) oxide. Copper (I) oxide can oxidize to copper (II) oxide or a disproportionation reaction can occur regenerating more copper metal and forming some copper (II) oxide. However, these are not the only reactions that occur in this system as electron spin resonance shows that there is no copper (II) in the fully matured red glaze. Copper (II) therefore appears to interact with copper metal between 1,000 °C and 1,200 °C to form copper (I). To summarize, the following reactions are thought to occur:

$$4Cu^O + O_2 \xrightarrow{\text{below 400 °C}} 2Cu_2O$$

$$2Cu^O + O_2 \xrightarrow{\text{below 400 °C}} 2CuO$$

or perhaps also

$$Cu_2O \xrightarrow{\text{below 400 °C}} CuO + Cu^O$$

so that at 400 °C, copper metal, copper (I) oxide and copper (II) oxide are all present. Then:

$$Cu^O + CuO \xrightarrow{\text{1,000 °C-1,200 °C}} Cu_2O$$
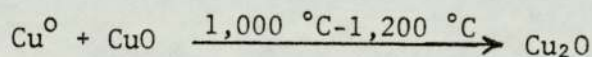
so that the fully matured glaze contains copper predominantly in a +1 oxidation state.

4.10.5 Copper Strontium Glaze Recipes

Strontium was added in various proportions to copper (II) oxide, potash feldspar, quartz and whiting, as shown in Table XXVI, and fired

to 1,280 °C in air in order to see if replacement of calcium by strontium in any way modified the structure of the fully matured glaze. Electron spin resonance studies indicated that no modification of the environment of the copper (II) cation could be observed by different initial concentrations of strontium.

4.11 CHROMIUM-STRONTIUM GLAZE RECIPES

A mixed oxide of strontium and chromium has been reported[51] by heating strontium chromate, chromium trioxide, and strontium hydroxide to 1,000 °C.

$$SrCrO_4 + CrO_3 + 5Sr(OH)_2 \xrightarrow{\;1,000\ ^\circ C\;} 3Sr_2CrO_4 + 5H_2O$$
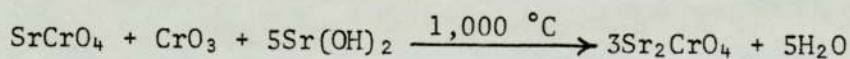
This reaction was carried out and a dark blue powder formed with a magnetic moment of 2.90 Bohr magnetons. This compound was added to a glaze recipe as shown in Table XXVII. A dark green fully matured glaze was formed on firing in air to 1,200 °C although some areas of blue were observed. Initially it was hoped that the addition of this compound to a ceramic glaze recipe would lead to the entrapment of chromium IV in the glaze, to give a rich blue finish.

An extremely strong electron spin resonance signal was obtained at g = 2.0 while the powdered visible spectrum gave an asymmetric absorption centred around 608 nm, indicating that reduction of

FIGURE 24

Visible spectra of Cr glass compared to some acidic solutions of Cr (III)

Powder Glass

8 molℓ^{-1} H_2SO_4

12 molℓ^{-1} H_2SO_4

16 molℓ^{-1} H_2SO_4

Absorption

wavelength nm
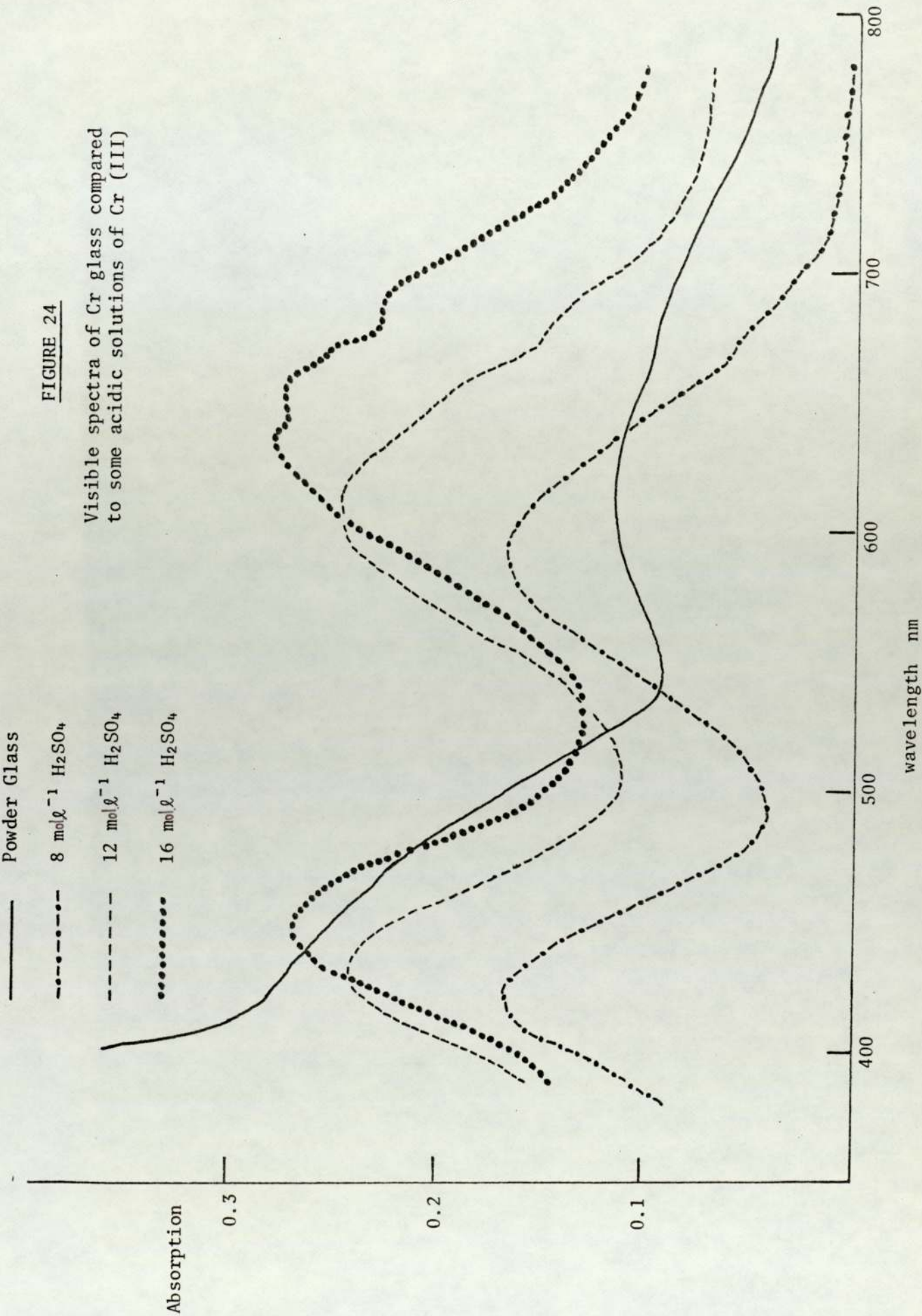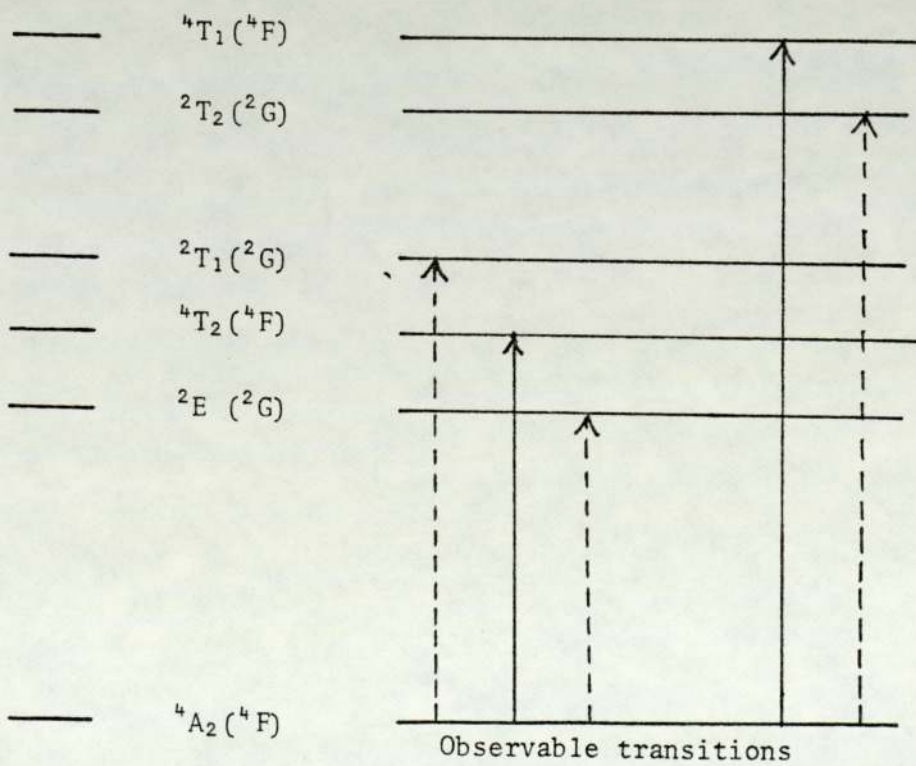
chromium (IV) occurs to give a chromium (III) containing glaze.

However, the visible spectrum of this glaze was compared with the solution spectra of some acidic chromium (III) solutions in order to give an insight into the sort of ligand field strengths present within the glaze. This comparison is necessary because if the visible spectrum of the glaze sample is studied alone, it is not clear whether the absorption at 608 nm is due to the $^4T_2 \leftarrow {}^4A_2$ transition of the ^4F electronic state of chromium (III) or whether it is due to the $^4T_1 \leftarrow {}^4A_2$ transition within the same electronic state. The powdered spectrum does display a certain amount of asymmetry although the absorption cuts off towards the blue end of the visible region as expected due to absorption by quartz. It is unclear, by just looking at the powdered glaze spectrum, whether the shelf between 400 nm and 500 nm is due to a transition metal absorption or if it is characteristic of the quartz absorption. Figure 24 compares acidic chromium solution spectra with the powdered glaze spectrum. It can be seen that the sample containing 4×10^{-4} mol .ℓ^{-1} chromium (III) and 12.0 mol ,ℓ^{-1} H_2SO_4 most closely matches the glaze spectrum but it also now becomes clear that the shelf between 400-500 nm is part of the chromium (III) electronic spectrum. It can be seen that the absorption peak at 608 nm is due to the $^4T_2 \leftarrow {}^4A_2$ transition of the ^4F electronic state, whilst the shelf between 400 and 500 nm is due to the $^4T_1 \leftarrow {}^4A_2$ transition. This point can be further illustrated by considering the strongest acidic solution spectrum in which this absorption can now be seen to be composed of three distinct components. By referring to Figure 25, it can be seen that this absorption is a composition of absorptions

FIGURE 25

$^4T_1(P)$

$^2A_1$

^2G

^4P

^4F

$^4T_1(F)$

$^2T_2$

$^4T_2$

$^2T_1$

^2E

$^4A_2$

Δ_o
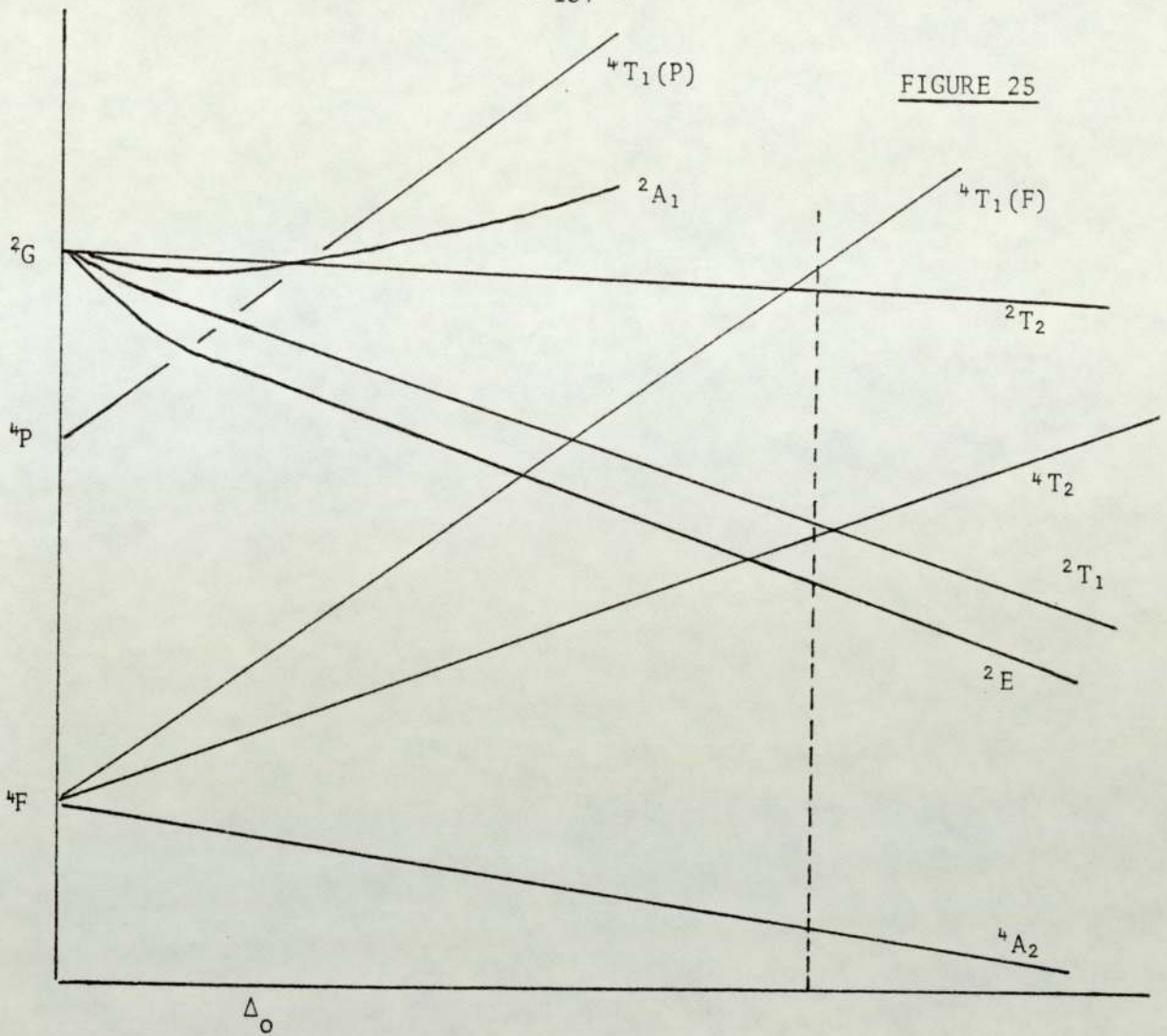
Energy level diagram v ligand field strength for octahedral Cr(III)

$^4T_1(^4F)$

$^2T_2(^2G)$

$^2T_1(^2G)$

$^4T_2(^4F)$

$^2E\ (^2G)$

$^4A_2(^4F)$

Observable transitions

between the $^4A_2$ ground state and (i) $^4T_2$ state of the ^4F electronic state, (ii) ^2E state of the ^2G electronic state and (iii) the $^2T_1$ state of the ^2G electronic state. The latter two transitions are spin forbidden and owe their high intensities to an intensity stealing effect.

The fact that this absorption can be resolved into three parts confirms that it is the $^4T_2 \leftarrow ^4A_2$ transition. The maximum number of components that the $^4T_1 \leftarrow ^4A_2$ transition could be expected to be resolved into is two as the $^2T_2(^2G) \leftarrow ^4A_2$ spin forbidden transition could possibly be observed.

Tanabe and Sugano[52] have published a set of semiquantitative energy level diagrams for d^2 to d^8 electronic configurations in octahedral symmetry. The diagram for a d^3 electronic configuration, such as chromium (III), is illustrated in Figure 26. The diagrams are a plot of E/B against Δ/B where B is a quantity called the Racah parameter which is a function of the particular ion under consideration, E is the absorption energy and Δ is a measure of the ligand field strength. The Racah parameter for a free chromium (III) ion is quoted by Tanabe and Sugano to be equal to 1,030 cm^{-1}. 608 nm is equivalent to 16,444 cm^{-1} so that E/B is equal to 15.96. This ratio for E/B compares roughly on the Tanabe-Sugano diagram to a Δ/B value of about 16, which is equivalent to a value of 16,480 cm^{-1} for the ligand field strength, Δ . It cannot be emphasised strongly enough that this calculation is only approximate as no account is taken of distortions from regular octahedral symmetry. Nevertheless Cotton and Wilkinson[53] report that Δ_o for complexes of the first transition

FIGURE 26

Tanabe Sugano diagram for d^3 configurations
$B = 766$ cm^{-1} for V^{II}
$= 1030$ cm^{-1} for Cr^{III}
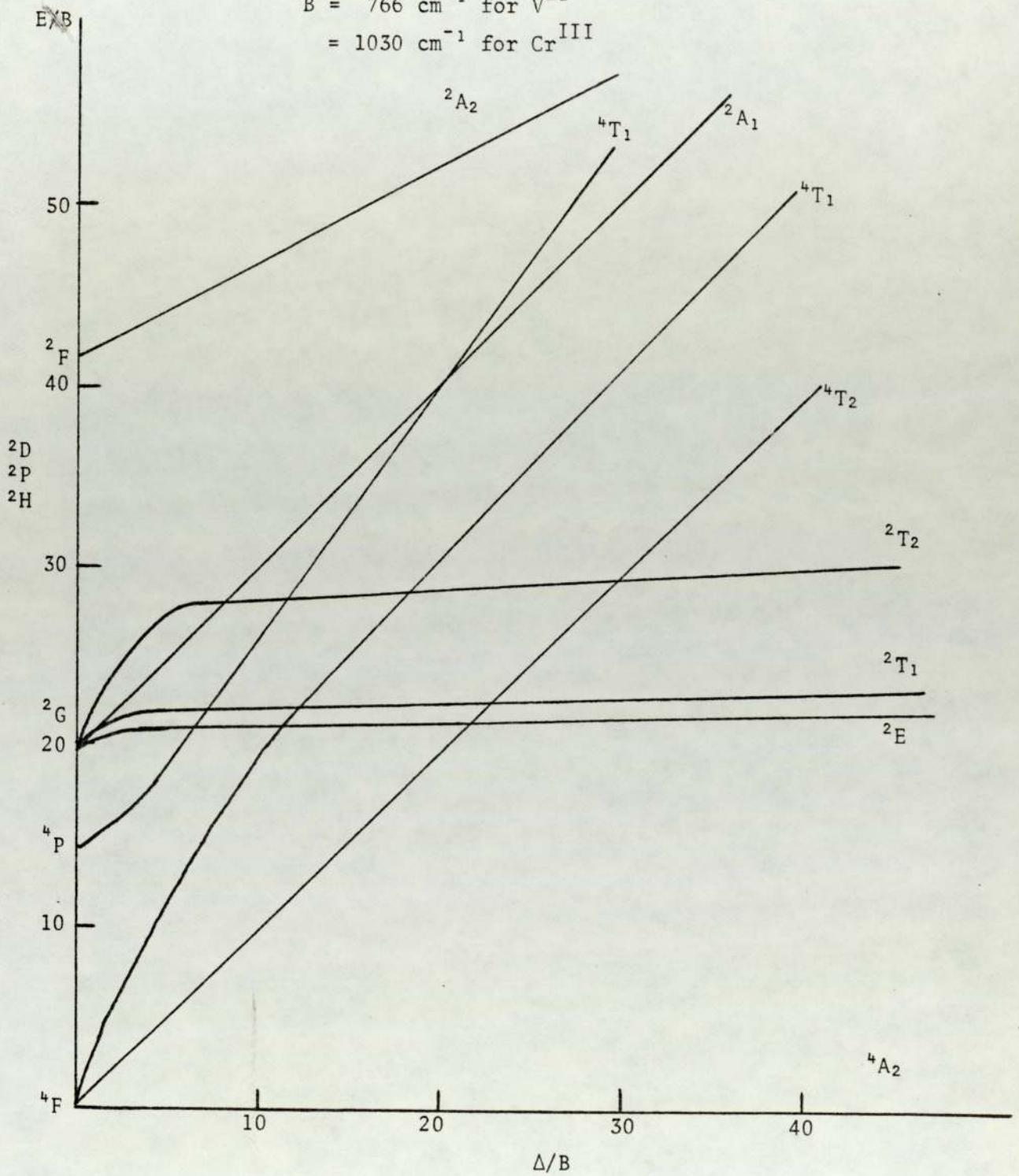
series are generally within the range 14,000-25,000 cm^{-1} for trivalent

ions so that the figure of 16,480 cm^{-1} calculated for the chromium

containing glaze shows that the ligand strength although well within

the expected range for trivalent ions of the first transition series

is definitely an indication of the fact that the ligand field is weak.

A convenient arbitrary definition of weak and strong field

strengths is often taken to be the field strength at which high to

low spin transitions occur in octahedral first row transition metal

ions. This does not apply to chromium (III) complexes, for which

there are no low spin octahedral species; however Figure 27 compares

the ligand field strength measured above with ligand field strengths

in the spin crossover region for some first row transition metal

trivalent cations. Again it can be clearly seen that the glaze

environment provides a ligand field very much towards the weak end

of the scale.

Ion	Δ	
Mn(III)	30,888 cm^{-1}	Calculated from
Fe(III)	31,100 cm^{-1}	Tanabe-Sugano
Co(III)	21,300 cm^{-1}	Diagrams
Cr(III)	16,480 cm^{-1}	Calculated from the present work

FIGURE 27

Chromium Trioxide and various amounts of Strontium oxalate were

added to mixtures of potash feldspar, quartz and whiting in the

proportions shown in Table XXVII. Visible spectra were obtained for

the dark green glazes obtained on firing these samples to 1,200 °C

FIGURE 28

Visible spectra of strontium containing
glaze recipes fired in air to 1,200 °C

•••••• 1.3% Sr oxalate

– – – 9.2% Sr oxalate

Absorption

wavelength nm
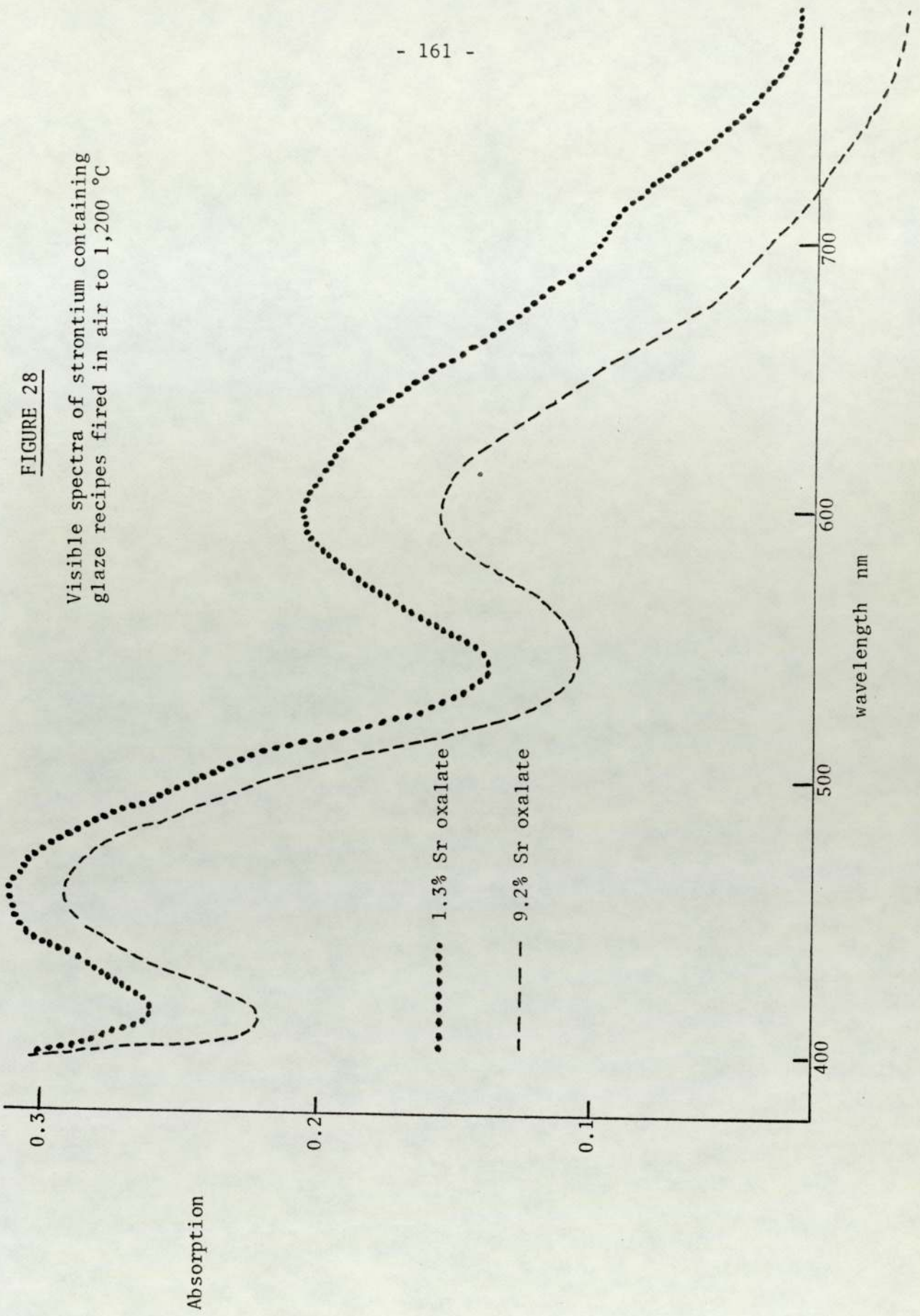
in air. These are illustrated in Figure 28 and it can be seen that
there is no difference between the positions of absorption for the
low strontium containing glaze compared to the high strontium
containing glaze. This indicates that the ligand field strength
experienced by the chromium (III) ions in the glazes studied is not
affected by the presence of different amounts of strontium. This is
further evidence that strontium does not appear to alter the
environment of transition metal ions in ceramic glazes.

4.12   CONCLUSION

The interaction of chromium, iron and copper transition metal
ions in ceramic glaze recipes has been studied using a variety of
spectroscopic techniques. Iron was initially introduced into the
glaze recipe in the form of ferrous oxalate which was shown to
decompose both in air and in an atmosphere of nitrogen below 400 °C.
Mössbauer spectroscopy showed conclusively that ferrous oxalate
decomposes in air to form haematite. The interaction of haematite,
formed on firing ferrous oxalate, with a mineral glaze recipe was
compared with its interaction with a soda glass system. Haematite
interacted with the soda glass systems at around 800 °C, although
no intermediate iron containing species could be positively identified
before glass formation occurred at 1,280 °C. In contrast to this,
haematite was identified as the only iron containing species even
in samples fired to 1,100 °C. Two iron sites were identified in the

soda glass, the Mössbauer parameters being consistent with iron (III) in octahedral and tetrahedral sites. Mössbauer spectra of the mineral glaze indicated that iron (III) was present only in octahedral sites. X-ray diffractogram results for the two systems showed that the soda glass was totally amorphous whilst crystalline quartz and potash feldspar diffraction peaks could be identified in the fully matured mineral glaze. The reagent grade calcium carbonate used in the soda glass recipe was shown to be a mixture of calcite and aragonite. The aragonite to calcite phase transformation was seen to occur between 400 °C and 600 °C whilst the decomposition of calcite was shown to occur between 600 °C and 800 °C. However no crystalline calcium oxide could be detected in samples fired above 600 °C although samples fired to 900 °C and 1,000 °C showed traces of $CaSiO_3$. Whiting was shown to consist of only one of the crystalline forms of calcium carbonate, calcite. The decomposition of calcite was shown to occur between 600 °C and 800 °C in samples of the mineral glaze system. However, as with the soda glass system, no crystalline calcium oxide could be detected. No $CaSiO_3$ could be detected in the mineral glaze system. The curious behaviour of calcium oxide led to a separate investigation being undertaken. Samples of reagent grade calcium carbonate and amorphous silica were fired in air to 900 °C. X-ray results indicated that the only crystalline species present was $CaSiO_3$. However samples of reagent grade calcium carbonate and quartz when fired in air to 900 °C gave X-ray powder diffractogram patterns indicating that calcium oxide and quartz were the only crystalline species present. This is considered to be strong evidence for the fact that calcium oxide interacts with a component of the mineral glaze recipe, other than quartz, and does not crystallise out after

the decomposition of calcium carbonate. Also this result demonstrates a difference in reactivity between amorphous silica and quartz at elevated temperatures in the presence of calcium oxide. It was not conclusively shown that either of these species was responsible for the difference in behaviour of haematite in the mineral glaze system compared to the soda glass system as this could be due to the presence of sodium carbonate in the soda glass system. Electron spin resonance studies of the fully matured iron containing glazes gave no valuable information; however mineral glaze recipe samples fired to 600 °C and below exhibited a complex multiline resonance spectrum. This was identified as being due to the nuclear magnetic hyperfine interaction of manganese (II), which is present to a small extent as an impurity in whiting. No resonance signal could be obtained for the manganese impurity in the mineral glaze recipe after the decomposition of whiting. However the decomposition of pure whiting was followed using electron spin resonance studies and the manganese impurity in calcium oxide was shown to give a characteristic resonance signal. This result confirms the X-ray diffraction result that calcium oxide does not crystallise out in the mineral glaze system after the decomposition of calcite.

The mineral glaze recipe was then fired in a nitrogen atmosphere in order to trap iron (II) in a glaze. Mössbauer spectroscopy showed that ferrous oxalate decomposes below 400 °C to form magnetite, Fe_3O_4, which then interacts with the rest of the mineral glaze components between 1,200 °C and 1,280 °C to give a black glaze containing octahedral iron (III) together with octahedral iron (II). Magnetite could not be detected by X-ray diffraction indicating that the particle size

is small.

Stoichiometric amounts of iron metal and haematite were added to potash feldspar, quartz and whiting in order to see if iron (II) could be produced in situ whilst firing under nitrogen. Mössbauer spectroscopy showed that the blue glaze formed on firing to 1,280 °C contained iron (II) in an octahedral site. No iron (III) could be detected. The most interesting result from this system is that samples fired to 800 °C were shown to consist of haematite and iron metal whilst the Mössbauer parameters of samples fired to 1,000 °C were very similar to those of the fully matured glaze even though the samples fired to 1,000 °C are light green powders. This indicates that the environment of the iron (II) cations is determined before glass formation. This againimplies that calcium oxide has some important structure determining role and that the Mössbauer spectrum of samples fired to 1,000 °C is due to a calcium iron (II) oxide, which then becomes trapped in a glass matrix. However no other spectroscopic evidence for this could be obtained.

Iron metal was also added to a glaze recipe and fired in nitrogen and Mössbauer spectroscopy showed that the iron metal does not interact with other components of the system until above 1,200 °C, when it then forms a light green glaze containing octahedral iron (II) only. Mössbauer parameters of the octahedral iron (II) and iron (III) sites in the different glaze recipes have been shown to be significantly different, even though the glass forming matrix, potash feldspar, is the same in all cases. The non-appearance of crystalline calcium oxide in mineral glaze recipes suggests that this species may have an active

role in determining the final glaze structure. The fact that no
calcium containing intermediate species could be positively identified
by any spectroscopic technique is not taken to mean that these do not
exist immediately prior to glass formation. The various different
environments of iron in fully matured glazes when introduced in
different forms may well be due not to the different ways in which
the original iron species interact with the glass matrix but due to
the manner in which the original iron species interacts with calcium
oxide, the products of which subsequently dissolve in the glass matrix.
It is suggested that it would be of great value in the future to study
the interactions between group II carbonates, particularly calcium
carbonate, and various oxides of iron at elevated temperatures, to
see if more evidence can be gained for the importance of such inter-
actions in determining the environment of transition metal ions in
glazes.

The Mössbauer parameters of a series of strontium-calcium
containing glazes were compared in order to investigate Shteinberg's
claim that group II cations are the most important structure deter-
mining species in glazes. The Mössbauer results indicate that the
presence of different group II cations in different concentrations
do not directly modify the local environment of iron (II) and iron (III)
glass sites in the systems studied.

Copper was initially introduced into glaze systems as a 10%
addition of copper (II) oxide and the electron spin resonance spectrum
of the fully matured green glaze formed on firing to 1,200 °C
indicates that the copper (II) ions have rhombohedral symmetry, although

the glaze samples are not magnetically dilute. 1% and 0.1% copper (II) oxide containing glazes gave spectra with much better resolution in which some nuclear hyperfine splitting was observed. By comparison dilute iron (III) containing glazes gave only marginally better resolution than more concentrated glazes. Comparison of the electron spin resonance spectra of both iron (III) and copper (II) containing glazes with previous work by Castner et al and Sands indicates that the results obtained in the present work are to be expected for copper (II) and iron (III) in network modifying positions. Again crystalline calcium oxide could not be detected by electron spin resonance or by X-ray diffraction after the decomposition of whiting indicating some active, perhaps structure determining, role. However, no modification of the electron spin resonance signal of the fully matured copper (II) glaze could be observed on the addition of various amounts of strontium.

Copper (I) oxide was introduced into the glaze recipe and fired in an atmosphere of nitrogen in order to trap Cu(I) in a glaze environment. However it was found that it was impossible to introduce copper (I) into a glaze by this method. X-ray diffraction confirmed the presence of Copper (II) oxide in samples fired as low as 400 °C, although this technique could not differentiate between whether oxidation or disproportionation is responsible for the presence of copper (II). Molar ratios of copper (II) oxide and copper metal were added to a glaze system and fired in nitrogen to form a fully matured red glaze containing no copper (II) ions. It is interesting to note the similarity between this system and the method used to introduce iron (II) into a glaze by a stoichiometric addition of iron metal and

haematite. Addition of various amounts of strontium to copper (II) glazes did not alter the electron spin resonance signal.

Visible spectra of chromium containing glazes were obtained and the ligand field strengths in these samples were shown to be 16,480 cm^{-1}. This is considered to be quite low for first row trivalent transition metal ions and is definite proof that the ligand field strength in glaze and glass systems is weak. Additions of various amounts of strontium to the glaze recipe did not affect the ligand field strength of the fully matured glazes. It is felt that the evidence for the fact that the presence of strontium in no way modifies the environment of the transition metal ions in the fully matured glaze systems studied is overwhelming.

The research was part technological in objective and a fair amount of technological success was achieved as reduction was shown not to be essential, although careful choice of raw materials was shown to be essential to achieve the desired effects under an inert atmosphere. Few problems of reproducibility were encountered, containment of a nitrogen atmosphere, on a small scale at least, proving to be relatively easy. The major chemical achievement of the research has been to highlight the importance of the role played by calcium oxide, after the decomposition of calcium carbonate, in determining the environment of transition metal ions in glasses and glazes. The detection of calcium oxide or calcium containing species has been difficult as these have often proved to be elusive, conspicuous often only by their absence. However the evidence for the fact that it plays an important structure determining role with its interaction with

transition metal oxides is strong and it is hoped that this
research project has opened the door for further investigation
in this area.

REFERENCES

1. Rado, P. "An introduction to the Technology of pottery", Pergamon Press (1969).

2. Grimshaw, R.W. "The Chemistry and Physics of clays and allied ceramic materials". 4th Edition, Benn (1971).

3. Zachariason, W.H., J.Am.Chem.Soc. 54, 3841 (1932).

4. Shteinberg, Y.G. "Strontium Glazes", 2nd Edition, pp5-12, Stroiizdat, Moscow (1967).

5. Belov, N.V. "Collection: Structure of Glass", p344, Academy of Sciences, USSR (1955).

6. Kingery, W.D., Bowen, H.K., Uhlmann, D.R. "Introduction to Ceramics" Second Edition, Interscience (1976).

7. Greenwood, N.N., Gibb, T.C. "Mössbauer Spectroscopy" Chapman and Hall (1971).

8. Emeleus, H.J. and Sharpe, A.G. "Modern Aspects of Inorganic Chemistry" Routledge and Kegan Paul, London (1973), p461.

9. "Modern Aspects of the vitreous state" MacKenzie, J.D. Butterworths, (1962), p195, Review entitled "Ligand Field Theory of Transition Metal Ions in Glasses".

10. Hedges, R.E.M., Nature, Vol.254, April 10th (1975), p501.

11. Tomov, T, Rushov, T. and Geogiev, S.A., Proc.Conf.Appl. Mössbauer Effect, Tihany, Hungary (1969), p 793.

12. Duncan, J.F., MacKenzie K.J.D. and Stewart, D.J. Symp.Faraday Soc. Mössbauer Effect (1967), p103.

13. Bancroft, G.M., Maddock, A.G. and Burns, R.G. Geochim.Cosmochim. Acta. 31, 2219 (1967).

14. Hussak, E. and Prior, G.T. Mineral Mag., 11, 302 (1897).

15. Donnay, J.D.H. and Nowacki, W., Crystal Data Determination Tables, 2nd Edition, American Crystallographic Association (1963).

16. Mason, B. and Vitaliano, C.J., Mineral Mag. 30,100 (1953).

17. Gakiel, U. and Malamud, M., Amer.Mineral. 54, 299 (1969).

18. Bancroft, M.G., Burns, R.G. and Maddock, A.G. Acta Cryst 22, 934 (1967).

19. Duncan, J.R. and Stewart, D.J. Trans. Faraday Soc., 63, 1031, (1967).

20. Yusfin, Y.S., Voitkovskii, Y.B., Savitskaya, L.I. and Generalov, O.N., Vyssh.Ucheb.Zaved,Cern.Met. 26, (1974).

21. Gallagher, P.K. and Kurkjian, C.R. Inorganic Chemistry 5, 214, (1966).

22. Gallagher, P.K., MacChesney, J.B. and Buchanan, D.N.E., Chem. Phys. 43, 516 (1965).

23. Ichida, T., J.Solid State Chem. 7, 308, (1973).

24. Cousins, D.R. and Charmawardena, K.G., Nature 223, 733-734 (1969).

25. Kostikas, A., Simopoulos, A. and Gangas, N.H., J.Phys.Colloq.35, C1-107-115 (1974).

26. Janot, C., Delcroix, P., J.Phys.Colloq.35, C6-557-561 (1974).

27. Bouchez, R., Coey, J.M.D., Coussement, R., Schmidt, K.P, Van Rossum, M., Aprahamiam, J. and Deshayes, J., J.Phys.Colloq.35, C6-541-546 (1974).

28. Abragam, A. and Bleaney, G., Electron Peramagnetic Resonance of Transition Ions, Clarendon Press (1970).

29. Wertz, J.E., Chem.Rev.55, p829-955 (1955).

30. Ayscough, P.B. "Electron Spin Resonance in Chemistry", Methuen, (1967).

31. Cotton, F.A. and Wilkinson, G., "Advances in Inorganic Chemistry" Wiley Interscience, p905.

32. Castner, T., Newell, G.S., Holton, W.C. and Slichter, C.P., J.Chem.Phys.32, 668 (1960).

33. Sands, R.H., Phys.Rev. 99, 1222 (1965).

34. Figgis, B.N. and Lewis, J., "Magneto-chemistry of Complex Compounds" Edited by Lewis, J. and Wilkins, R.G., Interscience.

35. Lancaster, J.C., PhD Thesis, The University of Aston in Birmingham, (1971).

36. Fernandopulle, M.E., PhD Thesis, The University of Aston in Birmingham (1972).

37. McWhinnie, W.R., Kulasungam, G.C. and Draper, J.C., J.Chem.Soc. A. 1253 (1967).

38. Lancaster, J.C. and McWhinnie, W.R., J.Chem.Soc.A.2673 (1970).

39. Cox, M., Darken, J., Fitzsimmons, B.W., Smith, A.W., Larkworthy, L.F. and Rogers, K.A., J.Chem.Soc. Dalton 1192 (1972).

40. Fitzsimmons, B.W., Smith, A.W., Larkworthy, L.F. and Rogers, K.A., J.Chem.Soc. Dalton 676, (1973).

41. Wickman, H.H. and Trozzolo, A.M., Inorg.Chem.7, 63, (1968).

42. Hall, L.H., Spijkerman, J.J. and Lambert, J.L., J.Am.Chem.Soc.90, 2044 (1968).

43. Axtmann, R.C., Hazony, Y. and Hurley, J.W., Chem.Phys. Letters 2,673 (1968).

44. McWhinnie, W.R., Poller, R.C. and Thevarasa, M., J.Chem.Soc. A.1671 (1967).

45. The International Rubber Handbook. The Rubber Co. Ltd., (1972).

46. Shaw, K. "Ceramic Glazes", Elsevier, p68.

47. Coey, J.M.D., Morrish, A.H. and Sawatzky, G.A. (1971), J.Phys. 32, C1-271.

48. Evans, B.J. and Lu-San Pan. Workshop in Chemical Applications of Mössbauer Spectroscopy, Abstract 13" Seeheim, W. Germany (1978).

49. Bhat, V.K., Manning, C.R. and Bowen, L.H., J.Am.Ceram.Soc. 56, 459 (1973).

50. Hatfield, W.E. and Whyman, Transition Metal Chemistry, 5,47 (1969).

51. Cotton,F.A. and Wilkinson, G. "Advanced Inorganic Chemistry" Wiley Interscience, Third Edition (1972), p840.

52. Tanabe and Sugano, J. Phys.Soc.Japan 9, 753 (1954).

53. Cotton, F.A. and Wilkinson, G. "Advanced Inorganic Chemistry" Wiley Interscience, Third Edition (1972), p 577.